applied sciences

MDPI

Article

Analysis of Chainsaw Emissions during Chestnut Wood Operations and Their Health Implications

Paola D'Antonio, Francesco Toscano, Nicola Moretti, Nicolino De Iorio and Costanza Fiorentino *

School of Agricultural, Forestry, Environmental and Food Sciences, University of Basilicata, 85100 Potenza, Italy; paola.dantonio@unibas.it (P.D.); francesco.toscano@unibas.it (F.T.); nicola.moretti@unibas.it (N.M.); nicola.deiorio@outlook.it (N.D.I.)

* Correspondence: costanza.fiorentino@unibas.it

Abstract: In Italy, the use of chainsaws for field operations such as Felling (FE), Delimbing (DE), and Bucking (BU) is widespread due to the topography, the medium–small size of farms, and the predominant presence of broad-leaved forests managed through coppicing. However, this has led to an increase in injuries and illnesses due to exposure to physical factors (e.g., noise, dust, and vibrations) and chemical agents (e.g., various volatile compounds). Occupational health and safety legislation in Italy has undergone several phases, including the approval of U.T. 81/2008. The present study aims to evaluate the noise generated by chainsaws and the concentration of pollutants (CO, VOC, and C_6H_6) present in chainsaw exhaust gases during interventions in a chestnut coppice in relation to the limits set by current legislation. The analysis of the noise generated by chainsaws during chestnut cutting operations showed that it exceeded the legal noise limits during all chainsaw activities, with peak levels of about 110 dB. The detected noise could cause important critical issues in relation to the health and safety of specialized operators. Furthermore, the correlation between the specific work (FE, DE, and BU) and the ratio between maximum and average values of CO and VOC emissions was evaluated. Notably, comparable levels of maximum VOC emissions were observed during the FE and BU phases. However, the average emission values during these phases exhibited significant differences, suggesting higher VOC production when the engine was running but not actively engaged in cutting. The highest emissions were recorded during the FE phase (CO = 135 ppm, VOC = 17.28 ppm, and C_6H_6 = 2.13 ppm).

Keywords: chainsaws; occupational health and safety; noise; gas emissions; forest-work injuries

Citation: D'Antonio, P.; Toscano, F.; Moretti, N.; De Iorio, N.; Fiorentino, C. Analysis of Chainsaw Emissions during Chestnut Wood Operations and Their Health Implications. *Appl. Sci.* **2024**, *14*, 2496. https://doi.org/10.3390/app14062496

Academic Editor: José Miguel Molina Martínez

Received: 19 February 2024
Revised: 5 March 2024
Accepted: 13 March 2024
Published: 15 March 2024

1. Introduction

The proliferation of portable equipment for urban green care, maintenance, and recreational activities has engendered significant challenges concerning operator safety and ergonomics [1]. These tools are frequently acquired online without the provision of any training prior to their utilization. Furthermore, in the forestry sector, despite the introduction of cutting-edge machinery and systems, the chainsaw remains unequivocally the primary apparatus employed for felling operations, delimbing logs, and segmenting timber into diverse assortments. The rationale behind this lies in the intricate topography of the Italian terrain. It is distinguished by a notable slope, which is even more pronounced within wooded regions, as lowland and hillside forests have long since relinquished their existence to agricultural land. Additionally, the majority of Italian forestry companies fall into the medium- or small-scale category, thereby often lacking the financial capacity to procure, depreciate, and manage state-of-the-art machinery. Another influential factor contributing to the presence of inadequate machinery fleets [2] is the organizational structure and composition of the forestry companies' wood capital. According to data derived from the RAF Italy 2017–2018 report, approximately 66% of forests nationwide are privately owned, while the remaining 34% are under public ownership. As far as private companies,

there exists a marked fragmentation of land ownership, compounded by the prevalence of broadleaf forests frequently subject to coppice management practices, thereby rendering the implementation of Harvester and analogous techniques rather arduous. Often, the presence of low-value woody capital results in management strategies that further increase the phenomena of soil degradation [3]. Moreover, Italian silviculture is primarily geared towards the production of low-value timber or, in some cases, biomass for energy purposes [4]. Consequently, the yield that can be extracted from the majority of Italian forests is not particularly lucrative, rendering it incompatible with management models predicated on advanced mechanization [5].

From the literature analysis, exponential growth in the number of publications in this area over the past five years is notable, indicating a significant level of interest within the scientific community regarding the discussed topic. Specifically, the issue of safety on forestry sites, which was previously predominantly regulated and monitored by public agencies, has now become a subject of research and experimentation, making it highly relevant.

The topic of chainsaw emissions, in particular, has historically received limited attention, at least until 2000. This partly explains the scarcity of available literature on the subject and the absence of standardized operating procedures for evaluating emissions in open-field conditions. Furthermore, a considerable proportion (~44%) of the specific contributions analysed pertain to the field of medicine rather than agricultural engineering.

Greater involvement of agricultural engineering in this field would obviously be desirable to integrate medical knowledge with the design and development of safer, more efficient, and ecologically sustainable chainsaws. Multidisciplinary collaboration between medicine, agricultural engineering, and other relevant disciplines could lead to more comprehensive and cutting-edge solutions to address the challenges associated with chainsaws.

The main objective of our research was the analysis of data on airborne pollutant and noise emissions during work activities conducted on forestry sites, with a focus on the respiratory safety of operators. This study aims to provide accurate information regarding the potential health risks and safety considerations for workers using chainsaws, contributing to informed decision-making and the development of appropriate safety measures and guidelines.

The specific objectives of the present work are as follows:

1. To assess the concentration of pollutants present in the exhaust gases of chainsaws with internal combustion engines, focusing on their impact on the respiratory health and safety of workers;
2. To evaluate the noise emitted by chainsaws with internal combustion engines during different activities involved in chestnut coppice utilization, with a particular emphasis on its impact on the respiratory health and safety of workers.

2. Material and Methods

2.1. Study Sites

The experiments were conducted within a chestnut coppice managed by the clear-cutting method. The experimental area was located in southern Italy, in Basilicata, in the municipality of Sassano ('Gravola'), at an altitude between 900 and 1000 m above sea level. The investigated silvicultural operations were as follows: felling (FE), delimbing (DE), and bucking (BU). All tests were conducted under clear weather conditions with light wind and an average temperature of 9 ± 3 °C. Experimental trials were conducted in accordance with current safety protocols and regulations. The sampling analysis lasted 8 working days. The measurements were conducted on 25 contiguous sample sites belonging to the same chestnut coppice forest. All operators had proven experience in site operations. The equipment was in good condition and carefully maintained. Precautions were taken to ensure the safety of researchers and operators involved in silvicultural operations. Attention was paid to the proper use of tools and equipment, as well as to the proper management of waste generated during the experimental activities. In addition, a preliminary analysis

of the terrain and surrounding ecosystem was conducted to assess the potential impact of silvicultural operations on the local soil, vegetation, and fauna.

2.2. Equipment

The experimental tests were carried out with a Husqvarna chainsaw model 357xp (Stockholm, Sweden). The instrumentation used was in perfect condition (sharpening, lubrication, etc.) and had 107 working hours prior to the experimental tests conducted for this work. On the market, it is possible to find a wide assortment of chainsaws, distinguished by individual characteristics and nominal powers [6]; the one chosen is designed for demanding cutting tasks and is among the most used in the forestry sites involved in the experimentation. The chainsaw is equipped with a 56.5 cm^3 engine with 3.2 kW of power, a recommended bar length of 40 cm, and a weight of 5.5 kg, which make it powerful but versatile for various applications. The chainsaw operates at a maximum speed of 9600 rpm and offers low levels of handle vibration (3.9/4.2 m/s^2). It produces sound power levels of 100 dB(A) and pressure levels of 112 dB(A). Additionally, it features a 0.68 L fuel tank and a 0.38 L oil tank, ensuring long-lasting operation without frequent refuelling or oil top-ups.

To evaluate the overall perception arising from complex sound or acoustic emissions, a Noise sensor TES 1355 dosimeter (TES Electrical Electronic Corp., Taipei, Taiwan) was employed, designed to replicate the response characteristics of the human auditory system. This dosimeter measures sound pressure levels and converts sound pressure levels into decibels. The experimental tests incorporated a TES 1355 dosimeter, encompassing a microphone, preamplifier, frequency weighting circuit, third-octave analysis capability, root mean square (RMS) circuit, analogue output, integrator circuit, and a comprehensive display system.

In order to assess the potential exposure of personnel to airborne pollutants emitted by chainsaw exhaust, a MultiRAE PGM-50 plus professional gas monitor (RAE Systems, San Jose, CA, USA) was employed. This programmable multi-gas monitor facilitates continuous real-time monitoring of toxic gases, oxygen levels, and combustible gases. The instrument detects and records the instantaneous concentration of gases in parts per million (ppm) for toxic gases, in percent volume (%vol) for oxygen, and in percent volume relative to the lower explosive limit (%vol of LEL) for combustible gases. The captured data were stored within the integrated data logger for subsequent analysis.

2.3. Data Collection

Noise measurements were conducted during the various silvicultural operations (FE, DE, and BU) on a sample of 30 trees. A total of 1260 observations were made, with 420 observations for each silvicultural operation. To capture a comprehensive range of scenarios encountered by operators, individuals with varying diametrical classes were included in the study. The dosimeter was directly affixed to the operator during chainsaw cutting operations to simulate the actual stress experienced by the auditory system (Figure 1). Such positioning ensured that data were acquired at a constant distance of 50 cm to 70 cm.

Specifically, the index of exceedance of exposure limits was calculated, both based on the recorded average values and the corresponding medians (Table 1). The following formula was employed to determine the indices:

$$i_{AV} = \frac{AV\ [\text{dB}]}{Lim\ [\text{dB}]} \quad (1)$$

$$i_{MED} = \frac{MED\ [\text{dB}]}{Lim\ [\text{dB}]} \quad (2)$$

where AV is the average value, MED refers to the median value of the variable, and Lim is the threshold established by law.

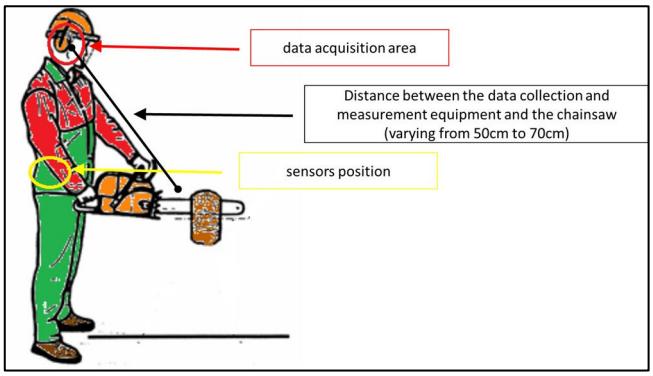

Figure 1. Operating scheme of data collection using Noise sensor TES 1355.

Table 1. Descriptive statistics for each type of machining and in relation to different diametric classes.

	DIAMETER (cm)	*AVERAGE*	*MEDIAN*	*MAX*	*SD*	*VARIANCE*	*CV*
FELLING	**5**	86.4	82.1	110.1	12.6	159.1	14.6
	7	88.4	83.8	111.3	87	162.1	14.4
	9	90.6	87	114.4	13	169.6	14.4
DELIMBING	**12**	90.8	89.8	110.9	13.6	185.5	15
	16	92.3	89.7	115.9	13.7	188.6	14.9
	18	94.9	96	116.5	14	196.1	14.8
BUCKING	**10**	90.7	90.5	108.9	12.4	154.1	13.7
	15	94.3	99.8	112.4	13.3	177.3	14.1
	20	101.5	107.6	122	14.3	204.8	14.1

For exhaust gas sampling, including CO, VOC, and C_6H_6, specialized clips were utilized to securely attach the instrumentation to the operator's belt (Figure 2). This approach yielded reliable results, as it ensured proximity between the gas analyser and the worker's mouth, which is a crucial requirement according to standards [7].

Figure 2. Operating scheme of data collection using gas emission sensor MultiRAE PGM-50.

Pollutants that are close to the operator's airway access are captured by a gentle current of air generated at the connecting tube port, to be transmitted to the sensor that provides data acquisition.

In this case, 432 measurements were taken on a sample of 30 trees, including 144 for each silvicultural operation. The collected data were clustered into 8 groups (one for each

day of data acquisition). Instantaneous measurements of the three gas emission variables were acquired at 15 min intervals throughout each processing phase (FE, DE, and BU).

In both cases, the descriptive statistics were calculated for each dataset, encompassing maximum values (V_{max}), minimum values (V_{min}), averages, and standard deviations for each time interval and work process. In particular, to estimate the variability of the parameters, the coefficient of variation was computed:

$$CV(\%) = \frac{\sigma\,[\mathrm{dB}]}{|\mu|[\mathrm{dB}]} \times 100 \quad (3)$$

where σ is the standard deviation and μ is the mean value of the variable.

The frequency of exceeding limits is given by the following formula:

$$f = 100 \times \left(\frac{Na}{Ntot} \right) \quad (4)$$

where *Na* are the readings above the threshold and *Ntot* is the total number of events.

3. Results and discussion

3.1. Noise Exposure

In order to assess the levels of acoustic pressure on the hearing apparatus of operators, a statistical analysis was carried out on a total sample of 1260 observations. For each operation, the three most representative diametric classes were identified:

1. Delimbing (DE): 5 cm; 7 cm; 9 cm;
2. Bucking (BU): 12 cm; 16 cm; 18 cm;
3. Felling (FE): 10 cm; 15 cm; 20 cm.

It should be noted that according to the current legislation in Italy (D.P.R. 81/2008), which is the Consolidated Law on occupational health and safety, the following weighted limits of exposure are set for workers operating on construction sites:

1. Lim1—80 dB (below this limit, there is no risk to the health of workers);
2. Lim2—85 dB (between 80 and 85 dB, the employer provides PPE, trains operators, and appoints a competent physician);
3. Lim3—87 dB (between 85 and 87 dB, workers are required to use PPE, health surveillance is activated, and workplaces must be properly cordoned off and marked).

Above 87 dB, measures are required to bring exposure below the limit value. Consolidation Act 81/2008 also sets peak values, that is, the maximum value of instantaneous sound pressure. These limits are as follows:

1. Lim1_peak: 135 dB;
2. Lim2_peak: 137 dB;
3. Lim3_peak: 140 dB.

For each diametric class related to a specific silvicultural operation, the following noise emission values (dB) were identified:

1. Average of the sound emission values;
2. Median of the sound emission values;
3. Maximum sound emission value recorded;
4. Standard deviation;
5. Coefficient of variability.

The analysis of the data from the various samples revealed coefficients of variation (CVs) below 15 percent. This indicates moderate relative variability from the mean, suggesting a good quality of the data acquisition methodology. Consequently, the mean and median values can serve as reliable indicators for conducting further analyses. Table 1 presents the descriptive statistics for each silvicultural operation and for each diametric class.

It is evident from Table 2 that the legal limits are consistently exceeded, and this situation is further exacerbated by the lack of proper personal protective equipment at forestry sites [8]. However, it is worth noting that the recorded values do not come close to the peak values mandated by law.

Table 2. Exceedance rates of noise thresholds stipulated by current Italian regulations.

	DIAMETER (cm)	$\frac{AV}{Lim1}$	$\frac{AV}{Lim2}$	$\frac{AV}{Lim3}$	$\frac{MED}{Lim1}$	$\frac{MED}{Lim2}$	$\frac{MED}{Lim3}$
FELLING	5	1.08	1.02	0.99	1.03	0.97	0.94
	7	1.10	1.04	1.02	1.05	0.99	0.96
	9	1.13	1.09	1.04	1.09	1.02	1.00
DELIMBING	12	1.13	1.07	1.04	1.12	1.06	1.03
	16	1.15	1.09	1.06	1.12	1.06	1.03
	18	1.19	1.12	1.09	1.20	1.13	1.10
BUCKING	10	1.13	1.07	1.04	1.13	1.20	1.04
	15	1.18	1.11	1.08	1.25	1.17	1.15
	20	1.27	1.19	1.17	1.35	1.27	1.24

Further investigations have been conducted to provide a more detailed understanding of the dynamics present in these contexts.

Values exceeding 1 indicate the surpassing of the analysed critical threshold, along with a percentage indicator relative to the threshold itself. For instance, in the case of felling operations on logs with a diameter falling within the 7 cm class, an exceedance of 10% for Lim1 is reported. The percentage of exceedance ranges from 8% to 27%, with an average of 11% for DE, 19% for FE, and 16% for BU, in relation to Lim1. It is important to emphasize that even small differences of a few dB in noise levels can result in a significant increase in perceived noise intensity. Noise is measured on a logarithmic scale, where a 3 dB increase corresponds to a doubling of perceived noise intensity.

Figure 3 shows the comparison between the average values of sound emissions detected for each diametric class, along with the respective legal limits (a–c). Additionally, it presents the maximum recorded values for each diametric class, along with the corresponding peak limit set by law (d).

The analysis also confirms that in at least 50 percent of the activities the limits imposed by current regulations are exceeded. The rate at which the thresholds, set by current regulations, are exceeded for each individual operation and for each diametric class were calculated; the results are shown below, in Table 3.

Table 3. Frequencies of exceeding legal limits for each type of processing and for each diametric class.

	DIAMETER (cm)	*Rate_Lim1* (%)	*Rate_Lim2* (%)	*Rate_Lim3* (%)
FELLING	**5**	57	44	44
	7	64	48	46
	9	69	52	50
DELIMBING	**12**	69	54	52
	16	76	65	58
	18	77	64	63
BUCKING	**10**	65	56	54
	15	74	66	64
	20	83	79	76

In relation to Lim1, during DE operations, the exceedance rate varies from 57% for the smallest diameter trees to 69% for the largest diameters. Similarly, for FE and BU operations, the rates vary from 65% to 83% and 69% to 77%, respectively. Even considering the other statutory limits (Lim2 and Lim3, where operators should wear hearing protectors), the

recorded rates show major criticalities for workers' health and safety, being on average at 48% and 47% for DE, 67% and 65% for FE, and 61% and 58% for BU. The analysis highlights not only that the thresholds are regularly disregarded, but that this dynamic is prevalent during the majority of construction operations.

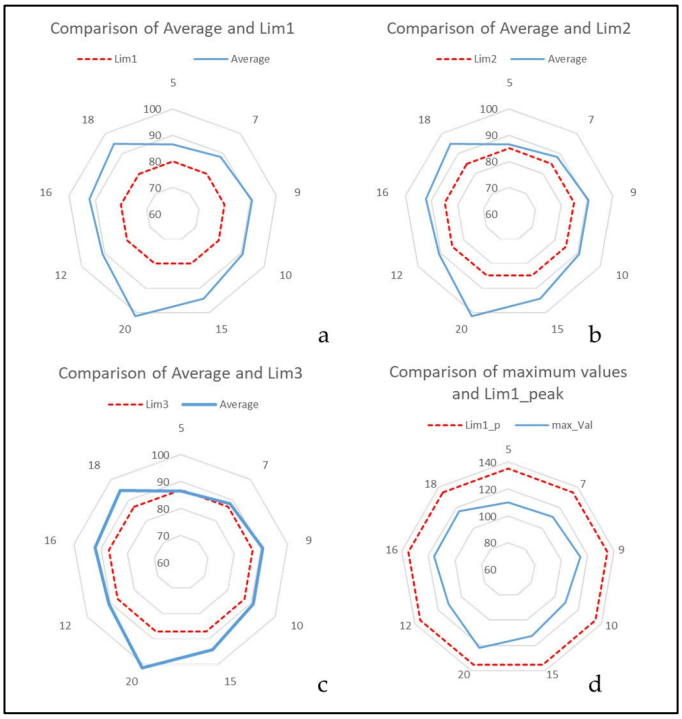

Figure 3. Comparisons between the average noise values measured for each diametric class and the relevant legal limits (**a**–**c**). Comparisons between the maximum values recorded for each diametric class and the relevant peak limits set by law (**d**).

3.2. Exposure to Airborne Pollutants

Table 4 shows the average values of the maximum detections obtained in each of the eight repeated measurements, along with the corresponding mean values of the same measurements. The table also includes the relative standard deviations (SDs) and coefficients of variation (CVs) for the measurements.

Table 4. Gas emissions detected during the different cutting operations.

	MED (Max)			**SD (Max)**			**CV (Max)**		
	CO	**VOC**	**C_6H_6**	**CO**	**VOC**	**C_6H_6**	**CO**	**VOC**	**C_6H_6**
Felling—FE	135.96	17.28	2.51	25.75	4.63	0.48	0.19	0.27	0.19
Delimbing—DE	33.09	2.65	1.13	11.15	1.07	0.21	0.34	0.40	0.18
Bucking—BU	76.26	15.24	1.73	11.31	4.12	0.55	0.15	0.27	0.32
	MED (Av)			**SD (Av)**			**CV (Av)**		
	CO	**VOC**	**C_6H_6**	**CO**	**VOC**	**C_6H_6**	**CO**	**VOC**	**C_6H_6**
Felling—FE	36.66	2.81	1.16	16.09	2.18	0.26	0.44	0.78	0.22
Delimbing—DE	20.21	0.60	0.76	5.02	0.44	0.33	0.25	0.73	0.43
Bucking—BU	27.08	0.96	0.98	1.92	0.57	0.28	0.07	0.59	0.29

Figure 4 shows the average concentrations of CO, VOC, and C_6H_6 detected during each of the eight time intervals monitored for each process by using the Multi-RAE PGM-50 plus professional gas detector. The graphs also display the legally established emission

limits. The graphical representations reveal noticeable changes in the measured variables, particularly in the emissions observed during the FE phase.

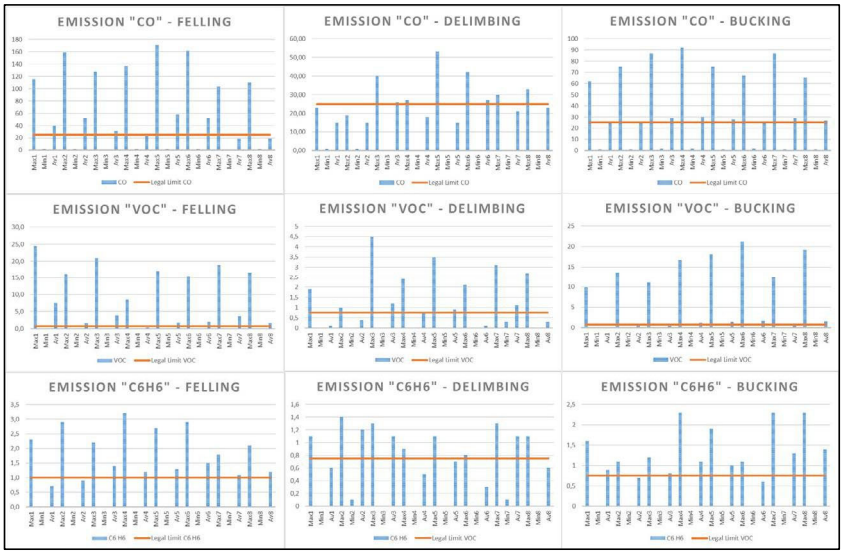

Figure 4. Average CO, VOC, and C_6H_6 (ppm) emissions detected in each reference interval. The red line represents the legal limits for each machining operation.

To assess the variability of the data, the average of the maximum values was considered more reliable, despite the potential presence of momentary peaks. This choice is justified because during the period of 15 min of constant detection, the chainsaw engine often remains running without actively cutting. In line with this rationale, the coefficients of variation calculated on the maximum values were relatively low, whereas those calculated on the averages exhibited higher values (as shown in Table 5). The coefficients of variation were particularly higher for delimbing operations compared to other cases. This variability can be attributed to the significant diameter variations observed among branches of the same tree. The coefficients of variation computed on the average values were generally high, except for CO emissions during BU (bucking) operations, which showed a CV value of 7%.

Table 5. Comparison between gaseous emissions measured in the field during wood processing and the imposed thresholds.

	L _Leg (ppm			$\frac{\text{MED(Max)}}{Lim\_Leg}$			$\frac{\text{MED(Vm)}}{Lim\_Leg}$		
	CO	**VOC**	**C_6H_6**	**CO**	**VOC**	**C_6H_6**	**CO**	**VOC**	**C_6H_6**
FE—Felling	25	0.75	1	5.44	23.03	2.51	1.47	3.75	1.16
DE—Delimbing	25	0.75	1	1.32	3.53	1.13	0.81	0.8	0.76
BU—Bucking	25	0.75	1	3.05	20.3	1.73	1.08	1.28	0.98

Table 5 shows that the maximum values observed during the three different interventions significantly exceeded the thresholds established by international regulations. However, observing the average values, the situation appears less critical. It should be highlighted that maximum emission values are rarely reached in the experimental time intervals during the various operations. Bucking operations (BU) showed average emissions lower than the threshold, and DE operations recorded values slightly higher and close to the limits. The most critical scenario occurred during Forest Extraction (FE) operations, with emissions exceeding the permitted threshold, in particular for volatile organic compounds (VOCs). These results highlight the greater need to use personal protective equipment

(PPE) to safeguard the respiratory system, especially during the FE phase. During this phase, in fact, a significant risk emerged for operators' health and safety.

A comparison between the average of the maximum values and the average values obtained during field operations is shown in Table 5. The presence of consistent peaks in VOC emissions for all three operations is evident. In particular, during FE operations, the maximum values recorded were approximately 16 times higher than the corresponding average values.

The results found in the present work are in accordance with those of Neri et al. [9]. Indeed, work operations, from the point of view of the chainsaw required effort, can be characterized differently depending on the emissions of CO and C_6H_6. During felling, the high emissions of CO and C_6H_6 are linked to the greater efforts of the chainsaw. However, important intervals of inactivity are recorded in the sampling interval of 15 min, and this depends both on the technical/operational characteristics linked to the particular activity (FE, DE, and BU) and on the specific fatigue of the operator. During cutting, the chainsaw is subjected to medium efforts; the high CO and C_6H_6 emissions are probably due to the shorter time intervals in which the chainsaw is on but not cutting than the previous operation (FE). During delimbing, the chainsaw makes small efforts, releasing moderate quantities of CO and C_6H_6 into the environment; furthermore, the intervals in which the engine is on but not running during the 15 min of detection are extremely reduced compared to previous operations. The chainsaw, in accordance with Kováč et al. [10], produces high VOC emissions when it is switched on but not operating at the cut. During the logging operations, the following can be observed:

1. The maximum emissions recorded, 17.28 ppm for FE and 15.24 ppm for BU, are similar, and higher in the abatement phase;
2. The average emissions recorded during FE (2.81 ppm) and BU (0.96 ppm) operations are very different, 2.9 times higher in the abatement phase;
3. The high risk of exposure occurs in the abatement phase, when VOC emissions are particularly higher than the threshold;
4. The lowest-risk situation, on the other hand, occurs during delimbing operations when the chainsaw's non-working intervals are minimal.

3.3. Health Implications

The chainsaw is currently the predominant machine used in the forestry sector. Workers engaged in moto-manual chainsaw operations face unfavourable environmental conditions that may adversely affect their long-term occupational health [11]. Both professional and consumer chainsaws are equipped with two-stroke engines, which have distinct advantages over four-stroke engines. This technology, although simpler and less expensive to produce than the other, offers a lower weight/power ratio and can be used in various positions, such as vertical, horizontal, or lateral [12]. Extensive investigations carried out systematically since the 1960s have unveiled numerous critical concerns associated with the persistent and continuous use of such portable equipment. In addition, concerning the results of the present study, motorized and manual forestry operations are intrinsically characterized by elevated hazard rates [13]. The analyses indeed highlight significant exceeding of the thresholds set by law in terms of both noise and gaseous emissions. Prolonged exposure to these physical and chemical agents [14] is the main cause of various occupational diseases.

Furthermore, our analysis conforms to numerous studies showing that chainsaws can emit noise levels above 90 dB(A) [15], thus posing a significant risk of hearing damage to operators [16]. The vibrations transmitted to the hand–arm system, in turn, cause irreversible damage to the peripheral circulatory system of the hands, leading to capillary rupture and the onset of Raynaud's syndrome, or 'white fingers' disease [17]. Despite the critical nature of these issues, there is extremely limited scientific literature explicitly addressing airborne pollutant emissions from machinery such as chainsaws [9] and specifically forestry operator exposure to BTEX and PAHs [18]. Both temporary and chronic harm, resulting from the

inhalation of exhaust gases emitted by chainsaws and brush-cutters, have been hitherto considered in broad and generalized terms, often compared to those encountered in other contexts involving the use of hand-guided power tools such as lawnmowers and motor-hoes. The literature on exhaust emissions during harvesting has often focused on laboratory tests. Field operational tests are a recently developed approach, but they are essential for determining emissions based on actual engine or vehicle conditions [19]. Several studies have explored related issues, albeit with different methodologies. Ref. [20] undertook an examination of the composition of chainsaw engine exhaust emissions, concentrating on the chemical constituents present. However, the monitoring of operators' exposure to emissions and therefore the assessment of the actual implications and risks linked to the health of the operators have been neglected. Baldauf et al. [21] conducted an assessment of the occupational exposure to airborne contaminants experienced by operators engaged in activities within urban and peri-urban green areas. However, their study did not explicitly differentiate between different tools employed, including brush-cutters and chainsaws. Dimou et al. [22] proposed a comparison of the exhaust emissions of nitrogen monoxide and methane produced by the engines of two conventional chainsaws (one professional and one amateur) with those produced by a catalytic one. Other authors [23] adopted a distinct approach by monitoring the occupational exposure of loggers to chainsaw exhaust emissions. In [24], the measurement of carboxyhemoglobin levels was utilized as an indicator of exposure to exhaust emissions. Other elements, such as the demanding nature of chainsaw tasks, contribute significantly to operator fatigue [25], increasing the heart rate and consequently accelerating breathing, potentially leading to a respiratory rate above 60 litres per minute. This further aggravates the operator's exposure to airborne pollutants, comprising both combustion gases and the non-combusted fraction expelled along with residual residues (approximately 30% of the initial mixture utilized in two-stroke engines). Several combustion products, including BTEX (benzene, toluene, ethylbenzene, and total xylenes), have negative impacts on the lower respiratory system [26] and central nervous system [27]. Studies by [28,29] showed that PAHs (polycyclic aromatic hydrocarbons) can be present either in the particulate form or associated with the gas phase in diluted exhaust gases. The present study analyses the emissions of a chainsaw in relation to work-site safety during forestry activity in a chestnut coppice. To address these critical concerns, a series of national and EU legislative measures have been implemented over the past few decades to regulate permissible exposure levels and prescribe preventive measures to be employed accordingly. One of the most pivotal and current Italian regulations in the occupational health and safety domain is Legislative Decree No. 81 of 9 April 2008, commonly referred to as the 'Consolidation Act on Health and Safety in the Workplace'. This innovative and continually updated legislation aims to restructure and integrate all pertinent regulations in a comprehensive manner, reflecting the progressive nature of the field.

4. Conclusions

In the present study, we proposed a comprehensive analysis of noise and gaseous emissions from a chainsaw during silvicultural operations on a chestnut coppice. The analysis of worker exposure to the noise produced by the chainsaw in the different operational phases (FE, DE, and BU) and for the different diametric classes showed strong criticalities for health and safety. The exposure limits set by the Italian regulations are almost never respected. The issue becomes more complex considering the low propensity of operators and employers in the training, use, and maintenance of PPE. The noise emission levels, despite the use of PPE contributing considerably to mitigating the acoustic pressure on workers' hearing apparatus, were higher than the specific thresholds (Lim2 and Lim3) in at least 50% of cases.

The risk assessment of workers' exposure to airborne pollutants is alarming. The computation of individual exposure based on measurements obtained during the sampling process showed, according to current regulations, that few operational situations reveal a moderate limit for carbon monoxide (CO) emissions. In all other samplings, the chemical

risk associated with CO, VOC (volatile organic compound), and benzene inhalation was found to be non-moderate. The felling operation (FE) proved to be the most critical activity for carbon monoxide emissions.

Author Contributions: Conceptualization, P.D., F.T. N.M. and C.F.; methodology, F.T. and C.F.; software, F.T.; validation, C.F. and P.D.; formal analysis, F.T., N.D.I. and P.D.; investigation, F.T.; resources, P.D. and F.T.; data curation, F.T. and C.F.; writing—original draft preparation, P.D., F.T. and C.F.; writing—review and editing, P.D. and F.T.; visualization, C.F.; supervision, P.D. and C.F.; project administration, P.D. and C.F.; funding acquisition, P.D. All authors have read and agreed to the published version of the manuscript.

Funding: This research received no external funding.

Institutional Review Board Statement: Not applicable.

Informed Consent Statement: Informed consent was obtained from all subjects involved in the study.

Data Availability Statement: The data presented in this study are available on request from the corresponding author.

Acknowledgments: This work was realized as part of a collaboration between the University of Basilicata and 'Casa delle Tecnologie Emergenti di Matera, Laboratorio del Giardino delle tecnologie emergenti—CTEMT'. Activities were conducted in the framework of the PSR 16.2 'SMART IRRIFERT' project CUP: G19J21004870006.

Conflicts of Interest: The authors would like to hereby certify that there are no conflicts of interest in the data collection, analyses, and interpretation in the writing of the manuscript, or in the decision to publish the results. The authors would also like to declare that the funding of the study has been supported by the authors' institutions.

Abbreviations

FE	Felling
DE	Delimbing
BU	Bucking
CO	Carbon monoxide
VOC	Volatile organic compounds
C_6H_6	Benzene
AV	Average noise
MED	Median
Lim	Law Limit
iAV	Average index
iMED	Median index
σ or *SD*	Standard deviation
μ	Average pollutants
CV	Coefficient of variation
BTEX	Benzene, toluene, ethylbenzene, and Xylenes
PAHs	Polycyclic aromatic hydrocarbons
PPE	Personal protective equipment

References

1. Toscano, F.; D'Antonio, P.; D'Antonio, C.; De Iorio, N.; Modugno, F.; Fiorentino, C. Experimental Analysis of Chainsaw Emissions in Chestnut Wood Operations. *Lect. Notes Civ. Eng.* **2023**, *337*, 957–965.
2. Fiorentino, C.; Crimaldi, M.; Libergoli, P.; D'Antonio, P.; Scalcione, V. Farm Management Information Systems: Digital Register of Farm Management in Southern Italy. *Lect. Notes Civ. Eng.* **2022**, *252*, 337–354.
3. AbdelRahman, M.A.E.; Metwalli, M.R.; Gao, M.; Toscano, F.; Fiorentino, C.; Scopa, A.; D'Antonio, P. Determining the Extent of Soil Degradation Processes Using Trend Analyses at a Regional Multispectral Scale. *Land* **2023**, *12*, 855. [CrossRef]
4. D'Antonio, P.; D'Antonio, C.; Evangelista, C.; Doddato, V. The assessment of the sawmill noise. *J. Agric. Eng.* **2013**, 44. [CrossRef]
5. Di Marzio, N. An Overview of Forest Cover and Management in Italy. *Nova Meh. Šumarstva* **2020**, *41*, 63–71. [CrossRef]

6. Da˛browski, A. Analysis and Laboratory Testing of Technical Injury Prevention Measures for Portable Combustion Chainsaws. *Forests* **2020**, *11*, 276. [CrossRef]
7. Dimou, V.; Anezakis, V.D.; Demertzis, K. Comparative analysis of exhaust emissions caused by chainsaws with soft computing and statistical approaches. *Int. J. Environ. Sci. Technol.* **2018**, *15*, 1597–1608. [CrossRef]
8. Albizu-Urionabarrenetxea, P.; Tolosana-Esteban, E.; Roman-Jordan, E. Safety and health in forest harvesting operations. Diagnosis and preventive actions. A review. *For. Syst.* **2013**, *22*, 392–400. [CrossRef]
9. Neri, F.C.; Foderi, A.; Laschi, F.; Fabiano, M.; Cambi, G.; Sciarra, M.C.; Aprea, A.; Cenni, E.; Marchi, M. Determining exhaust fumes exposure in chainsaw operations. *Environ. Pollut.* **2016**, *218*, 1162–1169. [CrossRef]
10. Kovác˘, J.; Krilek, J.; Dado, M.; Beno, P. Investigating the influence of design factors on noise and vibrations in the case of chain-saws for forestry work. *FME Trans.* **2018**, *46*, 513–519. [CrossRef]
11. Ålander, T.; Antikainen, E.; Raunemaa, T.; Elonen, E.; Rautiola, A.; Torkkell, K. Particle Emissions from a Small Two-Stroke Engine: Effects of Fuel, Lubricating Oil, and Exhaust Aftertreatment on Particle Characteristics. *Aerosol Sci. Technol.* **2005**, *39*, 151–161. [CrossRef]
12. Nuti, M. *A Variable Timing Electronically Controlled High Pressure Injection System for 2T S.I. Engines*; SAE Technical Paper 900799; SAE International: Warrendale, PA, USA, 1990. [CrossRef]
13. Micheletti Cremasco, M.; Giustetto, A.; Caffaro, F.; Colantoni, A.; Cavallo, E.; Grigolato, S. Risk Assessment for Musculoskeletal Disorders in Forestry: A Comparison between RULA and REBA in the Manual Feeding of a Wood-Chipper. *Int. J. Environ. Res. Public Health* **2019**, *16*, 793. [CrossRef] [PubMed]
14. Rukat, W.; Barczewski, R.; Jakubek, B.; Wróbel, M. The comparison of vibro-acoustic impact of chainsaws with electric and combustion drives. In Proceedings of the 17th International Conference Diagnostics of Machines and Vehicles, MATEC Web of Conferences, Bydgoszcz, Poland, 30 July 2018; p. 02020. [CrossRef]
15. Neri, F.; Laschi, A.; Bertuzzi, L.; Galipò, G.; Frassinelli, N.; Fabiano, F.; Marchi, E.; Foderi, C.; Marra, E. A Comparison between the Latest Models of Li-Ion Batteries and Petrol Chainsaws Assessing Noise and Vibration Exposure in Cross-Cutting. *Forests* **2023**, *14*, 898. [CrossRef]
16. Iftime, M.D.; Dumitrascu, A.E.; Ciobanu, V.D. Chainsaw operators' exposure to occupational risk factors and incidence of professional diseases specific to the forestry field. *Int. J. Occup. Saf. Ergon.* **2022**, *28*, 8–19. [CrossRef] [PubMed]
17. Tavares Jesus, A.; Fiedler, N.C.; de Assis do Carmo, F.C.; Silva Juvanhol, R. Exposure of operators to chainsaw vibration in forest harvesting. *Floresta* **2020**, *50*, 1653–1659. [CrossRef]
18. Magagnotti, N. Exposure of Mobile Chipper Operators to Diesel Exhaust. *Ann. Occup. Hyg. March* **2014**, *58*, 217–226. [CrossRef]
19. Lijewski, P.; Merkisz, J.; Fuc´, P. Research of exhaust emissions from a harvester diesel engine with the use of portable emission measurement system. *Croat. J. Eng.* **2013**, *34*, 113–122.
20. Magnusson, R.; Nilsson, C.; Andersson, K.; Andersson, B.; Gieling, R.; Wiberg, K.; Östman, C.; Rannug, U. Determination of Chemical Composition and Mutagenicity in Particles from Chainsaw Exhaust. Experimental Set-Up, Stability and Results from Two Different Fuels. *Environ. Technol.* **2000**, *21*, 819–829. [CrossRef]
21. Baldauf, R.; Fortune, C.; Weinstein, J. Air contaminant exposures during the operation of lawn and garden equipment. *J. Expo. Sci. Environ. Epidemiol.* **2006**, *16*, 362–370. [CrossRef]
22. Dimou, V.; Kantartzis, A.; Malesios, C.; Kasampalis, E. Research of exhaust emissions by chainsaws with the use of a portable emission measurement system. *Int. J. For. Eng.* **2019**, *30*, 228–239. [CrossRef]
23. Bünger, J.; Bombosch, F.; Mesecke, U.; Hallier, E. Monitoring and Analysis of Occupational Exposure to Chain Saw Exhausts. *Am. Ind. Hyg. Assoc. J.* **1997**, *58*, 747–751. [CrossRef] [PubMed]
24. Hooper, B.; Parker, R.; Todoroki, C. Exploring chainsaw operator occupational exposure to carbon monoxide in forestry. *J. Occup. Environ. Hyg.* **2017**, *14*, D1–D12. [CrossRef] [PubMed]
25. Hinze, A.; König, J.L.; Bowen, J. Worker-fatigue contributing to workplace incidents in New Zealand Forestry. *J. Saf. Res.* **2021**, *79*, 304–320. [CrossRef] [PubMed]
26. Moskal, A.; Makowski, L.; Sosnowski, T.R.; Gradoń, L. Deposition of Fractal-Like Aerosol Aggregates in a Model of Human Nasal Cavity. *Inhal. Toxicol.* **2006**, *18*, 725–731. [CrossRef]
27. Oberdörster, G.; Sharp, Z.; Atudorei, V.; Elder, A.; Gelein, R.; Kreyling, W.; Cox, C. Translocation of Inhaled Ultrafine Particles to the Brain. *Inhal. Toxicol.* **2004**, *16*, 437–445. [CrossRef]
28. Westerholm, R.N.; Alsberg, T.E.; Frommelin, A.B.; Strandell, M.E.; Rannug, J.U.; Winquist, L.; Grigoriadis, V.; Egebaeck, E.K. Effect of fuel polycyclic aromatic hydrocarbon content on the emissions of polycyclic aromatic hydrocarbons and other mutagenic substances from a gasoline-fuelled automobile. *Environ. Sci. Technol.* **1988**, *22*, 925–930. [CrossRef]
29. Westerholm, R.N.; Almen, J.; Li, H.; Rannug, J.U.; Egebaeck, K.E.; Graegg, K. Chemical and biological characterization of particulate-, semivolatile-, and gas-phase-associated compounds in diluted heavy-duty diesel exhausts: A comparison of three different semivolatile-phase samplers. *Environ. Sci. Technol.* **1991**, *25*, 332–338. [CrossRef]

Smart Sensors and Artificial Intelligence Driven Alert System for Optimizing Red Peppers Drying in Southern Italy

Costanza Fiorentino, Paola D'Antonio, Francesco Toscano, Nicola Capece, Luis Alcino Conceição, Emanuele Scalcione, Felice Modugno, Maura Sannino, Roberto Colonna, Emilia Lacetra and Giovanni Di Mambro

Pubblicazione: Rivista Sustainability, editore MDPI (Volume 17, Issue 4, Articolo 1682, Anno 2025)
https://doi.org/10.3390/su17041682

sustainability

MDPI

Article

Smart Sensors and Artificial Intelligence Driven Alert System for Optimizing Red Peppers Drying in Southern Italy

Costanza Fiorentino [1,*], Paola D'Antonio [1,*], Francesco Toscano [1], Nicola Capece [2], Luis Alcino Conceição [3], Emanuele Scalcione [4], Felice Modugno [1], Maura Sannino [5], Roberto Colonna [2,6], Emilia Lacetra [1] and Giovanni Di Mambro [7]

1 Department of Agriculture, Forest, Food and Environmental Sciences, University of Basilicata, Via dell'Ateneo Lucano, 10, 85100 Potenza, Italy; francesco.toscano@unibas.it (F.T.); fely.mod@gmail.com (F.M.); emilialacetra@gmail.com (E.L.)
2 Department of Engineering, University of Basilicata, Via dell'Ateneo Lucano, 10, 85100 Potenza, Italy; nicola.capece@unibas.it (N.C.); roberto.colonna@unibas.it (R.C.))
3 VALORIZA—Research Center for Endogenous Resource Valorization, Polytechnic Institute of Portalegre, 7300-110 Portalegre, Portugal; luis_conceicao@ipportalegre.pt
4 Lucanian Agency of Innovation and Development in Agriculture (ALSIA), Via Annunziatella, 75100 Matera, Italy; emanuele.scalcione@alsia.it
5 Department of Agricultural Sciences, University of Naples Federico II, Via Università, 100, Portici, 80055 Naples, Italy; maura.sannino2@unina.it
6 Space Technologies and Applications Centre (STAC), Satellite Application Centre (SAC), 85100 Potenza, Italy
7 Elaisian SRL, Via Ostiense, 92, 00154 Roma, Italy; giovanni.dimambro@elaisian.com
* Correspondence: costanza.fiorentino@unibas.it (C.F.); paola.dantonio@unibas.it (P.D.)

Abstract: The Senise red pepper, known as peperone crusco, is a protected geographical indication (PGI) product from Basilicata, Italy, traditionally consumed dried. Producers use semi-open greenhouses to meet PGI standards, but significant losses are caused by rot from microorganisms thriving in high moisture, temperature, and humidity, which also encourage pest infestations. To minimize losses, a low-cost alert system was developed. The study, conducted in summer 2022 and 2023, used external parameters from the ALSIA Senise weather station and internal sensors monitoring the air temperature and humidity inside the greenhouse. Since rot is complex and difficult to model, an artificial intelligence (AI)-based approach was adopted. A feed forward neural network (FFNN) estimated greenhouse climate conditions as if it were empty, comparing them with actual values when peppers were present. This revealed the most critical period was the first 3–4 days after introduction and identified a critical air relative humidity threshold. The system could also predict microclimatic parameters inside the greenhouse with red peppers, issuing warnings one hour before risk conditions arose. In 2023, it was tested by comparing predicted values with previously identified thresholds. When critical levels were exceeded, greenhouse operators were alerted to adjust conditions. In 2023, pepper rot decreased.

Keywords: red pepper; weather station; machine learning; smart sensors; greenhouse

Academic Editors: Pawel Sobczak, Jacek Mazur, Piotr Markowski and Andrzej Anders

Received: 9 January 2025
Revised: 10 February 2025
Accepted: 12 February 2025
Published: 18 February 2025

Citation: Fiorentino, C.; D'Antonio, P.; Toscano, F.; Capece, N.; Conceição, L.A.; Scalcione, E.; Modugno, F.; Sannino, M.; Colonna, R.; Lacetra, E.; et al. Smart Sensors and Artificial Intelligence Driven Alert System for Optimizing Red Peppers Drying in Southern Italy. *Sustainability* **2025**, *17*, 1682. https://doi.org/10.3390/su17041682

1. Introduction

1.1. Problem Statement and Context

Since ancient times, humans have relied on solar drying as a natural and effective way to preserve agricultural and animal products. This method leverages the sun, a free and renewable energy source, to remove moisture and extend the life of these products. The Senise red pepper belongs to this category of products, and due to its characteristics and properties, it has obtained a PGI (protected geographical indication) designation

from the Basilicata region. Traditionally, it was dried during the summer months by threading peppers into necklaces and hanging them under porticoes or balconies during the summer months. Today, Senise peppers are not only consumed locally but also distributed throughout Europe, with a growing local demand due to increased tourism. Consequently, producers cannot remain tied to traditional drying methods but must adapt their systems to meet today's business needs (quantity, quality, traceability, and healthiness of production). The economy of the Basilicata region, centered around its premium products, is founded on the high natural value of the territories, from which the stringent PGI regulations originate [1]. Current rules require that the peppers be dried in open-air environments, allowing only lightweight coverings that facilitate ventilation and can be easily removed. This effectively excludes the use of modern smart greenhouses equipped with automated systems to regulate the temperature, humidity, and ventilation. Many producers face significant challenges during the drying process, with some reporting losses exceeding 20% and, in extreme cases, up to 60% of the dry matter. Factors contributing to these losses include poor handling practices, suboptimal production methods, and inadequate storage facilities. Spoilage is primarily caused by microorganisms that thrive in the high moisture content of vegetables. Moreover, high temperature and relative humidity gradients can accelerate rot and create conditions conducive to pest and insect attacks [2]. The objective of the present study was to develop a low-cost monitoring system that complied with existing drying regulations while minimizing farmers' losses. The research focused on optimizing greenhouse production and drying methods, prioritizing sustainability and product quality. Technological advancements, such as the Internet of Things (IoT), cloud computing, and big data analytics, are increasingly integrated into agricultural practices. These tools enable the development of new process control systems, innovative services, and higher-quality products [3,4]. Real-time data analysis is critical for addressing complex challenges, such as complying with regulations, minimizing losses, optimizing timelines, and ensuring quality [5]. Advanced multivariate methodologies are necessary to achieve these objectives [6].

1.2. Current Advances and Relevance to the Problem

Modeling the greenhouse microclimate depends on its intended application and can involve two main categories of models: physical models, which study the behavior and interactions of monitored parameters, and black-box models. Physical models analyze the relationships between variables and their behavior but can be challenging to develop due to the nonlinear dynamics involved [7–9]. Conversely, black-box models rely on input–output data to bypass these complexities and deliver reliable results without requiring detailed knowledge of the underlying physical processes [10]. To develop black-box models, a training and testing dataset is required, along with the appropriate model structure and parameterization [11]. Given the complex interactions between internal and external climatic variables, a black-box approach using AI and neural networks is the most suitable solution. The integration of artificial intelligence and Internet of Things technologies in smart greenhouses is transforming modern agriculture. These advanced systems enhance productivity, resource management, and sustainability [12]. Through AI-driven automation, environmental parameters such as air temperature and relative humidity can be controlled with remarkable precision [13]. Additionally, IoT-enabled wireless sensors allow for continuous, real-time data monitoring and analysis [14]. Smart greenhouses have demonstrated the ability to achieve targeted temperature settings with 90% accuracy and provide highly accurate humidity level estimations [15]. Data from multiple sensors are centralized and managed through cloud-based platforms, enabling remote monitoring and system adjustments [14,16]. Machine learning techniques, particularly artificial neural

networks (ANNs), play a critical role in modeling complex drying processes and facilitating both real-time monitoring and process control [17]. These methods are also used to improve product quality metrics [18]. AI applications in smart greenhouses extend to various tasks, including automated pesticide spraying, efficient irrigation management, and pest identification using image processing technologies [12]. IoT-based monitoring systems further enhance efficiency by collecting temperature and humidity data in real time, enabling improved decision-making and operational optimization, particularly in industrial drying processes [19]. AI-powered systems are increasingly employed to refine greenhouse climate management and drying procedures. AI controllers can simulate and regulate complex variables, such as temperature and humidity, ensuring stable growing or drying environments [20]. For instance, in AI-enhanced greenhouses, temperature predictions achieve a 90% accuracy rate, while humidity levels are estimated with comparable precision [13]. By considering the enhancements in the farming system for tobacco crops [21], in the tobacco drying process, ANNs have been utilized to forecast temperature and humidity, with prediction errors consistently below 2% [22]. Choi et al. [23] developed an MLP neural network using external and internal greenhouse conditions as input variables. The model successfully predicted indoor temperature and relative humidity for intervals ranging from 10 to 120 min. The neural network employed four hidden layers and a variable number of nodes for predicting temperature and humidity separately. Similarly, Petrakis [24], in a 2022 study, introduced an ANN-based model capable of predicting indoor greenhouse conditions, including temperature and humidity, based on factors such as external temperature, wind speed, solar radiation, and prior internal conditions. The model provided accurate predictions up to 30 min in advance. Multiple studies have demonstrated the effectiveness of ANNs in estimating temperature and humidity within greenhouses [25–27]. Various ANN architectures, including multilayer perceptron (MLP), recurrent neural networks with long short-term memory (RNN-LSTM), and nonlinear autoregressive exogenous (NARX) models, have been employed for this purpose [25,27]. RNN-LSTM models have shown particularly high accuracy in predicting temperature and humidity over extended time periods [25]. Several studies have explored the use of artificial neural networks (ANNs) for predicting temperature and humidity in greenhouses. Feed forward neural networks (FFNNs) have shown promising results in estimating these parameters [28]. These findings suggest that ANNs can be valuable tools for precise greenhouse management and climate control.

1.3. Research Challenges and Objective

The research aimed to develop a low-cost alert system to monitor microclimatic variations inside the drying greenhouse and prevent spoilage. Due to the complexity of rot formation and the constraints imposed by PGI regulations, commercially available smart greenhouses are not suitable for drying Senise peppers. To address this, the study employed an FFNN, to analyze climate data from IoT sensors inside the greenhouse and external meteorological data from the ALSIA Senise weather station.

The primary objectives of this study were as follows:

(1) To design and implement an AI-based system capable of predicting the air temperature and relative humidity fluctuations inside the greenhouse;
(2) To identify critical humidity thresholds that contribute to pepper spoilage;
(3) To develop an early warning system that notifies operators one hour before critical conditions arise.

By achieving these objectives, the study sought to enhance the efficiency and sustainability of the drying process, reducing economic losses for producers.

The present study highlights the importance of AI-enhanced monitoring systems in addressing weather variability, a longstanding challenge in agro-food production. The developed warning system aligns with regulatory requirements while optimizing decision-making through real-time meteorological data and predictive models, enhancing both sustainability and efficiency. While no scientific evidence currently links the discussed issues to climate change, climatic variations in the Senise area are undeniable. In this context, the study demonstrates how an alert system can improve drying conditions without violating regulations, while future adjustments to guidelines may be necessary to adapt to evolving climatic conditions.

2. Materials and Methods

2.1. The Study Area

Senise peppers are a traditional variety grown in the Pollino National Park in the Basilicata region (in southern Italy), predominantly in the Sinni and Agri valleys, an area encompassing several municipalities, including Senise, from which the pepper variety takes its name. The peppers are planted between February and March, transplanted in May, and harvested in mid-to-late summer, with August being the peak month. Harvesting is performed manually, with great care taken to avoid damaging the stems. The unique genetic characteristics of this pepper variety make it especially ideal for natural drying and the subsequent production of paprika. Senise red peppers can be pointed, trunked, or hooked. They are particularly known for their high vitamin C content and their ability to maintain their vibrant red color even after drying. The distinct taste and characteristics of these peppers, coupled with their strong regional identity, led to their recognition as a protected geographical indication (PGI) by the EU in 1996.

In the upper left corner of Figure 1, the drying infrastructure is shown; it was a rectangular greenhouse (48 m × 9 m) with a PVC roof. The ridge height was 4.00 m, while the sidewalls were 2.20 m high. Inside the greenhouse, a shading net was positioned around 2.00 m in height. Additionally, two large openings on the shorter sides of the greenhouse served as entry and exit points, as well as a natural ventilation system.

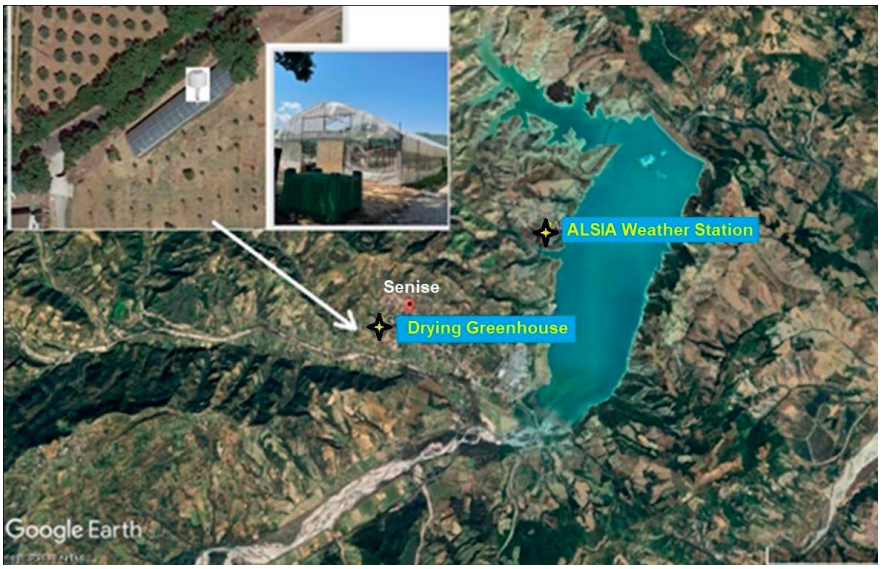

Figure 1. The drying greenhouse. The 2 yellow placeholders indicate the positions of the weather stations: the outdoor weather station was part of the regional monitoring network of the ALSIA agency, and the indoor sensors were from Elaisian SPA.

For monitoring outdoor agrometeorological variables, the Senise ALSIA weather station, located nearest to the greenhouse, was utilized, while temperature and humidity sensors were set up inside the drying greenhouse, approximately in the center of the structure (see Figure 1). The 2 yellow placeholders in Figure 1 indicate the positions of the weather stations.

The greenhouse was located approximately 2 km from the production area; the pepper harvest, in 2022 and 2023, took place from August to September, and the product was stored in the greenhouse in different stages, as shown in Table 1.

Table 1. Quantity and dates of storage of red peppers in the drying greenhouse.

Time	Quantity (kg)
17 August 2022	4500
26 August 2022	3800
12 September 2022	3700
24 September 2022	3900
5 August 2023	3300
20 August 2023	4700
8 September 2023	3800
16 September 2023	4100

2.2. The Climate Parameters

The data acquired by the ALSIA weather station of Senise are available online on the website of the agency. Elaisian provided the air temperature and humidity sensors positioned inside the greenhouse. The complete station "Enterprise" measured the air temperature (accuracy ±0.3 °C), relative humidity (±3%), precipitation (resolution 0.1 mm), and dew point (resolution 0.1 °C). The sensors were positioned at a height between 1.50 and 1.70 m to ensure representative measurements. Additionally, extra sensors were used: an ultrasonic anemometer to measure wind speed (sensitivity 0.12 m/s) and wind direction and a leaf wetness sensor to monitor the wetness hours. The parameters were acquired every 15 min and transmitted to the server every 60 min. This transmission interval was configurable to suit specific monitoring needs. In the event of mobile network connectivity problems, the station internally stored data from the last few days and restored the measured values to the cloud once the connection was re-established. The monitoring node was a Raspberry Pi (Raspberry Pi Foundation, Cambridge, UK). The primary programming language employed on the Raspberry Pi was Python 3.10, chosen for its versatility and extensive library support. The Raspberry Pi was a small but complete PC on a single board. The Raspberry Pi received data from the sensors and sent it to the Elaisian IoT platform, where parameter measurements were stored and displayed in real time. In case there was any sudden change in the air humidity value, the IoT-based device was able to send an autogenerated SMS alert to the owner's mobile phone.

From June to September 2021, relative humidity and temperature sensors were placed outside the greenhouse to evaluate whether the data acquired by the ALSIA station, located approximately 4 km away from the greenhouse, were representative of the study area. A correlation analysis was carried out on these data, and Pearson correlation coefficient values of 0.89 for temperature and 0.76 for relative humidity were found. The parameters were pre-processed to remove any outliers. In 2022 the sensors were placed inside the greenhouse.

The analysis procedure consisted of two steps:

(a) The first step aimed to highlight whether the variations in temperature and humidity inside the greenhouse, being a semi-open structure, were significantly influenced by

the presence of the red peppers. For this purpose, a feed forward neural network (FFNN) trained on the climate parameters acquired in the greenhouse when it was empty and the data of the Alsia outdoor weather station were used to predict the humidity and temperature parameters inside the greenhouse when the product was present. The neural network was trained on a dataset comprising hourly temperature and humidity readings collected daily over a 50-day period, from late June to 16 August 2022. The parameters estimated, as if the greenhouse were empty, were compared with those acquired by the indoor sensors from 17 August to the end of September. From the comparison between the predicted and measured parameters, it was possible to identify the time intervals in which the values of humidity and temperature became higher to intervene by improving the natural ventilation of the greenhouse. The system was tested in August and September 2022, when the pepper was in the greenhouse for drying.

(b) In the ensuing phase, the neural network was trained from 17 August 2022 to 30 September 2022, when the peppers were dried in the greenhouse. Therefore, the system was also able to predict the values of the microclimatic parameters inside the greenhouse in the presence of red peppers, issuing warnings one hour before a risk condition arose. The alert system was tested during the 2023 experimental year by comparing the predicted values with the thresholds previously identified. When the critical level was exceeded, the greenhouse operators were alerted to improve conditions inside the drying structure.

To ensure the maximum reliability of the data, specific measures were implemented during the pre-processing phase. In particular, we found that the readings from the Elaisian station and the ALSIA platform contained no missing data. However, for gaps shorter than two hours, a linear interpolation algorithm was applied to maintain the system's ability to make reliable predictions. Outliers were identified using a criterion based on the standard deviation (3σ) and confirmed with the Grubbs test. The detected outliers were then replaced with the weighted average of the surrounding values. These strategies enhanced the data quality and neural network accuracy, ensuring greater model reproducibility.

2.3. The Neural Network

Feed forward neural networks (FFNNs) [29] are a class of artificial neural networks in which the connections between nodes do not form loops. The use of a neural network allows the extraction and analysis of complex characteristics among the multiple variables offered by the sensors used to collect agrometeorological data. To predict the temperature and humidity inside the greenhouse, an FFNN was implemented.

The FFNN architecture was selected due to the following advantages:

- The prediction of internal temperature and humidity was influenced by multiple climate variables with complex interdependencies. FFNNs are well suited for modeling such nonlinear relationships, whereas traditional statistical models may struggle to capture them effectively.
- The input features included time-lagged climate variables ($t - 1$ and $t - 2$), making FFNNs a suitable choice for learning temporal dependencies without requiring explicit time-series models like recurrent neural networks (RNNs), which can be more computationally expensive and prone to vanishing gradient issues.
- Compared with more complex deep learning models (e.g., LSTMs or GRUs), FFNNs require fewer computational resources while still providing high prediction accuracy. This makes them a practical choice for real-time applications in greenhouse monitoring.
- Through careful architecture design (e.g., reducing neurons in the second hidden layer and applying K-Fold cross-validation), the FFNN was optimized to generalize

well to unseen data while minimizing overfitting. Other machine learning models, such as decision trees or support vector machines (SVMs), may require extensive feature engineering.

This FFNN network was trained using the data collected from the climate variables inside and outside the greenhouse, also considering the temporal correlations detected by the preliminary statistical analysis. The inputs used for prediction at time "t" were based on data collected over the previous two hours (t − 1 and t − 2), both outside and inside the greenhouse:

- Internal temperature and internal humidity: T_OUT(t − 1) and H_OUT(t − 1); T_OUT(t − 2) and H_OUT(t − 2).
- External temperature and external humidity: T_IN(t − 1) and H_IN (t − 1); T_IN (t − 2) and H_IN (t − 2).

The model predicted the following outputs:

- Predicted internal temperature: T_IN_E(t).
- Predicted internal humidity: H_IN_E(t).

The neural network was designed with the following outputs:

(1) Input layer: 8 input features representing the past two hours of both internal and external temperature and humidity values.

(2) Hidden layers:
   - First hidden layer: 64 neurons with ReLU (rectified linear unit) activation function. The number of neurons was chosen based on empirical studies and the complexity of the problem. The number of neurons in the FFNN was determined based on preliminary experiments to achieve an optimal trade-off between the predictive accuracy and the computational efficiency.
   - Second hidden layer: 32 neurons with ReLU activation. This layer reduced the number of parameters to prevent overfitting and helped in extracting higher-order features.

(3) Output layer:
   - The output layer consisted of 2 neurons, one for predicting the internal temperature and the other for predicting the internal humidity for the next hour.
   - Activation: Since the problem was a regression task and the forecasts were continuous values, the output layer used a linear trigger function. It was chosen for its effectiveness in handling vanishing gradient problems and for its ability to introduce non-linearity into the model.

The schematic diagram of the architecture of the feed forward neural network (FFNN) used in this study is shown in Figure 2.

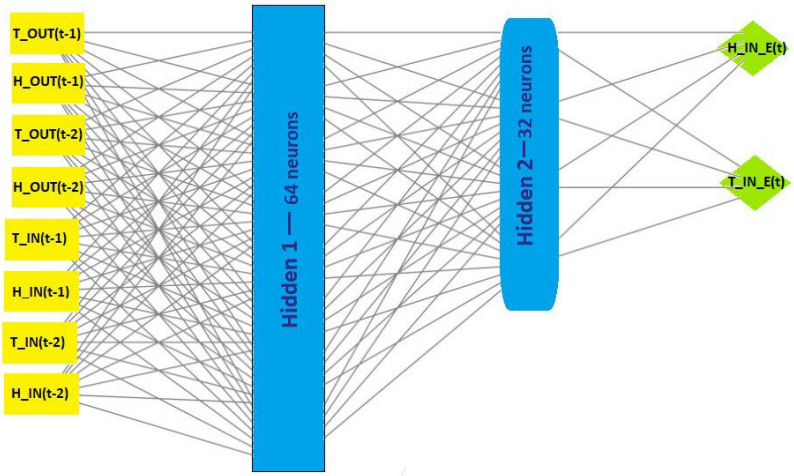

Figure 2. Schematic diagram of the feed forward neural network (FFNN). The diagram illustrates the structure of the neural network used to predict the internal air temperature and relative humidity inside the greenhouse.

The neural network was trained using the stochastic gradient descent (SGD) optimizer. The model was trained for 10,000 epochs to ensure adequate learning while monitoring the validation loss to prevent overfitting. Since MATLAB R2023a's Deep Learning Toolbox was employed, the batch size was automatically optimized based on the available computational resources and dataset size, ensuring efficient memory management during training. Hyperparameters such as weight initialization, activation functions, and dropout rates were set based on preliminary experiments to maximize model generalization and predictive accuracy.

During the training process, input data were propagated through the network. Each neuron, by summing the weighted inputs, adding a bias term, and applying the ReLU activation function in the hidden layers, calculated its activation function. The network predictions were compared with the actual values of the target variables T_IN and H_IN, and the error was calculated with the mean squared error (MSE) loss function. The error was subsequently backpropagated through the network to adjust the weights and biases. The backpropagation algorithm calculated the gradients of the loss function with respect to the weights and updated them to minimize the error.

2.4. The Neural Network Training and Validation

After training, the model was evaluated on a test set to assess its performance. The following metrics were used:

- Mean squared error (MSE): This was the main metric for evaluating the prediction accuracy. A lower MSE indicated better performance.
- Mean absolute error (MAE): The MAE was also tracked to assess the model's performance in terms of the absolute error in the predicted temperature and humidity.
- Cr oss-validation: The model's generalization ability was assessed using K-Fold cross-validation. This approach split the dataset into K subsets, training the model K times on different training/validation splits. This reduced the likelihood of overfitting to any single subset of data.

The dataset used in the training phase of the neural network was divided into three subsets: 70% for training, 20% for validation, and 10% for testing.

In Figure 3 the results of the neural network reliability analysis are shown; the plots are related to case (a) described in Section 2.2. In the scatter plots for training, validation, and testing (Figure 3a, along with the corresponding root mean square errors), the network

demonstrated a strong ability to predict humidity and temperature conditions inside the drying structure. The error histogram (Figure 3b) clearly showed that most of the air relative humidity predictions deviated by only ±0.215%, a low measurement in relation to the drying characteristics of the fresh peppers. Furthermore, only a very small percentage of the predictions showed errors greater than ±3%, making the system particularly efficient in predicting relative humidity values at practically any time of day or night.

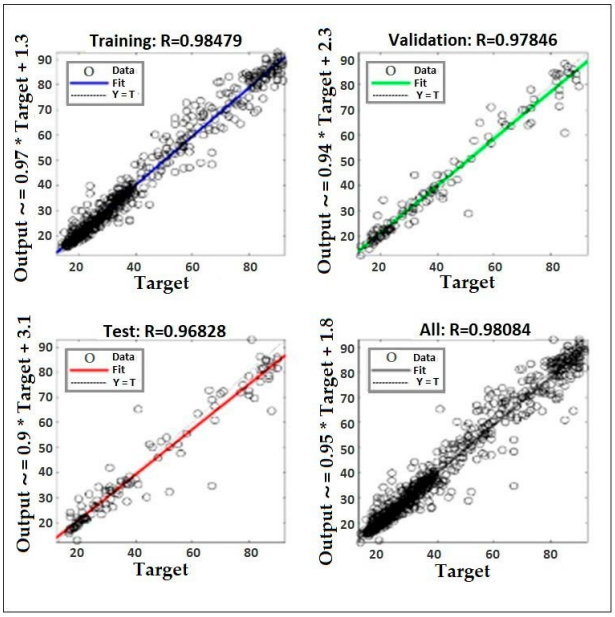

(**a**)

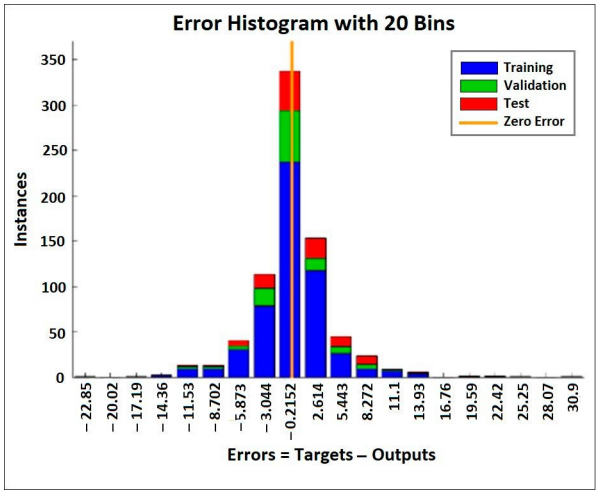

(**b**)

Figure 3. (**a**) Scatter plots of training, validation, and test dataset with the related root square errors of the neural network prediction of humidity and temperature conditions inside the drying structure. (**b**) Histogram of errors of predicted and measured air relative humidity.

When the neural network was trained to predict air temperature and humidity inside the greenhouse in the presence of the red peppers (case (b) in Section 2.2), the error histogram showed that most of the air relative humidity predictions deviated by only ±0.25%, a low measurement in relation to the drying characteristics of the fresh product, and also, in this case, a very small percentage of the predictions showed errors greater than ±3%.

3. Results and Discussion

The main objective of the present work was to identify the conditions that determine the onset of pepper rot phenomena and to develop an alert system to limit its occurrence, compatibly with the restrictions imposed by the PGI directive. It is crucial to emphasize the importance of designing a low-cost monitoring system due to the low profit margins that this crop often generates for farmers. These challenges arise both from the damage peppers can suffer during the growing phase (adverse weather conditions, pest attacks, diseases, etc.) and from losses caused by rotting during the drying phase. From this perspective, leveraging free data provided by the regional weather station is highly advantageous both for the reliability of the data, periodically validated by ALSIA operators, and for the presence in the Senise area of numerous drying greenhouses for peppers owned by producers organized into a consortium. The system was, therefore, designed to be easily applied also to other greenhouses in the area without the need to install external weather stations at each site, thereby avoiding additional costs.

In 2022, the FFNN was used to predict air temperature and humidity values inside the greenhouse in the absence of the red peppers. A comparison was conducted between the values measured in the presence of the product and those estimated by the neural network to evaluate the impact of the pepper's presence inside the greenhouse. This analysis aimed to assess the significance of these variations and their evolution over time and to calculate critical threshold values during the red pepper drying phase.

In 2023, the neural network was trained using data acquired in the previous year (17 August to 30 September) to predict relative humidity and temperature values inside the greenhouse in the presence of the product, with a one-hour lead time. By comparing the estimated relative humidity in the absence of the stored red peppers with that in its presence and applying the thresholds established in the prior year's study, it became possible to generate alerts and prompt timely interventions by farm operators.

Additionally, as the greenhouse was semi-open, excessive relative humidity could negatively impact the pepper drying process. As a result, the system was designed to alert producers whenever the relative humidity measured by the weather station outside the greenhouse exceeded 85% for more than two consecutive days. Studies have shown that to prevent fungal growth and mycotoxin production, it is essential to control drying and storage conditions using hazard analysis and critical control point systems. This is crucial as mycotoxin-producing fungi can thrive at relative humidity levels above 85–91% [30,31].

3.1. Analysis of Air Humidity and Temperature Patterns

Figure 4 shows the average daily values of temperature and relative humidity, inside and outside the greenhouse in the period from 1 August to 30 September 2022. The pepper began to be placed in the greenhouse for drying on 17 August, as shown in Table 1.

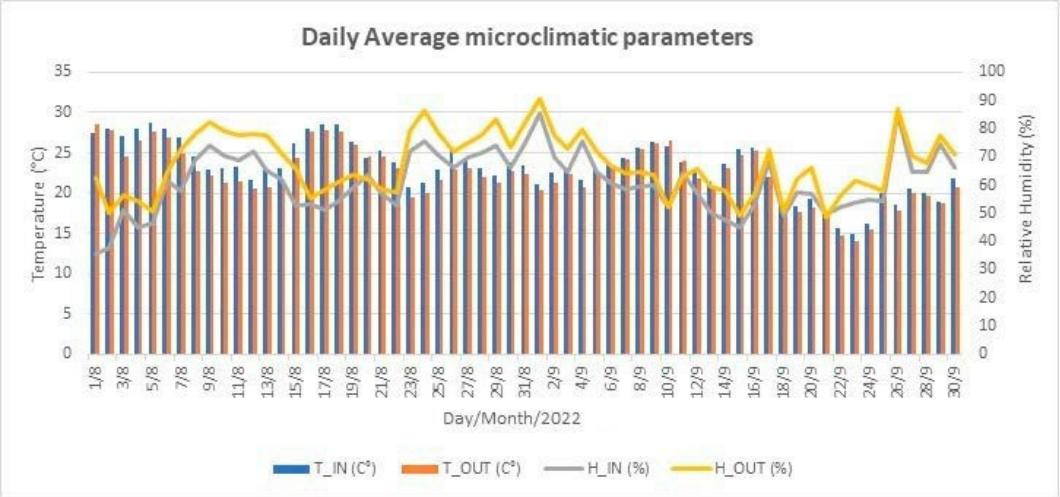

Figure 4. Mean daily values of temperature and relative humidity measured from the Senise Alsia weather station and the sensors located inside the greenhouse in August and September 2022.

Both measured parameters, outside and inside the greenhouse (Figure 4), showed very similar patterns when the Senise pepper was not present in the greenhouse (1–16 August). The relative humidity measured inside the greenhouse always showed lower values compared with the external measurements (ALSIA), while the temperature inside the greenhouse was higher than the corresponding values recorded outside. Under ideal ventilation conditions, humidity levels inside and outside the greenhouse should be the same. However, due to the presence of protective sheets and the positioning of the openings, this equilibrium was not achieved [32]. The dynamics between indoor and outdoor parameters were complex, and the indoor values at time t were influenced by external ones also relating to previous time steps. Figure 5 shows the hourly curves of the estimated and measured relative air humidity. The estimated and measured relative humidity curves in the greenhouse overlapped very well in the period in which the red peppers were not present in the greenhouse, while the former shifted toward lower values in the subsequent period. An ANOVA analysis was performed on the measured and estimated datasets by confirming the null hypothesis, i.e., that there was no significant difference between the means of the two datasets, in the period when the red pepper was not present in the greenhouse (1–16 August) and rejecting it in the period in which the pepper was present in the greenhouse. Both tests were performed with a significance level (p-value) of 0.05. A similar analysis was performed on the estimated and measured temperature data, yielding results closely aligned with those observed for relative humidity. However, since the most pronounced differences were found in the relative humidity data, the neural network was trained to incorporate both parameters (relative humidity and temperature). Nevertheless, for the development of the alert system, the analysis prioritized relative humidity measurements due to their greater significance.

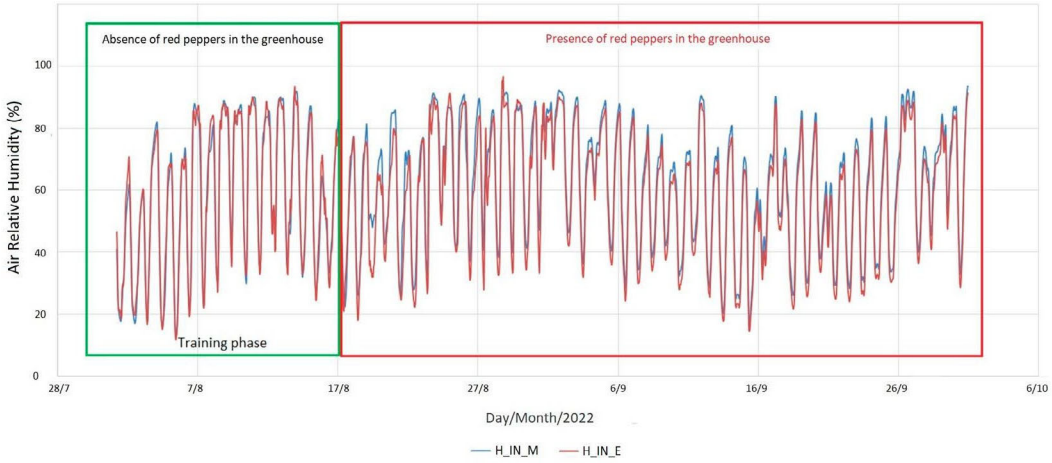

Figure 5. The measured (H_IN_M, blue line) and estimated (H_IN_E, red line) relative humidity inside the greenhouse. The graph shows the data starting from 1 August to 30 September; the period in which the neural network was tested is highlighted in green, while the period in which the peppers were present in the greenhouse is highlighted in red.

To highlight the significance of these differences, a targeted analysis was conducted [33]. Figure 6 shows the histograms of the differences between the estimated and measured relative humidity, relating to the period of absence of product (Figure 6a) in the greenhouse and to the following two weeks in which the peppers were introduced in the greenhouse (Figure 6b). While in Figure 6a, the distribution of deviations is almost symmetrical around the value 0, in the other graph, it moves toward positive values.

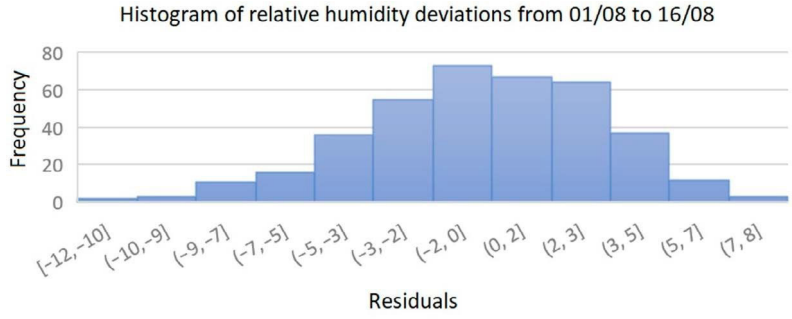

(**a**)

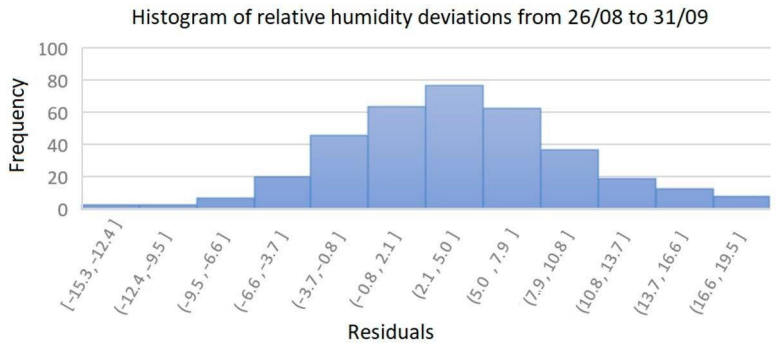

(**b**)

Figure 6. Histograms of the differences between the estimated and measured air relative humidity relating to the period of absence of red peppers (**a**) and in the presence of drying peppers in the greenhouse (**b**).

In Table 2, the coefficient of determination (R^2) and the root mean square error (RMSE) of the measured and estimated relative humidity were reported in relation to the different periods. The R^2 values, relating to the period in which the pepper was not present in the greenhouse, was very high, equal to 0.98, while it dropped to 0.88 when the product was present in the greenhouse. The coefficient of determination of the estimated and measured relative humidity values significantly reduced in the 4 days following the introduction of the Senise pepper in the greenhouse.

Table 2. R^2 and RMSE values for linear regression of measured and estimated datasets. The ID number is associated to the different periods following the date when the pepper was placed in the greenhouse.

ID	2022	R^2	RMSE
	1–16 August	0.98	3.4
	17 August to 30 September	0.89	6.9
1	17–19 August	0.86	7.4
	17–25 August	0.9	6.9
2	26–29 August	0.89	7.3
	26 August to 3 September	0.94	5.4
3	12–15 September	0.85	7.6
	12–20 September	0.91	6.7
4	24–28 September	0.88	7.4
	24–30 September	0.94	5.5

The climatic dynamics during the four periods when peppers were introduced into the greenhouse were different. From 17 to 20 August, higher average temperatures (25–28 °C) and lower relative humidity (51–62%) were recorded both inside and outside the greenhouse (Figure 4). In contrast, during the period from 26 to 29 August, the average temperatures decreased (22–25 °C), while the relative humidity increased (66–74%). From 12 to 15 September, the average temperatures were even lower (21–24 °C), with relative humidity ranging between 45% and 57%. Finally, from 24 to 27 September, the average temperatures further declined (15–20 °C), and the relative humidity ranged from 57% to 64%, peaking at 87% on 26 September, when 9.8 mm of rain was recorded.

Figure 7 shows the RMSE of the estimated and measured air relative humidity in the day following the placement of the red pepper in the drying greenhouse at four different times in the 2022 study year (as reported in Table 1).

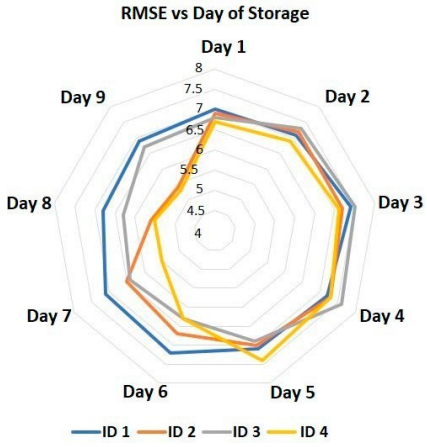

Figure 7. RMSE values for linear regression of measured and estimated datasets evaluated from the first to the ninth day after the red pepper was placed in the greenhouse at the different dates (ID number).

Temperature and relative humidity were the two most effective microclimatic variables in triggering sudden deterioration processes [34] of the peppers during the drying period. The RMSE values confirmed the highlights of the previous analysis. The drying process and storage conditions of the peppers were critical factors affecting their quality and safety. Moisture content and water activity played crucial roles in fungal growth and mycotoxin production during paprika processing [30]. The drying process typically involved three stages: a short induction phase, a linear drying rate period, and a slower diffusion-controlled phase [35].

During period ID-1 (Table 2), the correlation between the relative humidity values measured inside the greenhouse and those estimated as if the greenhouse were empty showed the lowest R^2 values during the first three days after the peppers were placed in the drying greenhouse. The increase in humidity inside the greenhouse, due to the presence of the product, occurred more rapidly because of higher external temperatures and lower relative humidity levels, in perfect agreement with the literature. Research on pepper drying has examined various factors affecting the process. The temperature directly influences the evaporation rate of water within the peppers [36], thus determining the drying rate. High temperatures can accelerate evaporation but may also cause thermal damage to the Senise red pepper, compromising its structural and nutritional quality [37]. Low relative humidity, while typically resulting in faster drying rates, can lead to excessively rapid and non-uniform drying. This creates moisture gradients within the pepper, compromising its integrity and causing cracking or breakage [38].

During periods ID-2 and ID-3, the minimum correlation between the two parameters occurred during the four days following the placement of the product in the greenhouse. In both cases, the temperatures were lower than in ID-1, and only in the case of ID-2 were the air humidity levels higher. Finally, during period ID-4, which occurred at the end of September, there was a further drop in temperatures along with higher external air humidity. In this case, the minimum correlation between the estimated and measured relative humidity inside the greenhouse was observed in the five days following the introduction of red peppers. This was the period during which the highest product losses occurred. Relative humidity plays a crucial role in maintaining an optimal hygroscopic balance. High relative humidity can reduce drying efficiency as water-saturated air impedes evaporation from the product [39,40]. This can lead to inadequate storage conditions, encouraging the growth of pathogenic microorganisms and increasing the risk of spoilage. Excessively low temperatures slow the drying process, increasing the risk of microbial proliferation and mold formation [38,41]. Air temperature and relative humidity, which regulate the rate of moisture evaporation and the risk of microbial growth, have a significant impact on the drying process of PGI Senise peppers. A noticeable increase in relative humidity was observed during the first three to four days after the peppers were placed in the greenhouse. This occurred because moisture from the fresh product was released into the surrounding air, temporarily altering the greenhouse microclimate. The results indicated that when external humidity levels remained high for several consecutive days, the drying process slowed down, increasing the risk of fungal contamination. However, sudden temperature fluctuations can accelerate moisture loss while simultaneously compromising the structural integrity of the peppers, potentially leading to uneven drying and quality deterioration.

3.2. The Alert System

In 2023, the FFNN was trained using data collected during the previous year (17 August 2022 to 30 September 2022) to predict relative humidity and temperature values when the peppers were stored inside the greenhouse, with a one-hour lead time. A comparison between the measured and predicted values of temperature and relative

humidity was performed. Statistical analysis of the output revealed that the RMSE and mean absolute error (MAE) for temperature predictions were 0.81 ˚C and 0.54 ˚C, respectively, while the RMSE and MAE for relative humidity predictions were 2.6% and 1.88%, respectively—results that can be considered satisfactory. Figure 8 illustrates the accuracy of the predicted versus measured parameters within the greenhouse in the presence of the product over a four-day sample period. The system remained operational throughout the entire pepper drying period in the greenhouse, from August to September 2023.

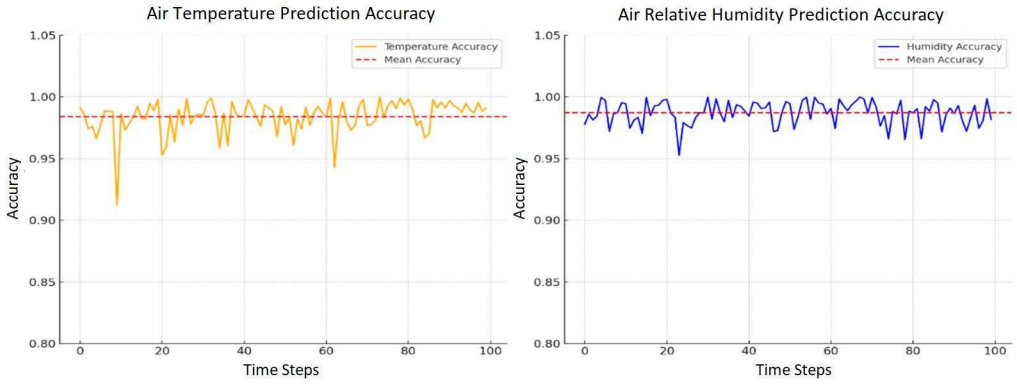

(**a**) (**b**)

Figure 8. (**a**) Graph showing the accuracy between estimated and measured temperatures in the presence of peppers inside the greenhouse over four consecutive days. (**b**) Accuracy between estimated and measured relative humidities in the presence of peppers inside the greenhouse.

The threshold system was developed on the data acquired in 2022, and it was based on comparing the hourly values of parameters estimated inside the greenhouse as if the peppers were not present, H_IN_E_WP, with those estimated when the product was present inside the greenhouse, H_IN_E_P. The threshold value was defined by referring to the histogram in Figure 6b, setting it equal to two standard deviations, as follows:

$$\text{Alert} \rightarrow \Delta H = \text{H\_IN\_E\_P} - \text{H\_IN\_E\_WP} > 12\%. \quad (1)$$

By applying the thresholds established in the 2022 study, it became possible to generate alerts and prompt timely interventions by farm operators. In fact, the developed alert system could issue a warning one hour before a risk condition arose, allowing the activation of appropriate preventive measures to improve the greenhouse microclimate. However, these interventions were focused on enhancing natural ventilation or solar irradiance due to the restrictions imposed by EU legislation, which grants the Senise pepper its PGI designation.

Figure 9 shows the graph of residuals between the estimated air relative humidity inside the greenhouse in the presence and absence of red peppers (ΔH), from 5 August to 30 September 2023. The outliers were removed from the graph.

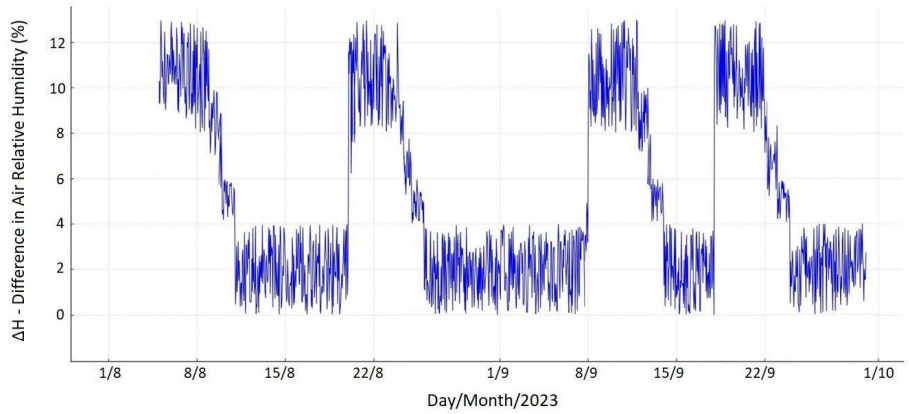

Figure 9. Residuals of estimated air relative humidity inside the greenhouse in the presence of the red pepper compared with its absence (ΔH) in summer 2023.

During this period, patterns influenced by both the presence of products and changes in environmental conditions were evident. Until 5 August 2023, the greenhouse was empty. On 5 August, the first batch of red peppers was placed inside the greenhouse (Table 1). From 5 to 9 August, external temperatures ranged between a minimum of 18 °C and a maximum of 28 °C. During this period, ΔH reached values of 13%. Subsequently, from 20 to 24 August, when additional peppers were placed in the greenhouse for drying, ΔH values increased again, while the external temperatures fluctuated between 22 °C and 35.5 °C, which probably contributed to amplify the observed humidity differences. A similar pattern was observed from 8 to 12 September, when temperatures moderated slightly, with averages ranging between 18.5 °C and 31 °C. The final highlighted period, from 16 to 20 September, showed temperatures stabilizing again at higher levels, between 22 °C and 34 °C. Following each of these highlighted periods, the graph indicates a gradual reduction in ΔH during the 2 days afterward, with differences dropping below 4–10%. For the remaining periods, when no significant events occurred, ΔH consistently remained below 4%. During the study period the alert system was activated several times, highlighting that the interventions carried out to improve natural ventilation inside the greenhouse were likely still insufficient to fully meet the intended objectives. Nevertheless, during 2023, product losses during the drying process were reduced.

Compared with studies on the use of predictive neural networks to predict microclimate conditions inside drying facilities currently in the literature, the present experimental approach has some key differences. Choi in 2019 [23] proposed an MLP model to predict the microclimate inside fully enclosed greenhouses, achieving 90% accuracy in predicting air humidity. The proposed model, however, addresses an even more complex and intriguing challenge, namely, the estimation—and relative management—of humidity and temperature in a semi-open environment. Compared with other studies, such as the one carried out by Petrakis in 2022 [24], which implemented a prediction system based on ANNs for smart greenhouses, the present study stands out due to the specificity of the application in a context characterized by extremely stringent regulations, which prevent complete automation, defining extremely critical or complex management challenges. Further studies are underway to refine the threshold system. Additionally, ongoing investigations aim to examine the presence of in-field infestations that could contribute to rot during the red pepper drying phase. To further improve this study, we acknowledge certain limitations. First, the system's applicability to other geographical regions with different environmental conditions may be affected by its reliance on the specific climate of the Basilicata region. Second, the dependence on IoT-based monitoring requires a stable data transmission infrastructure, which may not be available in all agricultural settings. Finally, although the

model accurately predicts temperature and humidity variations, it does not yet account for other critical factors that could enhance the accuracy of the alert system, such as air circulation patterns and potential external contamination. Future developments will aim to integrate these additional variables to improve predictive reliability and ensure wider applicability of the proposed method.

3.3. Potential Solutions to Optimize Red Pepper Drying Process

One potential solution to these challenges lies in the development of smart greenhouses as part of the Industry 4.0 framework. The focus of this industrial revolution is not merely on automation but on creating intelligent production systems that integrate data, making it easily accessible, analyzable, and actionable [42]. For instance, digital twin technologies can optimize production processes, energy consumption, and operational costs, all while accounting for key factors that influence the product quality and yield [22,43,44].

One potential approach could involve solar greenhouses, which offer an efficient and eco-friendly drying method for agricultural products. Compared with traditional sun-drying methods, solar greenhouses offer better quality by protecting crops from external contaminants [45]. They can function using either natural or forced convection systems, with the latter offering reduced drying times and improved control over humidity levels. Moreover, the incorporation of thermal storage solutions ensures consistent heat distribution throughout the drying cycle [46]. Unfortunately, current regional regulations prevent the use of this method, despite its potential compatibility with many of the guidelines already in place.

Growtronix is a modular system that monitors and controls greenhouse parameters like temperature, humidity, and lighting, allowing precise environmental customization. Monnit Greenhouse Monitoring is a solution that provides real-time monitoring and alerts for temperature, humidity, and other conditions to maintain optimal growth environments. Intel Edison-Based DIY Systems are projects using microcontrollers for smaller-scale or custom greenhouse solutions, showcasing flexibility and adaptability. Such systems are difficult to adapt to the specific case of Senise red peppers because the structural design of the greenhouse used for peppers may not align with the operational requirements of off-the-shelf smart systems, necessitating a tailored approach. Additionally, the requirements for maintaining the peppers' quality and preserving their geographical designation often involve specific drying directives imposed by the PGI protocol.

Drying technologies have undergone significant evolution [47], shifting from traditional methods like sun drying to modern techniques such as solar, convective, infrared, ultrasound, radio-frequency, microwave, and freeze drying [48]. While these innovations have improved efficiency, their positive impact on maintaining the sensory and bioactive qualities of chili peppers, such as color, texture, capsaicinoids, and antioxidants, should not be viewed as an unquestioned advantage. Advanced techniques often involve high energy costs and operational complexities that must be carefully weighed against the benefits in terms of product quality. Recent trends highlight the optimization of processes to improve product quality while minimizing energy consumption, raising questions about the long-term sustainability of these solutions. Although pre-treatment techniques, like blanching and cold plasma, have shown promising potential in preserving bioactive compounds, their actual scalability and economic impact remain to be fully established. Furthermore, hybrid methods that combine drying and pre-treatment strategies seem to promise an optimal balance between efficiency and quality, but a critical examination of the synergies and limitations of these solutions is necessary. Future research should focus on comparative analyses of different drying methods, considering not only product quality but also energy

efficiency, to guide researchers, policymakers, and industry stakeholders toward more sustainable and effective drying technologies.

4. Conclusions

While the alert system developed in this study is specifically designed for the Senise pepper drying process, with appropriate adjustments, it can be adapted to other contexts with similar management requirements. In fact, the Senise pepper is representative of other Italian realities subject to strict regulations in order to maintain the PGI status. In particular, the use of low-cost IoT sensors and publicly available meteorological data makes this technology highly accessible, even for small-scale producers, minimizing the need for complex and costly installations. This approach, based on AI algorithms, enables seamless integration into environments with varying microclimatic conditions, enhancing the efficiency of the drying process. Although smart greenhouses represent a promising solution for sustainable food production in the face of global challenges, they are often not applicable in such contexts. One of the main causes of Senise red pepper loss occurs in the greenhouse during the drying phase. Monitoring the microclimatic conditions in the greenhouse analyzing the data by using AI applications to enable targeted interventions has proven to be a very promising approach in reducing production losses. Further research is needed, including field monitoring of the crops, to assess potential nutritional deficiencies or the presence of pest attacks and diseases during the growing season of the peppers, which could also impact the drying phase. To address complex production challenges—such as meeting production standards, minimizing product loss, optimizing lead times, and ensuring product quality—there is a clear need for sustainable management strategies. These strategies must be based on the careful scientific analysis of real-time data, made possible by new technologies [49]. This underscores the importance of developing and prototyping decision support systems (DSSs) that are both effective and cost-efficient. As highlighted by Maraveas in 2023 [12], while these artificial intelligence applications show potential in improving agricultural sustainability and resource use efficiency, challenges remain, including cost, technology commercialization, and disparities between developed and developing regions. The adoption of these technologies represents a significant step toward more efficient and sustainable agricultural practices.

Author Contributions: Conceptualization, C.F., P.D., F.T., N.C., L.A.C., M.S. and R.C.; data curation, C.F., P.D., F.T., N.C., L.A.C., E.S., F.M., M.S., R.C., E.L. and G.D.M.; formal analysis, C.F., P.D., F.T., N.C., L.A.C., E.S., F.M., M.S., R.C., E.L. and G.D.M.; funding acquisition, C.F., P.D., F.T., L.A.C., E.S. and F.M.; investigation, C.F., P.D., F.T., N.C., L.A.C., E.S., F.M., M.S., R.C., E.L. and G.D.M.; methodology, C.F., P.D., F.T., N.C., L.A.C., E.S., F.M., M.S., R.C., E.L. and G.D.M.; project administration, C.F. and P.D.; resources, C.F., P.D., F.T., N.C., L.A.C., E.S., F.M., M.S., R.C., E.L. and G.D.M.; software, C.F., P.D., F.T., N.C., L.A.C., F.M., M.S. and R.C.; supervision, C.F., P.D., F.T., N.C., L.A.C., E.S., F.M., M.S., R.C. and E.L.; validation, C.F., P.D., F.T., N.C., L.A.C., E.S., F.M., M.S., R.C., E.L. and G.D.M.; visualization, C.F., P.D., F.T., N.C., L.A.C., E.S., F.M., M.S., R.C., E.L. and G.D.M.; writing—original draft, C.F., P.D., M.S. and R.C.; writing—review and editing, C.F., P.D., F.T., N.C., L.A.C., E.S., F.M., M.S., R.C., E.L. and G.D.M. All authors have read and agreed to the published version of the manuscript.

Funding: This work was supported by the University of Basilicata and "Casa delle Tecnologie Emergenti" of Matera, "Laboratorio del Giardino delle tecnologie emergenti"—CTEMT; Smart@Irrifert Project PSR Basilicata 2014–2020—Sottomisura 16.2, CUP G19J21004870006; and "Vertical gaRdens with Digital twin of plants" Viridiis Project, PRIN 2022, Cup C53D23000480006.

Institutional Review Board Statement: Not applicable.

Informed Consent Statement: Not applicable.

Data Availability Statement: The data presented in this study are available on request from the corresponding author.

Conflicts of Interest: Author Giovanni Di Mambro was employed by the company Elaisian SRL. The remaining authors declare that the research was conducted in the absence of any commercial or financial relationships that could be construed as a potential conflict of interest.

References

1. Fiorentino, C.; D'Antonio, P.; Toscano, F.; Donvito, A.; Modugno, F. New Technique for Monitoring High Nature Value Farmland (HNVF) in Basilicata. *Sustainability* **2023**, *15*, 8377. [CrossRef]
2. Esper, A.; Mühlbauer, W. Solar Drying—An Effective Means of Food Preservation. *Renew. Energy* **1998**, *15*, 95–100. [CrossRef]
3. Akyazi, T.; Goti, A.; Oyarbide, A.; Alberdi, E.; Bayon, F. A Guide for the Food Industry to Meet the Future Skills Requirements Emerging with Industry 4.0. *Foods* **2020**, *9*, 492. [CrossRef] [PubMed]
4. Babiceanu, R.F.; Seker, R. Manufacturing Operations, Internet of Things, and Big Data: Towards Predictive Manufacturing Systems. In *Service Orientation in Holonic and Multi-Agent Manufacturing*; Borangiu, T., Thomas, A., Trentesaux, D., Eds.; Springer: Cham, Switzerland, 2015; pp. 157–164. [CrossRef]
5. Hu, G.; You, F. Renewable Energy-Powered Semi-Closed Greenhouse for Sustainable Crop Production Using Model Predictive Control and Machine Learning for Energy Management. *Renew. Sustain. Energy Rev.* **2022**, *168*, 112790. [CrossRef]
6. Gautron, R.; Maillard, O.A.; Preux, P.; Corbeels, M.; Sabbadin, R. Reinforcement Learning for Crop Management Support: Review, Prospects and Challenges. *Comput. Electron. Agric.* **2022**, *200*, 107182. [CrossRef]
7. Lopez-Cruz, I.L.; Fitz-Rodríguez, E.; Salazar-Moreno, R.; Rojano-Aguilar, A.; Kacira, M. Development and Analysis of Dynamical Mathematical Models of Greenhouse Climate: A Review. *Eur. J. Hortic. Sci.* **2018**, *83*, 269–279. [CrossRef]
8. Su, Y.; Xu, L. Towards Discrete Time Model for Greenhouse Climate Control. *Eng. Agric. Environ. Food* **2017**, *10*, 157–170. [CrossRef]
9. Fiorentino, C.; AbdelRahman, M.A.E.; D'Antonio, P.; Toscano, F.; Sannino, M.; Abate, N.; Conte, D.; Lasaponara, R.; Masini, N. Space-to-tree: Architectural Framework for Real-time Monitoring of Pines in Natural and Historical Park. *Internet Technol. Lett.* **2024**, *7*, e574. [CrossRef]
10. Zhang, P. Industrial Control System Simulation Routines. In *Advanced Industrial Control Technology*, 1st ed.; Elsevier Inc.: Amsterdam, The Netherlands, 2010; pp. 781–810. [CrossRef]
11. Esteves, M.S.; Perdicoúlis, T.P.A.; dos Santos, P.L. System Identification Methods for Identification of State Models. In Proceedings of the 11th Portuguese Conference on Automatic Control (CONTROLO'2014), Porto, Portugal, 21–23 July 2014; Volume 321. [CrossRef]
12. Maraveas, C. Incorporating Artificial Intelligence Technology in Smart Greenhouses: Current State of the Art. *Appl. Sci.* **2023**, *13*, 14. [CrossRef]
13. González-Vidal, A.; Mendoza-Bernal, J.; Ramallo, A.P.; Zamora, M.Á.; Martínez, V.; Skarmeta, A.F. Smart Operation of Climatic Systems in a Greenhouse. *Agriculture* **2022**, *12*, 1729. [CrossRef]
14. Shamshiri, R.R.; Hameed, I.A.; Thorp, K.; Balasundram, S.K.; Shafian, S.; Fatemieh, M.; Sultan, M.; Mahns, B.; Samiei, S. Greenhouse Automation Using Wireless Sensors and IoT Instruments Integrated with Artificial Intelligence. In *Next-Generation Greenhouses for Food Security*; Intech: London, UK, 2021. [CrossRef]
15. López-Aguilar, K.; Benavides-Mendoza, A.; González-Morales, S.; Juárez-Maldonado, A.; Chiñas-Sánchez, P.; Morelos-Moreno, A. Artificial Neural Network Modeling of Greenhouse Tomato Yield and Aerial Dry Matter. *Agriculture* **2020**, *10*, 97. [CrossRef]
16. Kodali, R.K.; Jain, V.; Karagwal, S. IoT Based Smart Greenhouse. In Proceedings of the 2016 IEEE Region 10, Humanitarian Technology Conference (R10-HTC), Agra, India, 21–23 December 2016. [CrossRef]
17. Miraei Ashtiani, S.H.; Martynenko, A. Toward Intelligent Food Drying: Integrating Artificial Intelligence into Drying Systems. *Dry. Technol.* **2024**, *42*, 1240–1269. [CrossRef]
18. Sun, Q.; Zhang, M.; Mujumdar, A.S. Recent developments of artificial intelligence in drying of fresh food: A review. *Crit. Rev. Food Sci. Nutr.* **2018**, *59*, 2258–2275. [CrossRef]
19. Spagnuolo, A.; Vetromile, C.; Masiello, A.; De Santo, G.; Suriano, M.; Mercuri, G.; Pellegrino, M.; Piccolo, G.; Lubritto, C.; Di Cicco, M.R. Industrial Drying of Fruit and Vegetable Products: Customized Smart Monitoring and Analytical Characterization of Process Variables in the OTTORTO Project. *Processes* **2023**, *11*, 1635. [CrossRef]
20. Caponetto, R.; Fortuna, L.; Nunnari, G.; Occhipinti, L.; Xibilia, M.G. Soft Computing for Greenhouse Climate Control. *IEEE Trans. Fuzzy Syst.* **2000**, *8*, 753–760. [CrossRef]
21. Sifola, M.I.; del Piano, L.; Todisco, D.; Graziani, G.; Faugno, S.; Sannino, M.; Piscopo, R.; Salluzzo, A.; Cozzolino, E. A Multipurpose Sustainable Farming System for Tobacco Crops in the Mediterranean Area. *Sustainability* **2023**, *15*, 16636. [CrossRef]

22. Martínez-Martínez, V.; Baladrón, C.; Gomez-Gil, J.; Ruiz-Ruiz, G.; Navas-Gracia, L.M.; Aguiar, J.M.; Carro, B. Temperature and Relative Humidity Estimation and Prediction in the Tobacco Drying Process Using Artificial Neural Networks. *Sensors* **2012**, *12*, 14004–14021. [CrossRef] [PubMed]
23. Choi, H.; Moon, T.; Jung, D.H.; Son, J.E. Prediction of Air Temperature and Relative Humidity in Greenhouse via a Mutlilayer Perceptron Using Environmental Factors. *Prot. Hortic. Plant Fact.* **2019**, *28*, 95–103. [CrossRef]
24. Petrakis, T.; Kavga, A.; Thomopoulos, V.; Argiriou, A.A. Neural Network Model for Greenhouse Microclimate Predictions. *Agriculture* **2022**, *12*, 780. [CrossRef]
25. Jung, D.; Kim, H.S.; Jhin, C.; Kim, H.J.; Park, S.H. Time-series analysis of deep neural network models for prediction of climatic conditions inside a greenhouse. *Comput. Electron. Agric.* **2020**, *173*, 105402. [CrossRef]
26. Outanoute, M.; Lachhab, A.; Selmani, A.; Oubehar, H.; Guerbaoui, M. Neural network based models for estimating the temperature and humidity under greenhouse. *Int. J. Multi Discip. Sci.* **2016**, *3*, 26–33.
27. Taki, M.; Ajabshirchi, Y.; Ranjbar, S.F.; Matloobi, M. Application of Neural Networks and Multiple Regression Models in Greenhouse Climate Estimation. *Agric. Eng. Int. CIGR J.* **2016**, *18*, 29–43.
28. Singh, V.K.; Tiwari, K.N. Prediction of Greenhouse Micro-Climate Using Artificial Neural Network. *Appl. Ecol. Environ. Res.* **2017**, *15*, 767–778. [CrossRef]
29. Hornik, K.; Stinchcombe, M.; White, H. Multilayer feedforward networks are universal approximators. *Neural Netw.* **1989**, *2*, 359–366. [CrossRef]
30. Casquete, R.; Rodríguez, A.; Hernández, A.; Martín, A.; Bartolomé, T.; Córdoba, J.J.; Córdoba, M.G. Occurrence of Toxigenic Fungi and Mycotoxins during Smoked Paprika Production. *J. Food Prot.* **2017**, *80*, 2068–2077. [CrossRef]
31. Carbonell, J.V.; Piñaga, F.; Yusá, V.; Peña, J.L. The dehydration of paprika with ambient and heated air and the kinetics of colour degradation during storage. *J. Food Eng.* **1986**, *5*, 179–193. [CrossRef]
32. Mistriotis, A.; Bot, G.P.A.; Picuno, P.; Scarascia-Mugnozza, G. Analysis of the efficiency of greenhouse ventilation using computational fluid dynamics. *Agric. For. Meteorol.* **1997**, *85*, 217–228. [CrossRef]
33. Adhitya, R.Y.; Ramadhan, M.A.; Kautsar, S.; Rinanto, N.; Sarena, S.T.; Munadhif, I.; Syai'In, M.; Soelistijono, R.T.; Soeprijanto, A. Comparison methods of Fuzzy Logic Control and Feed Forward Neural Network in automatic operating temperature and humidity control system (Oyster Mushroom Farm House) using microcontroller. In Proceedings of the 2016 International Symposium on Electronics and Smart Devices (ISESD), Bandung, Indonesia, 29–30 November 2016; pp. 168–173. [CrossRef]
34. Mahmood, M.H.; Sultan, M.; Miyazaki, T. Significance of Temperature and Humidity Control for Agricultural Products Storage: Overview of Conventional and Advanced Options. *Int. J. Food Eng.* **2019**, *15*, 20190063. [CrossRef]
35. Vega-Gálvez, A.; Lemus-Mondaca, R.; Bilbao-Sáinz, C.; Fito, P.; Andrés, A. Effect of air drying temperature on the quality of rehydrated dried red bell pepper (var. Lamuyo). *J. Food Eng.* **2008**, *85*, 42–50. [CrossRef]
36. Sigge, G.O.; Hansmann, C.F.; Joubert, E. Effect of Temperature and Relative Humidity on the Drying Rates and Drying Times of Green Bell Peppers (*Capsicum annuum* L). *Dry. Technol.* **1998**, *16*, 1703–1714. [CrossRef]
37. Nouri, N.M.; Abbood, H.M.; Riahi, M.; Alagheband, S.H. A review of technological developments in modern farming: Intelligent greenhouse systems. *AIP Conf. Proc.* **2023**, *2631*, 030012. [CrossRef]
38. Sabudin, S.; Hakimi Remlee, M.Z.; Mohideen Batcha, M.F. Effect of relative humidity on drying kinetics of agricultural products. *Appl. Mech. Mater.* **2014**, *699*, 257–262. [CrossRef]
39. Tsafaras, I.; Campen, J.B.; Stanghellini, C.; de Zwart, H.F.; Voogt, W.; Scheffers, K.; Al Harbi, A.; Al Assaf, K. Intelligent greenhouse design decreases water use for evaporative cooling in arid regions. *Agric. Water Manag.* **2021**, *250*, 106807. [CrossRef]
40. Soussi, M.; Chaibi, M.T.; Buchholz, M.; Saghrouni, Z. Comprehensive Review on Climate Control and Cooling Systems in Greenhouses under Hot and Arid Conditions. *Agronomy* **2022**, *12*, 626. [CrossRef]
41. Mishra, S.; Verma, S.; Chowdhury, S.; Dwivedi, G. Analysis of recent developments in greenhouse dryer on various parameters—A review. *Mater. Today Proc.* **2021**, *38 Pt 1*, 371–377. [CrossRef]
42. Jamwal, A.; Agrawal, R.; Sharma, M.; Giallanza, A. Industry 4.0 Technologies for Manufacturing Sustainability: A Systematic Review and Future Research Directions. *Appl. Sci.* **2021**, *11*, 5725. [CrossRef]
43. Howard, D.A.; Ma, Z.; Veje, C.; Clausen, A.; Aaslyng, J.M.; Jørgensen, B.N. Greenhouse Industry 4.0–Digital Twin Technology for Commercial Greenhouses. *Energy Inform.* **2021**, *4*, 37. [CrossRef]
44. D'Antonio, P.; Fiorentino, C.; Abdelrahman, M.A.E.; Sannino, M.; Scalcione, E.; Lacertosa, G.; Modugno, F.; Marsico, A.; Donvito, A.R.; Conceição, L.A.; et al. Modeling Climatic, Terrain and Soil Factors Using AHP in GIS for Grapevines Suitability Assessment. *Sustain. Dev.* **2024**, *33*, 970–991. [CrossRef]
45. Nidhi, D.; Verma, P. A Review Paper on Solar Greenhouse. In Proceedings of the 3rd National Conference on Advances in Engineering, Technology & Management (AETM'16), Ambala, India, 9 April 2016; pp. 43–48. [CrossRef]
46. Ahmad, A.; Prakash, O.; Kumar, A.; Chatterjee, R.; Sharma, S.; Kumar, V.; Kulshreshtha, K.; Li, C.; Eldin, E.M.T. A Comprehensive State-of-the-Art Review on the Recent Developments in Greenhouse Drying. *Energies* **2022**, *15*, 9493. [CrossRef]

47. Burchi, G.; Chessa, S.; Gambineri, F.; Kocian, A.; Massa, D.; Milazzo, P.; Rimediotti, L.; Ruggeri, A. Information Technology Controlled Greenhouse: A System Architecture. In Proceedings of the 2018 IoT Vertical and Topical Summit on Agriculture—Tuscany (IOT Tuscany), Tuscany, Italy, 8–9 May 2018; pp. 1–6. [CrossRef]
48. Elmatsani, H.; Munarso, S.; Benyamin, B.; Budiyanto, A.; Yohanes, H.; Djafar, M.; Sjafrina, N.; Koeslulat, E.; Lukas, A.; Lanjar, L.; et al. Global perspective on red chili drying: Insights from two decades of research (2004–2023). *Front. Sustain. Food Syst.* **2024**, *8*, 1456938. [CrossRef]
49. Sannino, M.; Faugno, S.; Maresca, G.; Suardi, A.; Fiorentino, C.; Assirelli, A.; Panico, T. Olive growing in the Sorrento Peninsula: Operative, economic, and environmental evaluation trough LCA of mechanical harvesting. *Heliyon* **2024**, *10*, e40461. [CrossRef]

Recent Developments and Future Prospects in the Integration of Machine Learning in Mechanised Systems for Autonomous Spraying: A Brief Review

Francesco Toscano, Costanza Fiorentino, Lucas Santos Santana, Ricardo Rodrigues Magalhães, Daniel Albiero, Řezník Tomáš, Martina Klocová and Paola D'Antonio

Pubblicazione: Rivista AgriEngineering, editore MDPI (Volume 7, Issue 5, Articolo 142, Anno 2025)
https://doi.org/10.3390/agriengineering7050142

AgriEngineering

MDPI

Review

Recent Developments and Future Prospects in the Integration of Machine Learning in Mechanised Systems for Autonomous Spraying: A Brief Review

Francesco Toscano [1,*], Costanza Fiorentino [1], Lucas Santos Santana [2], Ricardo Rodrigues Magalhães [3], Daniel Albiero [4], Řezník Tomáš [5], Martina Klocová [5] and Paola D'Antonio [1]

[1] School of Agricultural, Forestry, Environmental and Food Sciences, University of Basilicata, 85100 Potenza, Italy; costanza.fiorentino@unibas.it (C.F.); paola.dantonio@unibas.it (P.D.)
[2] Agricultural Engineering Department, Federal University of Vale Jequitinhonha e Mucuri, Unaí 38610-001, Brazil; santana.santos@ufvjm.edu.br
[3] School of Engineering, Federal University of Lavras, Lavras 37200-900, Brazil; ricardorm@ufla.br
[4] Faculdade de Engenharia Agrícola, Universidade Estadual de Campinas, Campinas 13083-875, Brazil; dalbiero@unicamp.br
[5] Laboratory on Geoinformatics and Cartography, Department of Geography, Faculty of Science, Masaryk University, Kotlarska 2, 611 37 Brno, Czech Republic; tomas.reznik@sci.muni.cz (R˘.T.); martina.klocova@gmail.com (M.K.)
* Correspondence: francesco.toscano@unibas.it

Abstract: The integration of machine learning (ML) into self-governing spraying systems is one of the major developments in digital precision agriculture that is significantly improving resource efficiency, sustainability, and production. This study looks at current advances in machine learning applications for automated spraying in agricultural mechanisation, emphasising the new innovations, difficulties, and prospects. This study provides an in-depth analysis of the three main categories of autonomous sprayers—drones, ground-based robots, and tractor-mounted systems—that incorporate machine learning techniques. A comprehensive review of research published between 2014 and 2024 was conducted using Web of Science and Scopus, selecting relevant studies on agricultural robotics, sensor integration, and ML-based spraying automation. The results indicate that supervised, unsupervised, and deep learning models increasingly contribute to improved real-time decision making, performance in pest and disease detection, as well as accurate application of agricultural plant protection. By utilising cutting-edge technology like multispectral sensors, LiDAR, and sophisticated neural networks, these systems significantly increase spraying operations' efficiency while cutting waste and significantly minimising their negative effects on the environment. Notwithstanding significant advances, issues still exist, such as the requirement for high-quality datasets, system calibration, and flexibility in a range of field circumstances. This study highlights important gaps in the literature and suggests future areas of inquiry to develop ML-driven autonomous spraying even more, assisting in the shift to more intelligent and environmentally friendly farming methods.

Keywords: self-governing spraying systems; digital precision agriculture; agricultural mechanisation; agricultural robotics; agricultural plant protection

Academic Editor: Ray E. Sheriff

Received: 1 March 2025
Revised: 21 April 2025
Accepted: 24 April 2025
Published: 6 May 2025

Citation: Toscano, F.; Fiorentino, C.; Santana, L.S.; Magalhães, R.R.; Albiero, D.; Tomáš, R˘.; Klocová, M.; D'Antonio, P. Recent Developments and Future Prospects in the Integration of Machine Learning in Mechanised Systems for Autonomous Spraying: A Brief Review. *AgriEngineering* **2025**, *7*, 142. https://doi.org/10.3390/agriengineering7050142

1. Introduction

Climate change, sometimes shown in extreme weather or prolonged droughts, and the increasing complexity of weed and disease management can have a negative impact

on crop output [1]. Consumers are becoming increasingly aware of the significant issues with excessive fertiliser and pesticide use in relation to agricultural sustainability [2,3].

Over the decades, a series of technical and technological innovations have radically transformed modern agriculture [4]. Agricultural mechanisation, in particular, has enabled a dramatic increase in the productivity efficiency of agroecosystems. Mechanised systems have reduced manual labour and improved the precision of agricultural operations [5]. Modern mechanisation challenges are related to operational efficiency, precision, and the implementation of technologically innovative equipment [6]. A major limitation of mechanisation is the inability of these machines to dynamically adapt to variable field conditions and the specific needs of crops [7]. In this context, the implementation of artificial intelligence systems plays a decisive role in shaping the research and development lines in the sector. Specifically, machine learning (ML) represents one of the most promising and cutting-edge technologies for overcoming the typical limitations of traditional mechanised systems [8]. ML algorithms enable agricultural machines to dynamically learn new operational modes through data analysis, adapting with high precision to field variables and thus optimising agricultural operations in real time [9]. In agriculture, ML is proving essential for optimising crop management, reducing waste, and increasing sustainability.

Due to its ability to analyse large amounts of heterogeneous data, ML can enhance the effectiveness of mechanised systems and elevate them to a higher level. Among the main lines of development and implementation of these innovative systems, the following can certainly be found:

a. Detection of weeds, diseases, and crop stress: through computer vision algorithms, images or data collected by drones, onboard sensors, satellites, etc., can be analysed to proactively identify and assess the presence of weeds, diseases, or stress conditions (e.g., water stress) [10];
b. Optimization in the application of agronomic resources [11];
c. Automation of guidance systems [12];
d. Predictive analysis for strategic crop management [13].

The combination of agricultural mechanisation and machine learning has led to the development of intelligent, integrated systems, representing the future of crop management. This synergy offers unprecedented advantages, making agriculture more resilient, sustainable, and productive. Among the main practical examples of fruitful integration, we find autonomous robots with computer vision [14], intelligent tractors [15], drones for monitoring and spraying [16], intelligent sprayers with multispectral sensors [17], automated harvesting [18], digital precision irrigation [19,20], intelligent automated planning of management operations [21], predictive diagnostics for machinery maintenance [22], etc.

In this highly dynamic scenario, technological innovations driving digital precision agriculture (DPA) are called upon to play a central and significant role, optimising strategic resource management and improving production sustainability [23]. These technologies are particularly useful for effectively managing the main operational and management issues of various crops (e.g., fungal diseases, fertiliser management, phytosanitary product management, etc.).

The purpose of this study is to present an organised overview of the latest advances and potential directions in the use of ML in agricultural mechanised systems for autonomous spraying. This strategy is appropriate given the increasing need to improve agricultural methods in order to solve issues with food security, environmental sustainability, and production efficiency.

This paper also seeks to contribute to the understanding of the transformative potential of machine learning in agricultural mechanisation related to spraying systems in agriculture. In this landscape of practical applications, autonomous spraying [24] represents one of the most advanced and promising areas in precision agriculture, combining mechanical technologies and artificial intelligence to optimise the application of phytosanitary products, fertilisers, and other agronomic resources. In an autonomous sprayer operation, it is essential to define an accurate knowledge representation (KR) so that the state function is referenced in real time through data from sensors and communication systems so that artificial intelligence methods can make decisions [25].

Three main types of autonomous spraying systems are available: drones [26], ground robots [27], and tractor-mounted sprayers [28]. Drones are a cutting-edge autonomous spraying device that works especially well in challenging terrain. They provide remote sensing via multispectral or thermal cameras, quick coverage, and accurate application using GPS and sophisticated sensors. They optimise the application techniques, cutting waste and enhancing sustainability when combined with machine learning algorithms. Ground robots are self-driving vehicles with sophisticated sensors (thermal, LiDAR, and multispectral), self-navigating systems, and nozzles that can be adjusted to precisely manage crops. They may administer tailored treatments and cut down on waste by using computer vision to analyse real-time photos and identify illnesses or pests. Sprayers mounted on tractors, finally, represent a traditional and widely used solution in precision mechanisation, yet in recent years, they have been significantly improved through the integration of advanced technologies, such as field harvesters [29]. Equipped with multispectral sensors, assisted or autonomous guidance systems, and variable control nozzles, these sprayers optimise the application of products, reducing waste and ensuring precise operation even on uneven terrain.

2. Research Methodology

In this brief review, the state of the art regarding the integration of ML in mechanised autonomous spraying systems was analysed. This review was conducted through a systematic examination of recent progress in the field. A comprehensive literature review was carried out, with particular emphasis on the last 10 years (2014–2024), in order to locate the most relevant studies that had been published. The two main databases used for the search were Web of Science and Scopus. The search terms included combinations of keywords such as “machine learning”, “autonomous spraying”, “mechanized systems”, “precision agriculture”, “robotic sprayers”, “sensor integration”, and “agricultural robotics”. Scientific articles, conference papers, and book chapters were considered, and the findings of the latest available reviews in the literature were also analysed.

Following the identification of pertinent contributions, an examination was conducted of the technological elements (sensors, machine learning algorithms, and mechanised systems), the effectiveness, precision, and environmental impact of autonomous spraying systems, as well as particular machine learning applications like disease prediction, pest detection, and resource optimisation.

Inclusion criteria were defined to select peer-reviewed studies focusing on the application of machine learning techniques within autonomous or semi-autonomous spraying systems in agricultural settings. Exclusion criteria involved papers that addressed the general uses of machine learning in agriculture without specific reference to mechanised spraying, studies lacking empirical validation, and works published in non-English languages or not accessible through institutional databases.

Qualitative analysis was used to evaluate the research:

a. **Technological Trends:** The most widely utilised machine learning algorithms, sensors, and technology in autonomous spraying systems were determined. The integration of sensors (such as LiDAR and multispectral cameras) with machine learning models for real-time decision-making processes received particular attention.
b. **Progress in Automation:** Recent developments in autonomous systems, such as enhanced robot navigation, precise spraying, and the systems' capacity to adjust to changing field circumstances, were the main emphasis of this review.
c. **Effectiveness and Impact:** These systems' performance was assessed in terms of environmental sustainability, resource conservation, agricultural production enhancement, and operating efficiency.
d. **Challenges and Limitations:** The limitations and challenges highlighted in the studies, such as the need for high-quality data, system calibration, or field-specific adaptations, were critically analysed.

This scientific review's main goal was to comprehend and precisely characterise the ways in which machine learning is combined with sensor technologies in autonomous spraying systems.

Various machine learning model types that fall into three groups were examined and explored in this context:

a. **Supervised Learning:** Algorithms trained on labelled datasets to identify patterns and make predictions on crop health, pest infestations, or diseases.
b. **Unsupervised Learning:** Algorithms for detecting anomalies and grouping in sensor data, especially to find unanticipated occurrences like fungal infections or water stress.
c. **Deep Learning:** High-resolution photographs taken by drones or ground robots can be utilised to diagnose illnesses or infestations using sophisticated neural networks for image identification and analysis.

To provide a structured overview of the key aspects covered in this study, Figure 1 presents a conceptual map outlining the main themes explored, including machine learning approaches, technological trends, and existing challenges in autonomous spraying systems.

It should be mentioned that although this study offered a thorough examination of the most recent advances in the field, its focus was restricted to research conducted in the context of autonomous spraying. Developing control architectures for sprayers based on behaviours adapted to the unstructured agricultural environment directly leads to the need to develop machine learning methods with a 'decomposition' of behaviour into small sub-behaviours that can be modelled in supervised or unsupervised networks [25]. Crop management techniques other than mechanised spraying and general uses of machine learning in agriculture were excluded. This review's methodological approach is to provide a systematic and comprehensive overview of the present research situation, pointing out gaps in the literature and offering suggestions for future advancements in the incorporation of machine learning into autonomous spraying systems.

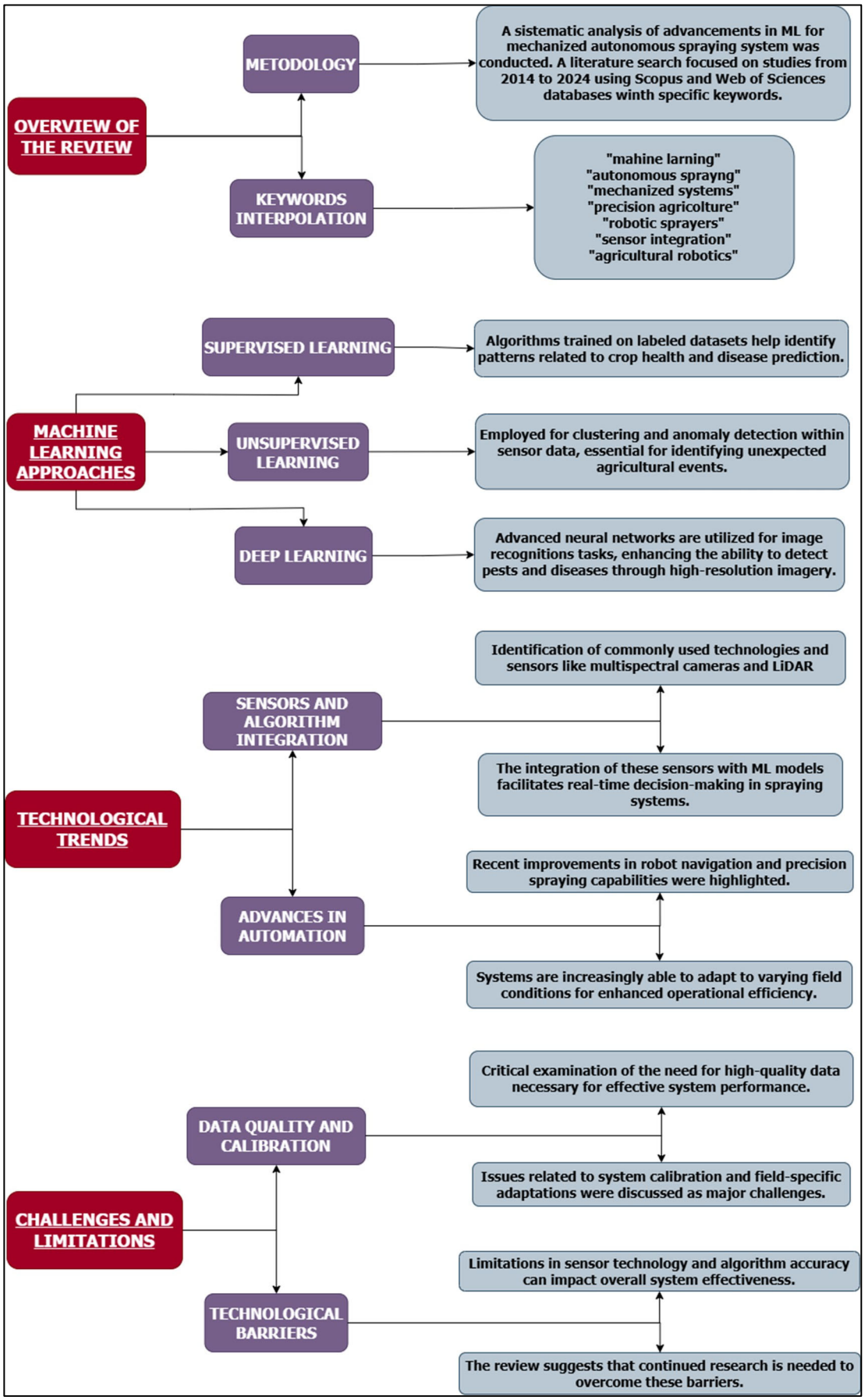

Figure 1. Conceptual map outlining the key aspects of this study, including an overview of this review, machine learning approaches, technological trends, and challenges in autonomous spraying systems.

3. Results

The integration of ML in mechanised autonomous spraying systems has made significant progress in recent years, with a growing focus on the use of advanced sensors and machine learning algorithms. The fusion of data from multiple sensors is crucial for enhancing the accuracy of autonomous spraying systems. The integration of RGB (red, green, and blue) cameras, LiDAR, and multispectral sensors provides a more comprehensive understanding of the agricultural environment. For example, Ban et al. [30] developed a method based on the fusion of data from a monocular RGB camera, a 3D LiDAR, and an inertial measurement unit (IMU) for the real-time extraction of navigation lines between corn rows (Figure 2). Using an advanced algorithm for creating maps of green features and filtering LiDAR data, the system achieved a 90% accuracy rate and an average angular error of 1.84°, significantly improving the navigation of agricultural robots in complex environments.

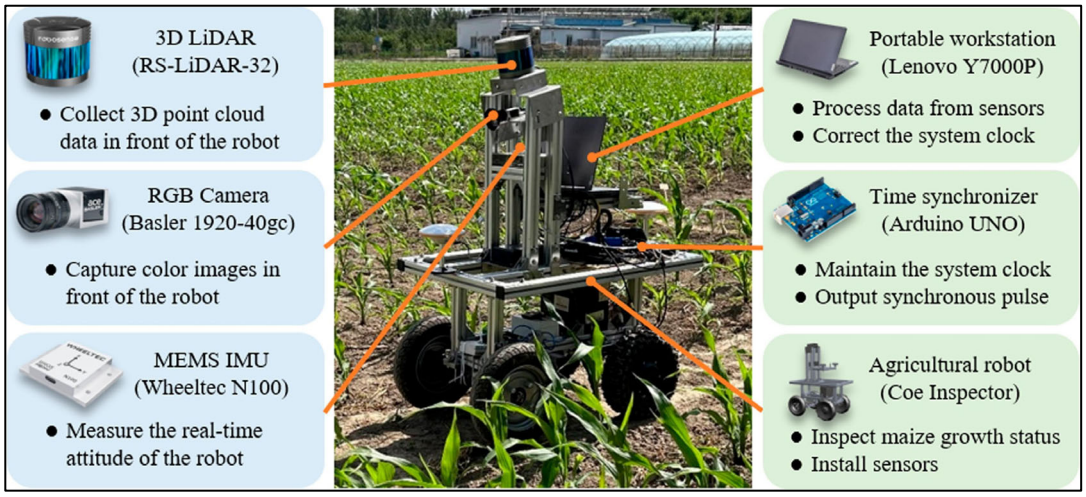

Figure 2. Multiple sensor device developed by Ban et al. Adapted from [30], © 2024, licensed under CC BY-NC-ND.

An advanced system based on fully convolutional networks (FCNs) was designed by Lottes et al. [31] for stem detection and pixel-wise classification of crops and weeds. By using RGB and NIR (near infrared) images, the model demonstrated a high level of generalisation, even on fields not included in the training phase. Additionally, Shi et al. [32] analysed advanced techniques for crop row detection, utilising sensors such as monocular, stereo cameras, and LiDAR, combined with deep learning algorithms like Faster R-CNN and YOLO. The multi-sensor fusion enhanced the robustness and accuracy of autonomous navigation in agricultural fields. In their paper, Arsalan et al. [33] compared the YOLOv5 and YOLOv6 models for tobacco plant detection and segmentation, using the TobSet dataset (Figure 3).

Aerial photos taken with a Mavic Mini drone were used to assess the models. While YOLOv5-seg fared better with smaller and overlapping plants, YOLOv6 showed higher accuracy and quicker recognition than YOLOv5. Later, Khan et al. [34] used sophisticated methods such dilated convolutions and the adaptive gradient algorithm to enhance the YOLOv8 algorithm for real-time segmentation of fruit tree canopies (Figure 4).

The study's average accuracy of 93.3% and the 40% reduction in spraying waste demonstrated the model's effectiveness in precision spraying for complex agricultural environments. In the study conducted by Jin et al. [35], the efficacy of deep convolutional neural networks (DCNNs) in recognising and distinguishing turfgrass weeds based on their herbicide sensitivity was demonstrated. The study looked at models like VGG-Net, ShuffleNet-v2, MobileNet-v3, and GoogLeNet. Similarly, a deep (CNN)-based method

for weed identification and classification in agricultural environments was developed and assessed by Pattanik et al. [36]. The work focussed on using sophisticated deep learning methods, including CNNs, rectified linear units (ReLUs), and the SoftMax classifier, to analyse images and differentiate between weeds and crops. To improve crop-weed classification accuracy, the proposed approach makes use of machine learning techniques including scale-invariant feature transform (SIFT) and speeded-up robust features (SURFs) as well as artificial visual analysis systems. When these technologies were combined with neural networks and ensemble learning techniques, it was shown that crop photos could be accurately classified. As an alternative, Huynh and Nguyen [37] provided a real-time droplet identification system for agricultural spraying systems that used a CNN for video input (Figure 5).

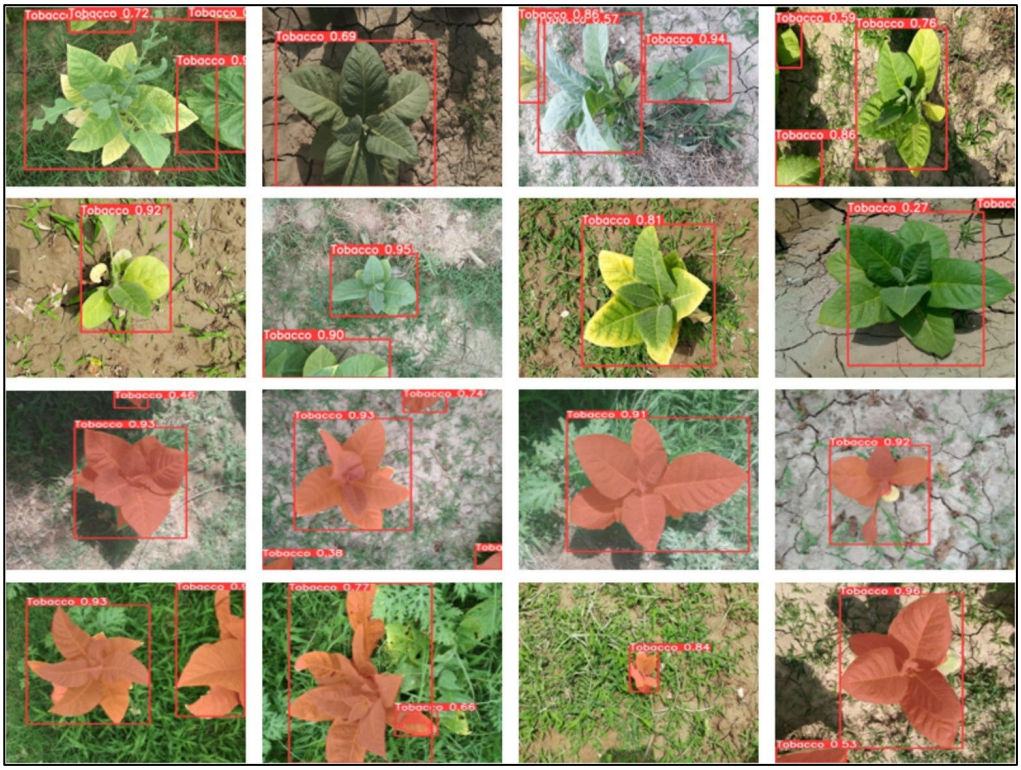

Figure 3. Comparison of tobacco plant detection using YOLOv5s and YOLOv6s Adapted from [33], © 2024, licensed under CC BY-NC-ND.

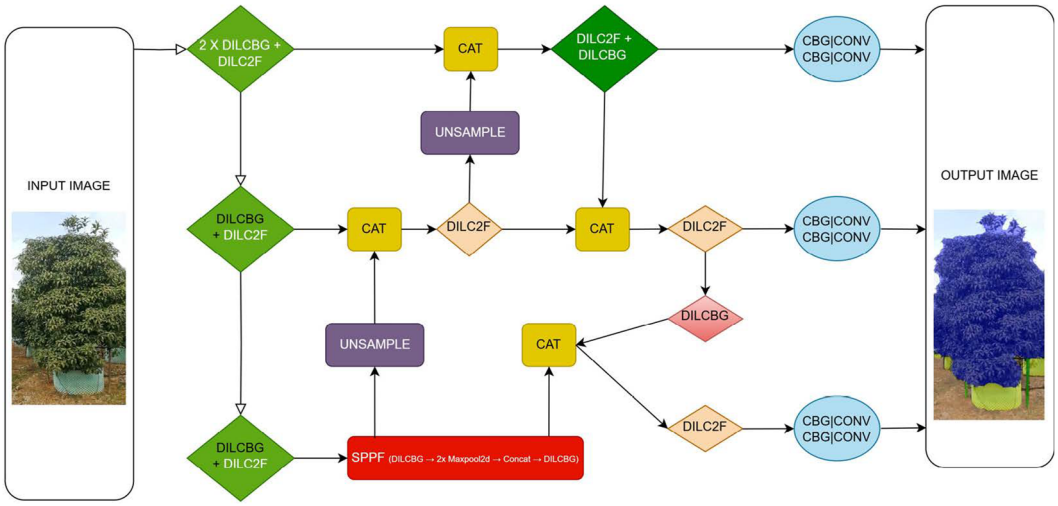

Figure 4. Schematic representation of the improved YOLOv8 model structure diagram.

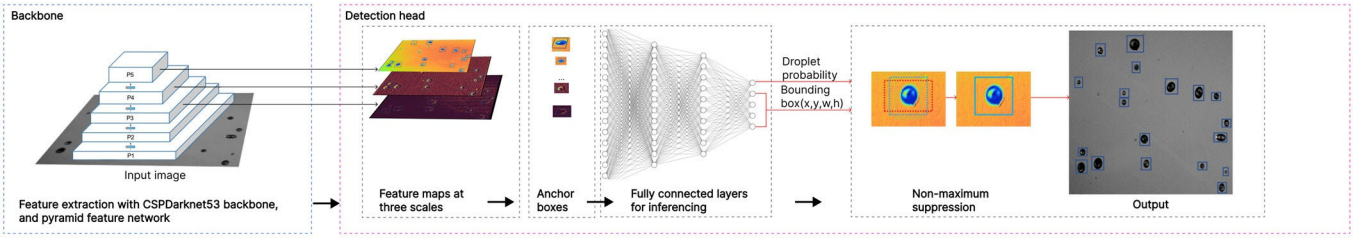

Figure 5. The framework of the droplet detector. Reproduced from [37], © 2024, licensed under CC BY 4.0.

The technology, which is intended for embedded devices with constrained resources, provides excellent droplet detection precision even in the presence of fast movement or low light levels. The system's capacity to maximise fertiliser and pesticide use, improving spraying operations' sustainability and efficiency, is highlighted in the results. Modi et al. [38] created a deep learning-based system for the autonomous identification of weeds in sugarcane fields (Figure 6) using a dataset of more than 5600 photos and testing models like DarkNet53 and ResNet50. The system achieved an accuracy of 96.6% and an F1 score higher than 99%, demonstrating the potential of deep learning in precise weed management.

Furthermore, Gao et al. [39] used a machine learning approach based on the mutual subspace method (MSM) to create a recognition system to detect spraying locations utilising unmanned aerial vehicles (UAVs). By efficiently differentiating between areas that need to be sprayed and those that do not, this system seeks to improve precision pesticide spraying while providing high computing speed and accuracy.

The automation of spraying systems has benefited from the use of autonomous vehicles, drones, and agricultural robots. Today, real-time agricultural monitoring systems based on deep learning and wireless sensors are available [40]. An autonomous unit detects weeds through a camera, transmits the images to a deep learning model, and activates targeted herbicide spraying. In their article, "The Deployment of Machine Learning and On-Board Vision Systems for an Unmanned Aerial Sprayer for Pesticides", Karrar S. Mohsin et al. [41] presented the development of an autonomous pesticide spraying system integrating machine learning and computer vision technologies. The drone can recognise and find target regions thanks to the computer vision technologies, and the system uses machine learning algorithms to evaluate the environmental data and optimise spraying parameters. By enhancing pesticide application efficiency and accuracy, this technology combination seeks to minimise environmental effects and chemical consumption. The suggested strategy provides a novel approach to agricultural management, encouraging more focused and sustainable methods.

Kameswari et al. [42] presented an autonomous pesticide-spraying robot based on machine learning techniques in the field of agricultural robotics with the goal of increasing crop output while lowering labour needs. The system employs an support vector machine (SVM) image classifier to automatically detect the path, operating with a supervised learning approach. As the robot moves, it captures images with a Pi-Camera, analyses them to identify the path, and sprays water or pesticides based on the needs. Additionally, it uses the Plantix app to monitor plant health by analysing real-time photographs. The Raspberry Pi 3 CPU controls the complete system and gives the motor driver instructions to manoeuvre the robot. This project is an innovative example of agricultural automation, utilising machine learning and robotics to boost the productivity of agricultural operations. Also, Wijesundara et al. [43] described the development of an autonomous agricultural robot designed for precise pesticide application. The system uses state-of-the-art computer vision technologies for accurate plant identification and RTK-GPS technology for

navigation along present paths. Positive outcomes from tests carried out in a field of potted plants demonstrated how well the robot works to increase agricultural productivity and encourage more environmentally friendly methods. Similar to this, Khan et al. [44] demonstrated a GPS-guided autonomous agricultural robot equipped with an automatic weeding and fertilisation system. This gadget selectively applies pesticides and detects weeds using machine learning techniques. The system combines Raspberry Pi, Arduino, and RTK GPS for precise navigation. Although weed recognition and the addition of more sophisticated sensors might be improved, experimental testing validated the robot's capacity to function independently in fields. Huynh et al. [45] described an autonomous agricultural robot that combines a deep learning algorithm for targeted plant spraying with a sophisticated navigation system. With the use of sophisticated sensors to identify impediments and optimise routes, the robot can move around the field at a steady pace and on its own. By identifying plants with high accuracy, the deep learning system increased spraying efficiency and decreased the usage of pesticides. The results from experiments support the system's efficacy and suggest that it might improve agricultural productivity and sustainability. Faikal et al. [46], on the other hand, have already created autonomous UAVs for pesticide spraying by combining artificial neural networks (PSO-ANNs) and optimisation approaches (particle swarm optimisation). The technology provided an efficient and long-lasting solution for autonomous crop management by increasing spraying accuracy and minimising environmental impact. Göktoglan and Sukkarieh [47] investigated UAV systems further and used unmanned aerial vehicles (UAVs) to monitor and control weeds in challenging regions. They tested using UAVs with multispectral sensors to create maps of infestations and automatically administer herbicides in different parts of Australia. The solution reduced costs and operational risks, demonstrating the effectiveness of UAVs in precision agriculture management. Significant gains in sustainability and operating efficiency have been demonstrated by autonomous spraying systems. Using a 2D LiDAR system to identify tree trunks and move between rows, Jiang et al. [48] created an autonomous robot for orchard spraying (Figure 7).

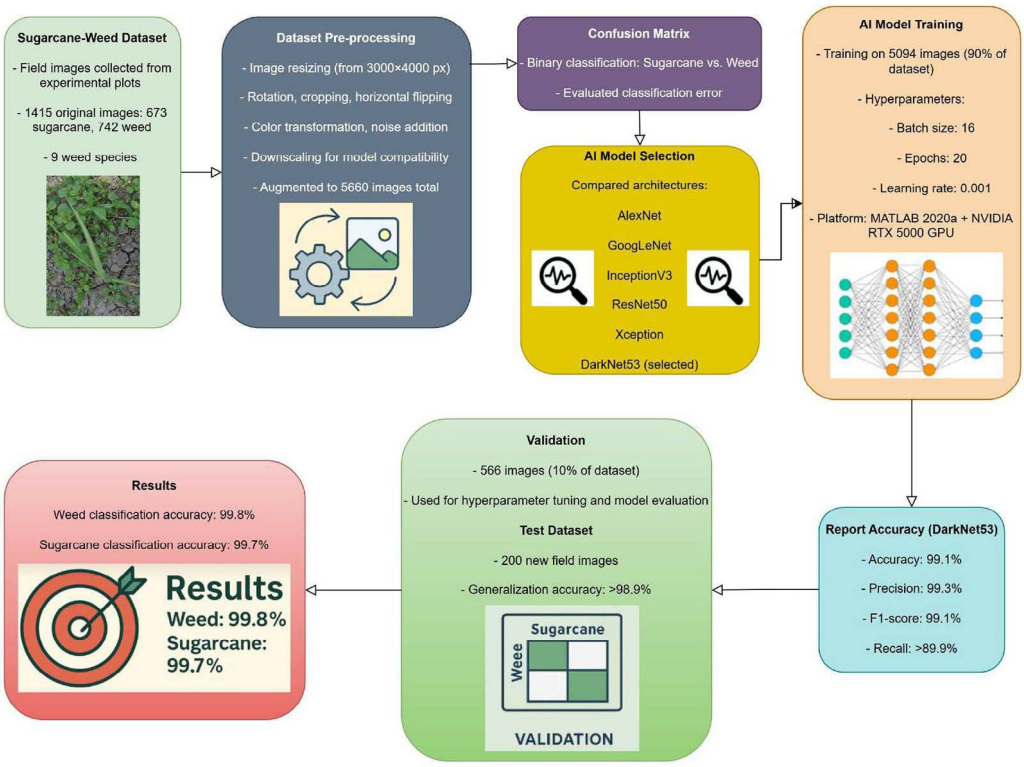

Figure 6. Synoptical deep learning map for autonomous weed identification in sugarcane fields.

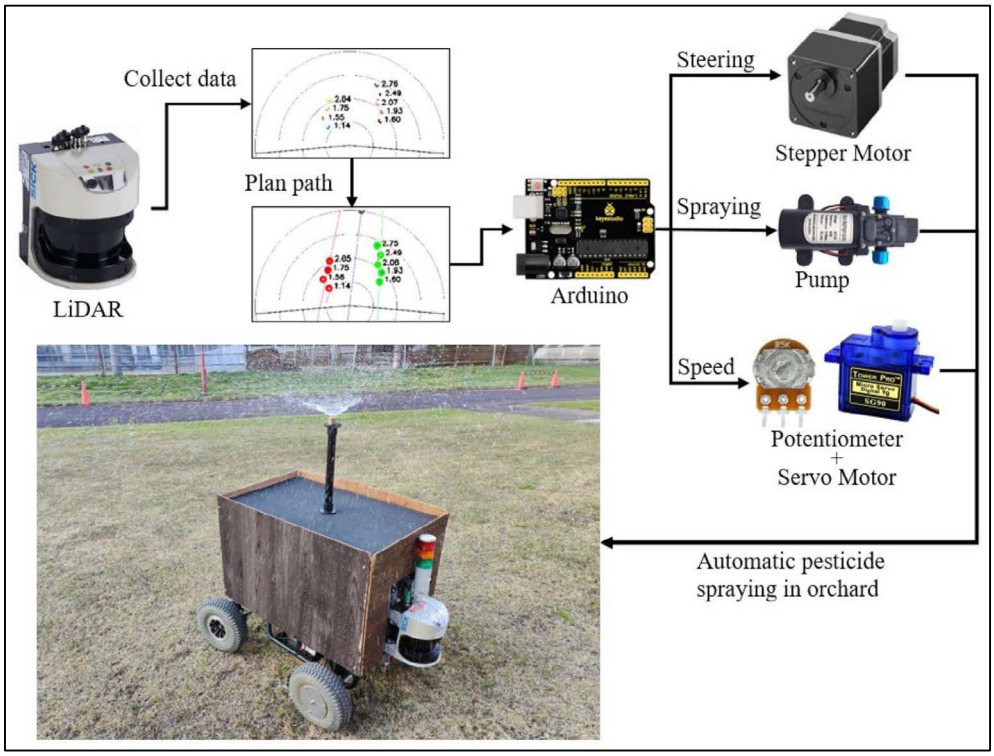

Figure 7. Two-dimensional LiDAR-based navigation system design for facilitated orchards using a converted electrical vehicle as a spraying robot. Reproduced from [48], © 2023, licensed under CC BY 4.0.

The system processes point clouds and plans the robot's itinerary using clustering techniques including DBSCAN, K-means, and RANSAC. With mean positioning errors varying from 11.4 cm to 15.5 cm depending on the terrain and turning orientation, field testing has shown that the robot can safely and efficiently perform spraying duties while calculating its path in real time. Researchers have studied the development of vision-based autonomous vehicles for agricultural applications in great detail. The use of machine learning algorithms including regressions, SVM, and KNN was studied by Thakur et al. [49]. The use of ensemble methods and hybrid algorithms, which integrate many base estimators to improve accuracy and resilience, is growing in popularity. These methods, which are mostly used with Python and R, increase the processing speed for big datasets and optimise farming operations like harvesting and spraying. When Balasingham et al. [50] created SPARROW, an autonomous agricultural robot for weed elimination, they integrated a targeted spraying algorithm to autonomously recognise weeds and arrange the direction of the nozzle, confirming the effectiveness of robot spraying. The robot can accurately follow crop rows by using a vision-based navigation system that synchronises with the spraying algorithm. This inexpensive approach seeks to minimise environmental effect, increase efficiency, and decrease the usage of herbicides. Additionally, Ji et al. [51] created an autonomous indoor irrigation robot by combining cutting-edge sensors and navigation algorithms to guarantee accurate and consistent watering. While the frame stays still, the robot may spray a large variety of walls since it travels along the Y-axis. Its sophisticated sensors enable accurate and autonomous navigation by tracking position and monitoring ambient variables. Effective irrigation is ensured by the spraying system's ability to distribute liquid uniformly across target surfaces. The robot's mechanical design increases its adaptability in interior areas by allowing it to adjust to different ambient conditions. The robot's autonomy has led to more efficient irrigation management, reducing the time and resources required for operation. This system guarantees precise and uniform irrigation, reducing human intervention and increasing process efficiency. Despite progress, a number

of obstacles still stand in the way of these technologies' widespread deployment. As noted in 2020 by Danton et al. [52], one of the main challenges in the creation of an autonomous agricultural robot intended for the accurate delivery of fertiliser is the requirement for high-quality data to train machine learning algorithms. The device incorporates sensors to track soil conditions, actuators to distribute fertiliser precisely, and GPS for self-navigating. Robot control is made simpler by the user interface and navigation algorithms. Adoption of such technology can encourage more sustainable farming practices, since field testing has shown effective waste reduction and increased agricultural efficiency. Moreover, in 2024, Alshbatat et al. [53] emphasised the difficulties in adapting these systems to variable environmental conditions, especially for early disease detection in medicinal herb plants. However, the authors succeeded in developing an intelligent autonomous agricultural robot to detect and treat diseases in medicinal herb plants. With the use of artificial intelligence and Internet of Things technology, the robot can identify problems like leaf yellowing early and halt movement to administer preventative therapies. The system's deep learning algorithms and Pixy camera allow producers to make quick judgements, increasing greenhouse plant disease management effectiveness. Lastly, Singh et al. [54] described the creation and experimental verification of an agricultural intelligent drone that uses machine learning and image processing methods to spray crops. By using machine learning algorithms to evaluate photos taken by onboard drone sensors, the suggested solution makes it possible to precisely identify regions that require treatment and apply fertiliser or pesticide where it is needed. By reducing excessive chemical use, this system seeks to minimise environmental damage and encourage more sustainable agriculture practices. The drone's ability to increase spraying efficiency, guarantee consistent treatment distribution, and lower operating costs has been shown through experimental validation.

Practically speaking, the findings and comparative analysis presented in this paper offer concrete recommendations for the selection and implementation of autonomous machine learning (ML)-based spraying systems across different agricultural settings. By analysing ML techniques and sensor integration—together with an evaluation of technological maturity, adaptability, and decision-making autonomy—this review provides practical insights to guide the identification of the most appropriate solutions based on crop type, farm size, and specific operational requirements.

As an example, platforms integrating Camera-LiDAR-IMU fusion with YOLOv8-based segmentation demonstrate strong perceptual performance and a high degree of technological maturity, positioning them as viable options for commercial deployment in structured environments like orchards and vineyards. In contrast, systems still in early development—such as autonomous sprayers for indoor agriculture—are currently better suited for experimental trials or use within controlled cropping systems. This study's comparative methodology also offers a helpful guide for making investment decisions. Larger operations could profit from more complex platforms combining UAVs, LiDAR, and cutting-edge deep learning techniques, while small and medium-sized farms might find it easier to implement lightweight and affordable solutions (such as CNNs combined with embedded video cameras).

The potential of integrating these technologies into broader digital agricultural platforms and decision support systems is highlighted by their emphasis on flexibility and decision autonomy. It is precisely this integration that allows autonomous spraying systems to be able to react instantaneously to crop conditions, weather patterns or insect outbreaks, thus facilitating more adaptable and sustainable agricultural management techniques.

4. Discussion

Mechanised autonomous spraying systems that use ML have shown notable improvements in accuracy, productivity, and environmental sustainability.

ML offers significant advantages over traditional, classical methods in precision agriculture, particularly in the context of autonomous spraying systems. These systems benefit from enhanced accuracy, efficiency, and sustainability when compared to conventional approaches, which often rely on uniform spraying techniques that can lead to overuse of chemicals and unnecessary environmental impact. ML-based systems, on the other hand, can dynamically adjust to specific environmental conditions, detect plant and weed types more accurately, and target pesticide application more precisely. This precision reduces the quantity of pesticides and fertilisers used, directly supporting sustainability goals by minimising waste and environmental harm. Furthermore, ML systems continuously improve through training, adapting to changing variables in the field—such as crop growth stages, weather conditions, and terrain diversity—enabling better decision-making and real-time adjustments that traditional methods simply cannot match. Nevertheless, in order to facilitate widespread adoption, a number of issues still need to be looked at and resolved. Large amounts of high-quality labelled data are required for ML-based technological solutions in order to guarantee correct generalisation and reduce mistakes throughout the spraying process. In this regard, obtaining good performance in machine learning models depends critically on the calibre and volume of data utilised for training. A fundamental aspect concerns the fusion of data from heterogeneous sensors, such as monocular cameras, LiDAR, and multispectral sensors.

The integration of advanced technologies into autonomous spraying systems is revolutionising precision agriculture by enhancing monitoring capabilities and enabling targeted interventions. Recent studies have highlighted the key role of unmanned aerial vehicles (UAVs) equipped with hyperspectral and multispectral sensors in supporting more accurate agronomic decisions. Sousa et al. [55] demonstrated how push-broom and snapshot sensors mounted on UAVs can optimise targeted spraying in viticulture applications, allowing for more precise pesticide distribution and reduced environmental impact. Similarly, Pádua et al. [56] showed the effectiveness of multi-temporal vegetation monitoring using UAV-based RGB imagery to improve vineyard spraying management, enabling timely and localised interventions. Furthermore, the adoption of machine learning algorithms for data analysis has opened new avenues for intelligent pest control. Guimarães et al. [57] developed a system based on multispectral UAV data and ML classifiers to detect aphids in vineyards, allowing for a more precise application of biological or chemical control agents. These findings confirm that the fusion of machine learning, advanced sensor technology, and UAV systems is one of the most promising strategies for optimising autonomous spraying, ensuring more efficient resource use and greater sustainability in agricultural practices. The integration of sensors that operate at different frequencies and provide information with varying levels of detail presents challenges that are still being optimised, despite the fact that data fusion approaches, like the one suggested by Ban et al. [30], have produced notable results in terms of accuracy and navigation. For instance, using RGB and LiDAR sensors together is beneficial for autonomous navigation management; nevertheless, it necessitates sophisticated data processing to synchronise and align data from various devices without sacrificing navigation system accuracy.

Another area of discussion involves the ability of ML models to adapt to variable conditions, such as terrain diversity, lighting variations, and weather conditions. According to Pattanik et al. [36], deep learning methods and models like CNNs have been created for weed identification; however, further testing and optimisation are needed to determine how well ML models function in dynamic agricultural situations. In particular, the resilience of the model has to be strengthened to manage situations in which environmental factors, such the presence of clouds or variations in sunshine, might impact the quality of pictures obtained by sensors. Thus, it is crucial to create deep learning algorithms that can adjust to changes in the environment in real time without sacrificing the precision of

plant and weed identification. The combination of computer vision and ML algorithms has shown promising results in the automation of targeted spraying. However, interoperability issues between different systems remain. For instance, the deployment of drones and autonomous robots for spraying requires synchronisation between visual sensors, GPS units, and navigation algorithms, as highlighted in the studies by Jiang et al. [48] and Thakur et al. [49]. The real-time management of these complex systems, especially in agricultural environments characterised by uneven surfaces and growing plants, necessitates continuous improvements in localisation and mapping models to minimise positioning errors and ensure precise and effective spraying operations. Choosing the right ML techniques and sensors to maximise detection and navigation is a critical step in the creation of autonomous spraying systems. The advantages, limitations, and primary uses of some of the most popular machine learning techniques and sensors are contrasted in Table 1. This comparison aids in understanding how various technical combinations might be used to optimise autonomous systems' efficiency in agricultural settings.

Table 1. Summary of machine learning methods and sensors for autonomous spraying in precision agriculture.

Machine Learning Method	Sensor Type	Advantages (ML)	Advantages (Sensor)	Disadvantages (ML)	Disadvantages (Sensor)	Main Applications	Reference
Fusion of RGB, LiDAR, and IMU	RGB Camera, 3D LiDAR, IMU	High accuracy in navigation line detection	Comprehensive environmental perception	Computationally intensive	LiDAR data filtering challenges	Autonomous navigation in crop fields	Ban et al. (2024) [30]
Fully Convolutional Networks (FCN)	RGB Camera, NIR Camera	High generalisation for plant classification	Improved plant segmentation	Requires large training dataset	NIR camera cost and complexity	Weed and crop classification	Lottes et al. (2019) [31]
YOLOv5, YOLOv6	RGB Camera, UAV	Fast object detection and segmentation	Aerial monitoring of crops	Inference time in real-time applications	Limitations in detecting overlapping plants	Crop monitoring and weed detection	Arsalan et al. (2024) [33]
Dilated Convolutions, Adaptive Gradient	RGB Camera	Enhanced feature extraction	Detailed canopy structure detection	Requires more computational power	Limited field adaptability	Precision spraying of fruit trees	Khan et al. (2024) [34]
DCNN (VGG-Net, ShuffleNet-v2, MobileNet-v3, GoogLeNet)	RGB Camera	High accuracy (>99%) in weed recognition	Reduced herbicide use	High dependency on training data	Variability in lighting conditions	Weed classification and herbicide optimisation	Jin et al. (2022) [35]
CNN + ReLU + SoftMax	RGB Camera	Effective weed-crop differentiation	Artificial visual analysis support	Computationally expensive	Errors in complex field scenarios	Crop–weed classification	Pattanik et al. (2023) [36]
CNN-based Droplet Detection	Video Camera	High precision in droplet detection	Adaptability to real-time processing	Limited to embedded systems	Performance affected by motion blur	Optimised pesticide application	Huynh and Nguyen (2024) [37]
DarkNet53, ResNet50	RGB Camera	High accuracy (96.6%) in weed detection	Robust deep learning features	High computational demand	Large dataset requirement	Weed identification in sugarcane fields	Modi et al. (2023) [38]
Mutual Subspace Method (MSM)	RGB Camera, UAV	Fast recognition of spraying areas	Efficient field coverage	Lower accuracy compared to deep learning	Weather dependency	Precision pesticide spraying	Gao et al. (2019) [39]
SVM (Support Vector Machine)	RGB Camera, Pi-Camera	Effective path detection	Real-time image analysis	Limited scalability	Low image resolution challenges	Autonomous pesticide spraying robot	Kameswari et al. (2022) [42]

Reducing the usage of pesticides and fertilisers is one of these technologies' main advantages, which has important sustainability ramifications.

Autonomous spraying systems, such those developed by Khan et al. [34], are more accurate in identifying and delivering chemicals, reducing spraying waste by 40%. In addition to lowering farmers' operational costs, this promotes more environmentally friendly farming practices and helps to conserve the environment.

Significant investments in infrastructure, technology, and training are needed to deploy autonomous agricultural drones and robots. Managing real-time data and the computing capacity required for image analysis provide additional difficulties, especially for small and medium-sized farms. However, due to ongoing developments in machine learning technologies, sensor miniaturisation, and production cost reductions, these challenges ought to be overcome in the years to come.

In evaluating the state-of-the-art swarm robotics technologies, thirty-four agricultural swarm robotics technologies were assessed from seven key aspects:

1. Technology Readiness Level (TRL): ranging from the basic principles of technology (TRL 1) to fully proven systems in operating environments (TRL 9).
2. Configurability (Config): the robot's ability to be configured for specific tasks.
3. Adaptability (Adapt): how well the system adjusts to different working scenarios.
4. Perception Ability (Perc): the robot's capacity to perceive its environment using various sensors.
5. Decision Autonomy (Decis): the ability of the robot to act autonomously, based on its environment and task requirements.

Each of these aspects was evaluated using a three-level scoring system (3 = fully addressed, 2 = partially addressed, 1 = not addressed), and this helped in drawing comparisons across technologies. This evaluation framework can be integrated with the analysis of machine learning approaches for autonomous spraying systems, as both domains share a focus on improving task execution efficiency and environmental adaptation in agricultural robotics (Table 2).

Table 2. Evaluation of ML-based autonomous spraying technologies. Technologies assessed on TRL, configurability, adaptability, perception, and decision autonomy.

Name Technology	Author	TRL	Config	Adapt	Perc	Decis
Camera-LiDAR-IMU Fusion Method	Chao Ban et al. (2024) [30]	7	3	2	3	2
Robust Joint Stem Detection	Lottes et al. (2019) [31]	6	2	1	1	2
Row Detection-Based Navigation	Shi et al. (2023) [32]	7	3	2	2	3
Real-Time Precision Spraying for Tobacco	Arsalan et al. (2024) [33]	7	3	2	3	2
YOLOv8 Instance Segmentation for Orchard Canopies	Khan et al. (2024) [34]	7	3	2	3	2
Deep Learning-Based Weed Detection in Turf	Jin et al. (2022) [35]	7	3	1	3	2
CNN Algorithm for Farm Weed Detection	Pattanaik et al. (2023) [36]	7	3	2	3	2
Real-Time Droplet Detection	Huynh and Nguyen (2024) [37]	6	2	1	1	2

Table 2. *Cont.*

Name Technology	Author	TRL	Config	Adapt	Perc	Decis
Automated Weed Identification Framework for Sugarcane	Modi et al. (2023) [38]	6	3	3	3	2
UAV-Based Spraying Area Recognition	Gao et al. (2019) [39]	7	3	2	3	1
Real-Time Agricultural Monitoring	Mukherjee et al. (2023) [40]	7	3	2	3	2
Machine Learning for UAV Sprayers	Mohsin et al. (2025) [41]	6	2	2	1	2
Autonomous Pesticide-Spraying Robot Using SVM	Kameswari et al. (2022) [42]	7	3	1	3	2
RTK and ML for Autonomous Field Robots	Wijesundara et al. (2023) [43]	6	2	1	3	1
GPS-Guided Autonomous Navigation	Khan et al. (2018) [44]	7	3	1	3	1
Droplet Tracking in Crop-Spraying	Huynh et al. (2024) [45]	6	3	1	3	2
Autonomous UAVs for Pesticide Application	Faical et al. (2016) [46]	6	2	1	3	3
Remote Sensing of Invasive Species with UAVs	Göktogan and Sukkarieh (2015) [47]	8	3	3	3	2
Navigation of an Autonomous Spraying Robot	Jiang and Ahamed (2023) [48]	5	1	1	3	2
Vision-Based Control for Agri-Robots	Thakur et al. (2024) [49]	6	1	2	3	3
SPARROW: Smart Precision Agriculture Robot	Balasingham et al. (2024) [50]	5	1	2	1	2
Fully Autonomous Indoor Spray Robot	Ji et al. (2023) [51]	5	1	2	1	1
Spraying Robot with Edge Following	Danton et al. (2020) [52]	6	1	2	1	1
Intelligent Autonomous Agricultural Robot	Alshbatat and Awawdeh (2024) [53]	6	2	1	2	2
Smart Agriculture Drone for Crop Spraying	Singh et al. (2024) [54]	4	1	2	1	1
Total by evaluation criteria			**54/72**	**39/72**	**56/72**	**45/72**

The assessment of autonomous spraying technologies [27,58] based on machine learning reveals significant variations in technological preparedness, adaptability, configurability, perceptual capacity, and decision autonomy. These elements provide information on the actual implementation and possible enhancement of these systems in precision farming. The majority of the evaluated systems are at advanced stages of development in terms of technological readiness, with several of them reaching TRL 6 or 7. This suggests successful demonstration in relevant or operational environments but indicates the need for further refinement before large-scale commercial adoption.

High technological maturity, for instance, positions the Camera-LiDAR-IMU Fusion Method (Ban et al. [30]) and YOLOv8 Instance Segmentation for Orchard Canopies (Khan et al. [34]) for integration into precision spraying applications. For autonomous spraying systems to be adapted to a variety of agricultural environments, configuration is crucial. Technologies with great configurability, such as deep learning-based weed identification [35] and row detection-based navigation [32], may adapt to different crop varieties and field circumstances. The intricacy of combining several sensors and machine learning models, however, is the main reason why certain systems still present customisation challenges. When it comes to optimising autonomous spraying systems, adaptability is still crucial. While many ML-based approaches show moderate adaptability, enabling them to cope with changes in environmental conditions such as lighting and crop growth stages, further improvements are necessary for optimal performance in dynamic settings [59]. Improving adaptability would make the systems more successful overall by allowing them to respond more quickly to changes in the agricultural environment. The perceptual ability of a system has a significant impact on its capacity to observe its surroundings and make precise spraying judgements. Because they increase the accuracy of object detection and segmentation, multi-sensor integration technologies, such as LiDAR and multispectral cameras, are typically linked to high perception scores. However, systems that just use RGB cameras could not work as effectively in inclement weather or when they are hidden by dense foliage.

Lastly, the ability of completely autonomous systems to make decisions on their own is referred to as decision autonomy. Even if a number of the technologies under evaluation have excellent decision-making skills, modifying spraying actions in response to real-time data, some still need to be optimised in order to reach full autonomy. In practical agricultural applications, system independence and accuracy might be further increased by refining decision-making algorithms and including reinforcement learning. Considering these developments, there are still obstacles to the broad use of these technologies. The high price of sophisticated technologies and the requirement for suitable infrastructure are two of the primary challenges.

In conclusion, integrating machine learning into autonomous spraying systems is one of the most promising approaches to addressing the problems brought up by precision agriculture. Even if operational and technological issues still need to be resolved, these systems have the potential to revolutionise agriculture through increased production, less environmental impact, and the encouragement of more sustainable agricultural methods with more research and refinement.

5. Future Prospects

Recent advances in agricultural nozzle design and the use of mechatronic spraying systems have greatly increased the accuracy, efficiency, and versatility of pesticide and agrochemical applications. These developments have established a strong foundation for the transition to more sustainable and digitally integrated plant protection methods.

Nonetheless, several key challenges still warrant deeper investigation—particularly when it comes to improving atomisation control in smart farming systems, minimising environmental footprints, and ensuring seamless data interoperability across platforms. Progress in spraying technologies will likely emerge from a multidisciplinary blend of robotics, digital agriculture, fluid mechanics, precision engineering, and artificial intelligence. Computational fluid dynamics (CFD) and additive manufacturing are effective techniques for improving both material properties and nozzle design. These methods help optimise the fit for specific crop structures and canopy types while allowing for the creation

of spray patterns that are finely tuned to improve efficiency and precision. As a result, they enhance droplet accuracy, reduce off-target drift, and optimise pesticide application.

More selective and energy-efficient droplet generation may also be facilitated by recent developments in biomimetic nozzle design. The integration of real-time sensing technologies—such as LiDAR, hyperspectral and multispectral imaging, and advanced machine vision systems—with AI-based control algorithms is poised to transform conventional spraying into a dynamic and site-specific process.

Current smart spraying systems are made to react instantly to field circumstances that change, such as abrupt weather changes, insect outbreaks, or signs of crop stress. They can instantly change important parameters like spray pressure, droplet size, and flow rate, guaranteeing that treatments remain accurate and efficient in a variety of situations.

Such adaptability is expected to drive the transition from conventional high-volume spraying toward ultra-low-volume (ULV) or micro-dosing techniques, maintaining treatment precision and efficacy while substantially lowering chemical usage and reducing environmental impact.

Another significant dimension of future spraying systems is their interoperability and digital traceability. The adoption of Internet of Things (IoT) communication protocols, blockchain infrastructures, and standardised data formats (e.g., ISOBUS) will support the secure, transparent, and tamper-proof recording of spraying data. These characteristics play a crucial role in meeting the demands of tightening regulatory standards, while also strengthening transparency, traceability, and accountability throughout the agri-food supply chain. Future advances in atomisation will be strongly related to the creation of self-governing robotic systems that can be smoothly combined with intelligent spraying technologies that can instantly adapt to changing field circumstances.

These systems, whether deployed on the ground or from the air, are capable of carrying out targeted interventions with minimal human oversight, delivering reliable results across diverse terrains and crop varieties. Integration with farm management platforms and digital twins could allow for fully autonomous planning, execution, and optimisation of spraying tasks at the field or even plant level.

Concurrently, there is an increasing need to understand and mitigate spraying technology's ecological and toxicological impacts. Future studies should look at how formulation chemistry, droplet size and speed, and interactions with non-target organisms—such as pollinators, aquatic animals, and soil fauna—affect the ecosystem. It is equally crucial to investigate the cumulative effects of repeated spraying, air drift, and residue behaviour in complex agroecosystems. To solve these difficulties, long-term, cross-disciplinary research will be required. It would also be necessary to actively include stakeholders through participatory procedures in order to develop spraying strategies that are both productive and ecologically sensitive.

Table 3 provides a concise overview of these futuristic approaches, outlining their main areas of emphasis, supporting technology, and expected advantages.

The future of spraying technologies will depend on the integration of advanced nozzle design, real-time sensing and processing capabilities, the possibility of data-driven control and environmentally sustainable agricultural practices, as well as lowering the cost of the technologies. These innovations are key to meeting the challenge of increasing food production while minimising the negative effects of spraying on human health and the environment. Achieving the full potential of new-generation spraying systems will require a coordinated, interdisciplinary approach to ensure the development of sustainable and resilient agri-food systems.

Table 3. Future prospects for agricultural spraying systems.

Focus Area	Objective	Emerging Technologies/Approaches	Expected Benefits
Precision Application	Optimise droplet size, spray angle, and volume for target coverage	Variable rate technology (VRT), real-time sensors, adaptive nozzles	Improved efficacy, reduced input use, minimisation of drift and off-target deposition
Smart Nozzles and Control Units	Achieve dynamic control of spraying parameters	Electromagnetic valves, AI-based controllers, digital twins	Tailored delivery per plant or zone, reduction in resource consumption
Detection and Mapping	Identify plant status, weed locations, and canopy structure	UAVs, multispectral/hyperspectral cameras, LiDAR	Site-specific spraying, increased selectivity and sustainability
Automation and Robotics	Enable autonomous operation with minimal human intervention	Autonomous ground vehicles (UGVs), drones, SLAM algorithms	Increased operational efficiency, safety, and scalability
Integration with DSS and IoT	Support data-driven decisions and remote monitoring	Decision Support Systems (DSS), IoT platforms, cloud analytics	Real-time monitoring, better farm management, predictive maintenance
Sustainability and Environment	Minimise environmental footprint and protect biodiversity	Biodegradable formulations, precision targeting, eco-risk models	Reduction in leaching/runoff, protection of beneficial insects and pollinators
Multifunctional Spraying	Combine spraying with additional functions (e.g., data collection, imaging)	Multi-sensor sprayers, modular platforms	Increased ROI per pass, streamlined field operations
Standardisation and Interoperability	Ensure compatibility across machines and systems	Open protocols, ISOBUS standards, blockchain for traceability	Transparent data exchange, improved traceability and certification

6. Conclusions

Significant gains in accuracy, productivity, and environmental sustainability have been demonstrated by the application of ML in automated spraying systems. Precision agriculture has significantly improved with the use of advanced machine learning models and multi-sensor fusion techniques. This has made it possible to identify plants in real time, apply pesticides precisely, and optimise navigation for autonomous agricultural robots.

By improving weed detection, crop row identification, and disease recognition, the studies reviewed highlight the effectiveness of advanced algorithms such as CNNs, YOLO, and FCNs. This leads to more sustainable agricultural practices by reducing the dependency on pesticides and herbicides. Furthermore, the ability to minimise pesticide use and runoff—factors that negatively affect neighbouring ecosystems—through the integration of machine learning into autonomous spraying systems on the one hand increases operational efficiency, and on the other promotes environmental sustainability. However, despite these important advances, several key challenges persist that prevent the widespread adoption of machine learning-based autonomous spraying systems.

Indeed, major obstacles include the need for high-quality labelled datasets to train robust models that can generalise across different field conditions and crop varieties. The scalability of such systems is limited by the significant resources needed for data collecting and annotation.

Precision farming can be significantly improved by integrating IoT-driven agricultural monitoring networks with machine learning-based autonomous spraying systems. By

offering real-time field monitoring, providing farmers with timely data, and optimising resource management, these technologies can enhance both sustainability and productivity. This approach fosters an eco-friendlier farming practice, promoting bio-diversity conservation and minimising the environmental impact of agricultural activities through waste reduction and better resource utilisation.

To ensure that these technologies are used appropriately, attention must also be paid to the ethical and legal considerations, in particular those related to data privacy, environ-mental impact, and acceptance by farmers (especially in settings with strong cultural traditions).

Moreover, the fusion of heterogeneous sensor data, including RGB cameras, LiDAR, and multispectral imagery, presents complexities of synchronisation and alignment that still require continuous refinement to ensure accurate real-time decision-making. The capacity of these systems to adjust to changing environmental factors, such as variations in sunlight, weather, and soil characteristics, is another crucial component. One of the primary areas of study continues to be ensuring dependable performance in various agricultural environments. Furthermore, real-time applications face difficulties due to the computational needs of deep learning methods, especially for embedded devices with constrained processing capacity. Optimising light-weight machine learning models that preserve high accuracy while cutting down on inference times should be the key goal of future research. In conclusion, even though ML has transformed autonomous spraying systems by increasing productivity and decreasing reliance on agrochemicals, more developments are needed to address operational and technological issues. To enable the smooth integration of these technologies into contemporary agriculture, future research should focus on enhancing sensor fusion techniques, creating adaptable machine learning models, and investigating energy-efficient computer options.

Author Contributions: Conceptualization, F.T. and P.D.; methodology, F.T., C.F., L.S.S., R.R.M., D.A., and R̆.T.; formal analysis, F.T., R.R.M., P.D., and C.F.; investigation, F.T., C.F., L.S.S., R.R.M., D.A., M.K., and R̆.T.; resources, F.T. and P.D.; data curation, F.T., C.F., L.S.S., R.R.M., D.A., M.K., and R̆.T.; writing—original draft preparation, F.T., R.R.M., P.D., and C.F.; writing—review and editing, F.T., C.F., L.S.S., R.R.M., D.A., P.D., M.K., and R̆.T.; visualization, L.S.S., R.R.M., D.A., P.D., and R̆.T.; supervision, F.T., R.R.M., C.F., and P.D.; project administration, F.T., C.F., and P.D.; funding acquisition, F.T. and P.D. All authors have read and agreed to the published version of the manuscript.

Funding: This research received no external funding.

Data Availability Statement: No new data were created or analysed during this study. All supporting data are available upon request from the corresponding author, subject to ethical and privacy restrictions.

Acknowledgments: This work was carried out within the framework of research activities and scientific collaboration between the University of Basilicata and international institutions, including the Agricultural Engineering Department at the Federal University of Vale Jequitinhonha and Mucuri (Brazil), the School of Engineering at the Federal University of Lavras (Brazil), the Faculty of Agricultural Engineering at the State University of Campinas (Brazil), and the Laboratory on Geoinformatics and Cartography at Masaryk University (Czech Republic). This research falls within the scientific-disciplinary fields of agricultural engineering. The authors acknowledge the University of Basilicata and the "Casa delle Tecnologie Emergenti" of Matera, "Laboratorio del Giardino delle Tecnologie Emergenti"—CTEMT; the Smart@Irrifert Project (PSR Basilicata 2014–2020—Sottomisura 16.2, CUP G19J21004870006); and the "Vertical gaRdens with Digital twin of plants" Viridiis Project (PRIN 2022, CUP C53D23000480006) for their support. Martina Klocová was provided with the support for student projects entitled "Dynamics of the natural and social environment in geographical perspective" (MUNI/A/1648/2024).

Conflicts of Interest: The authors declare that the research was conducted in the absence of any commercial or financial relationships that could be construed as potential conflicts of interest.

Abbreviations

The following abbreviations are used in this manuscript:

ML	Machine Learning
DPA	Digital Precision Agriculture
RGB	Red, Green, Blue
CPU	Central Processing Unit
GPS	Global Positioning System
LiDAR	Light Detection and Ranging
IMU	Inertial Measurement Unit
FCN	Fully Convolutional Network
VGG	Visual Geometry Group
NIR	Near-Infrared
YOLO	You Only Look Once
DCNN	Deep Convolutional Neural Network
CNN	Convolutional Neural Network
ReLU	Rectified Linear Unit
F1 score	Indicator of classification accuracy
SIFT	Scale-Invariant Feature Transform
SURF	Speeded-Up Robust Features
SVM	Support Vector Machine
MSM	Mutual Subspace Method
UAV	Unmanned Aerial Vehicle
RTK-GPS	Real-Time Kinematic-Global Positioning System
PSO-ANN	Particle Swarm Optimization–Artificial Neural Network
DBSCAN	Density-Based Spatial Clustering of Applications with Noise
K-means	A clustering algorithm
RANSAC	Random Sample Consensus
K-NN	K-Nearest Neighbours
TRL	Technology Readiness Level
Config	Configuration
Adapt	Adaptability
Perc	Perception Ability
Decis	Decision-making

References

1. Malhi, G.S.; Kaur, M.; Kaushik, P. Impact of Climate Change on Agriculture and Its Mitigation Strategies: A Review. *Sustainability* **2021**, *13*, 1318. [CrossRef]
2. Richard, B.; Qi, A.; Fitt, B.D.L. Control of crop diseases through Integrated Crop Management to deliver climate-smart farming systems for low- and high-input crop production. *Plant Pathol.* **2021**, *70*, 13493. [CrossRef]
3. Jacquet, F.; Jeuffroy, M.-H.; Jouan, J.; Le Cadre, E.; Litrico, I.; Malausa, T.; Reboud, X.; Huyghe, C. Pesticide-free agriculture as a new paradigm for research. *Agron. Sustain. Dev.* **2022**, *42*, 8. [CrossRef]
4. Khan, N.; Ray, R.L.; Sargani, G.R.; Ihtisham, M.; Khayyam, M.; Ismail, S. Current Progress and Future Prospects of Agriculture Technology: Gateway to Sustainable Agriculture. *Sustainability* **2021**, *13*, 4883. [CrossRef]
5. Sims, B.; Kienzle, J. Sustainable Agricultural Mechanization for Smallholders: What Is It and How Can We Implement It? *Agriculture* **2017**, *7*, 50. [CrossRef]
6. Daum, T. Mechanization and sustainable agri-food system transformation in the Global South. A review. *Agron. Sustain. Dev.* **2023**, *43*, 16. [CrossRef]
7. Emami, M.; Almassi, M.; Bakhoda, H.; Kalantari, I. Agricultural mechanization, a key to food security in developing countries: Strategy formulating for Iran. *Agric. Food Secur.* **2018**, *7*, 24. [CrossRef]

8. Scolaro, E.; Beligoj, M.; Estevez, M.P.; Alberti, L.; Renzi, M.; Mattetti, M. Electrification of Agricultural Machinery: A Review. *IEEE Access* **2021**, *9*, 164520–164541. [CrossRef]
9. Liakos, K.G.; Busato, P.; Moshou, D.; Pearson, S.; Bochtis, D. Machine Learning in Agriculture: A Review. *Sensors* **2018**, *18*, 2674. [CrossRef]
10. Domingues, T.; Brandão, T.; Ferreira, J.C. Machine Learning for Detection and Prediction of Crop Diseases and Pests: A Comprehensive Survey. *Agriculture* **2022**, *12*, 1350. [CrossRef]
11. Radoc˘aj, D.; Jurišic´, M.; Gašparovic´, M. The Role of Remote Sensing Data and Methods in a Modern Approach to Fertilization in Precision Agriculture. *Remote Sens.* **2022**, *14*, 778. [CrossRef]
12. D'Antonio, P.; Mehmeti, A.; Toscano, F.; Fiorentino, C. Operating performance of manual, semi-automatic, and automatic tractor guidance systems for precision farming. *Res. Agric. Eng.* **2023**, *69*, 179–188. [CrossRef]
13. Fiorentino, C.; D'Antonio, P.; Toscano, F.; Capece, N.; Conceição, L.A.; Scalcione, E.; Modugno, F.; Sannino, M.; Colonna, R.; Lacetra, E.; et al. Smart Sensor and AI-Driven Alert System for Optimizing PGI Red Peppers Drying in Southern Italy. *Sustainability* **2025**, *17*, 1682. [CrossRef]
14. Bai, Y.; Zhang, B.; Xu, N.; Zhou, J.; Shi, J.; Diao, Z. Vision-based Navigation and Guidance for Agricultural Autonomous Vehicles and Robots: A Review. *Comput. Electron. Agric.* **2022**, *192*, 107584. [CrossRef]
15. Heikkilä, M.; Suomalainen, J.; Saukko, O.; Kippola, T.; Lähetkangas, K.; Koskela, P.; Kalliovaara, J.; Haapala, H.; Pirttiniemi, J.; Yastrebova, A.; et al. Unmanned Agricultural Tractors in Private Mobile Networks. *Network* **2022**, *2*, 1–20. [CrossRef]
16. Toscano, F.; Fiorentino, C.; Capece, N.; Erra, U.; Travascia, D.; Scopa, A. Unmanned Aerial Vehicle for Precision Agriculture: A Review. *IEEE Access* **2024**, *12*, 3401018. [CrossRef]
17. Abbas, I.; Liu, J.; Faheem, M.; Noor, R.S.; Shaikh, S.A.; Solangi, K.A.; Raza, S.M. Different Sensor-Based Intelligent Spraying Systems in Agriculture. *Sens. Actuators A Phys.* **2020**, *312*, 112265. [CrossRef]
18. Kulbacki, M.; Segen, J.; Kniec´, W.; Klempous, R.; Kluwak, K.; Kulbacki, J.N.M. Survey of Drones for Agriculture Automation from Planting to Harvest. In Proceedings of the 2018 IEEE 22nd International Conference on Intelligent Engineering Systems (INES), Las Palmas de Gran Canaria, Spain, 21–23 June 2018; pp. 353–358. [CrossRef]
19. Alves, R.G.; Maia, R.F.; Lima, F. Development of a Digital Twin for Smart Farming: Irrigation Management System for Water Saving. *J. Clean. Prod.* **2023**, *388*, 135920. [CrossRef]
20. Obaideen, K.; Yousef, B.A.A.; AlMallahi, M.N.; Tan, Y.C.; Mahmoud, M.; Jaber, H.; Ramadan, M. An Overview of Smart Irrigation Systems Using IoT. *Nexus* **2022**, *7*, 100124. [CrossRef]
21. Mohamed, E.S.; Belal, A.A.; Abd-Elmabod, S.K.; El-Shirbeny, M.A.; Gad, A.; Zahran, M.B. Smart Farming for Improving Agricultural Management. *Eur. J. Remote Sens.* **2021**, *54*, 123–135. [CrossRef]
22. Ruiz-Sarmiento, J.-R.; Monroy, J.; Moreno, F.-A.; Galindo, C.; Bonelo, J.-M.; Gonzalez-Jimenez, J. A Predictive Model for the Maintenance of Industrial Machinery in the Context of Industry 4.0. *Eng. Appl. Artif. Intell.* **2020**, *82*, 103289. [CrossRef]
23. Muhie, S.H. Novel Approaches and Practices to Sustainable Agriculture. *J. Agric. Food Res.* **2022**, *8*, 100446. [CrossRef]
24. Gonzalez-de-Soto, M.; Emmi, L.; Perez-Ruiz, M.; Aguera, J.; Gonzalez-de-Santos, P. Autonomous Systems for Precise Spraying—Evaluation of a Robotised Patch Sprayer. *Biosyst. Eng.* **2016**, *146*, 79–97. [CrossRef]
25. Albiero, D.; Garcia, A.P.; Umezu, C.K.; de Paulo, R.L. Swarm Robots in Mechanized Agricultural Operations: A Review about Challenges for Research. *Comput. Electron. Agric.* **2022**, *193*, 106608. [CrossRef]
26. Shahrooz, M.; Talaeizadeh, A.; Alasty, A. Agricultural Spraying Drones: Advantages and Disadvantages. In Proceedings of the 2020 Virtual Symposium in Plant Omics Sciences (OMICAS), Bogotá, Colombia, 23–27 November 2020; pp. 1–5. [CrossRef]
27. Lochan, K.; Khan, A.; Elsayed, I.; Suthar, B.; Seneviratne, L.; Hussain, I. Advancements in Precision Spraying of Agricultural Robots: A Comprehensive Review. *IEEE Access* **2024**, *12*, 129447–129483. [CrossRef]
28. Honrao, D.V.; Awadhani, L.V. Design and development of agricultural spraying system. *Mater. Today Proc.* **2023**, *77*, 734–738. [CrossRef]
29. R˘ezník, T.; Herman, L.; Klocová, M.; Leitner, F.; Pavelka, T.; Leitgeb, Š.; Trojanová, K.; Štampach, R.; Moshou, D.; Mouazen, A.M.; et al. Towards the Development and Verification of a 3D-Based Advanced Optimized Farm Machinery Trajectory Algorithm. *Sensors* **2021**, *21*, 2980. [CrossRef]
30. Ban, C.; Wang, L.; Chi, R.; Su, T.; Ma, Y. A Camera-LiDAR-IMU Fusion Method for Real-Time Extraction of Navigation Line Between Maize Field Rows. *Comput. Electron. Agric.* **2024**, *223*, 109114. [CrossRef]
31. Lottes, P.; Behley, J.; Chebrolu, N.; Milioto, A.; Stachniss, C. Robust Joint Stem Detection and Crop-Weed Classification Using Image Sequences for Plant-Specific Treatment in Precision Farming. *J. Field Robot.* **2019**, *37*, 20–34. [CrossRef]
32. Shi, J.; Bai, Y.; Diao, Z.; Zhou, J.; Yao, X.; Zhang, B. Row Detection BASED Navigation and Guidance for Agricultural Robots and Autonomous Vehicles in Row-Crop Fields: Methods and Applications. *Agronomy* **2023**, *13*, 1780. [CrossRef]
33. Arsalan, M.; Rashid, A.; Khan, K.; Imran, A.; Khan, F.; Akbar, M.A.; Cheema, H.M. Real-Time Precision Spraying Application for Tobacco Plants. *Smart Agric. Technol.* **2024**, *8*, 100497. [CrossRef]

34. Khan, Z.; Liu, H.; Shen, Y.; Zeng, X. Deep Learning Improved YOLOv8 Algorithm: Real-Time Precise Instance Segmentation of Crown Region Orchard Canopies in Natural Environment. *Comput. Electron. Agric.* **2024**, *224*, 109168. [CrossRef]
35. Jin, X.; Liu, T.; Chen, Y.; Yu, J. Deep Learning-Based Weed Detection in Turf: A Review. *Agronomy* **2022**, *12*, 3051. [CrossRef]
36. Pattanaik, B.; Malibari, A.; Kumarasamy, M.; Nagaraj, V.; Gopikrishnan, M. Design and Evaluation of a Deep CNN Algorithm for Detecting Farm Weeds. *Int. J. Environ. Sci. Manag. Syst.* **2023**, *71*, 71–79. [CrossRef]
37. Huynh, N.; Nguyen, K.-D. Real-Time Droplet Detection for Agricultural Spraying Systems: A Deep Learning Approach. *Mach. Learn. Knowl. Extr.* **2024**, *6*, 259–282. [CrossRef]
38. Modi, R.U.; Kancheti, M.; Subeesh, A.; Raj, C.; Singh, A.K.; Chandel, N.S.; Dhimate, A.S.; Singh, M.K.; Singh, S. An Automated Weed Identification Framework for Sugarcane Crop: A Deep Learning Approach. *Crop Prot.* **2023**, *173*, 106360. [CrossRef]
39. Gao, P.; Zhang, Y.; Zhang, L.; Noguchi, R.; Ahamed, T. Development of a Recognition System for Spraying Areas from Unmanned Aerial Vehicles Using a Machine Learning Approach. *Sensors* **2019**, *19*, 313. [CrossRef]
40. Mukherjee, D.; Das, A.; Ghosh, N.; Nanda, S. Real Time Agricultural Monitoring with Deep Learning Using Wireless Sensor Framework. In Proceedings of the 2023 International Conference on Electrical, Electronics, Communication and Computers (ELEXCOM), Roorkee, India, 26–27 August 2023; pp. 1–6. [CrossRef]
41. Mohsin, K.; Chandravadhana, S.; Chaudhari, V.; Balasaranya, K.; Pari, R.; Srinivasarao, B. The Deployment of Machine Learning and On-Board Vision Systems for an Unmanned Aerial Sprayer for Pesticides. *J. Mach. Comput.* **2025**, *5*, 600–610. [CrossRef]
42. Kameswari, S.S.D.; Prabhakar, T.; Kishore, K.K. Autonomous Pesticide Spraying Robot Using SVM. In Proceedings of the International Conference on Wireless Communication, Mumbai, India, 8–9 October 2021; Vasudevan, H., Gajic, Z., Deshmukh, A.A., Eds.; Lecture Notes on Data Engineering and Communications Technologies. Springer: Singapore, 2022; Volume 92. [CrossRef]
43. Wijesundara, W.M.T.D.; Wanigathunga, T.D.; Waas, M.N.C.; Hithanadura, R.T.; Munasinghe, S.R. Accurate Crop Spraying with RTK and Machine Learning on an Autonomous Field Robot. *arXiv* **2023**. [CrossRef]
44. Khan, N.; Medlock, G.; Graves, S.; Anwar, S. GPS Guided Autonomous Navigation of a Small Agricultural Robot with Automated Fertilizing System. In *SAE Technical Paper*; SAE International: Warrendale, PA, USA, 2018. [CrossRef]
45. Huynh, T.N.; Burgers, T.; Nguyen, K.-D. Efficient Real-Time Droplet Tracking in Crop-Spraying Systems. *Agriculture* **2024**, *14*, 1735. [CrossRef]
46. Faical, B.S.; Ueyama, J.; de Carvalho, A.C.P.L.F. The Use of Autonomous UAVs to Improve Pesticide Application in Crop Fields. In Proceedings of the 2016 17th IEEE International Conference on Mobile Data Management (MDM), Porto, Portugal, 13–16 June 2016; pp. 32–33. [CrossRef]
47. Göktogan, A.H.; Sukkarieh, S. Autonomous Remote Sensing of Invasive Species from Robotic Aircraft. In *Handbook of Unmanned Aerial Vehicles*; Springer: Berlin/Heidelberg, Germany, 2015; pp. 2813–2834. [CrossRef]
48. Jiang, A.; Ahamed, T. Navigation of an Autonomous Spraying Robot for Orchard Operations Using LiDAR for Tree Trunk Detection. *Sensors* **2023**, *23*, 4808. [CrossRef] [PubMed]
49. Thakur, A.; Kumar, A.; Mishra, S.K. Control Techniques for Vision-Based Autonomous Vehicles for Agricultural Applications: A Meta-analytic Review. In *Artificial Intelligence: Theory and Applications*; Sharma, H., Chakravorty, A., Hussain, S., Kumari, R., Eds.; Lecture Notes in Networks and Systems; Springer: Singapore, 2024; Volume 843. [CrossRef]
50. Balasingham, D.; Samarathunga, S.; Arachchige, G.G.; Bandara, A.; Wellalage, S.; Pandithage, D.; Hansika, M.M.D.J.T.; De Silva, R. SPARROW: Smart Precision Agriculture Robot for Ridding of Weeds. In Proceedings of the 2024 5th International Conference for Emerging Technology (INCET), Belgaum, India, 24–26 May 2024; pp. 1–6. [CrossRef]
51. Ji, X.; Li, Y.; Hong, K.; Cao, J. Design of a Fully Autonomous Indoor Spray Robot. *Int. J. Intell. Robot. Appl.* **2023**, *7*, 763–777. [CrossRef]
52. Danton, A.; Roux, J.-C.; Dance, B.; Cariou, C.; Lenain, R. Development of a Spraying Robot for Precision Agriculture: An Edge Following Approach. In Proceedings of the 2020 IEEE Conference on Control Technology and Applications (CCTA), Montreal, QC, Canada, 24–26 August 2020; pp. 267–272. [CrossRef]
53. Alshbatat, A.I.N.; Awawdeh, M. On the Development of Intelligent Autonomous Agricultural Robot. In Proceedings of the 2024 Advances in Science and Engineering Technology International Conferences (ASET), Abu Dhabi, United Arab Emirates, 3–5 June 2024; pp. 1–8. [CrossRef]
54. Singh, E.; Pratap, A.; Mehta, U.; Azid, S.I. Smart Agriculture Drone for Crop Spraying Using Image-Processing and Machine Learning Techniques: Experimental Validation. *IoT* **2024**, *5*, 250–270. [CrossRef]
55. Sousa, J.J.; Toscano, P.; Matese, A.; Di Gennaro, S.F.; Berton, A.; Gatti, M.; Poni, S.; Pádua, L.; Hruška, J.; Morais, R.; et al. UAV-Based Hyperspectral Monitoring Using Push-Broom and Snapshot Sensors: A Multisite Assessment for Precision Viticulture Applications. *Sensors* **2022**, *22*, 6574. [CrossRef] [PubMed]
56. Pádua, L.; Marques, P.; Hruška, J.; Adão, T.; Peres, E.; Morais, R.; Sousa, J.J. Multi-Temporal Vineyard Monitoring through UAV-Based RGB Imagery. *Remote Sens.* **2018**, *10*, 1907. [CrossRef]

57. Guimarães, N.; Pádua, L.; Sousa, J.J.; Bento, A.; Couto, P. Identification of Aphids Using Machine Learning Classifiers on UAV-Based Multispectral Data. In Proceedings of the 2023 IEEE International Geoscience and Remote Sensing Symposium (IGARSS), Pasadena, CA, USA, 16–21 July 2023. [CrossRef]
58. Sitompul, E.; Gubarda, M.R.; Sihombing, P.; Simarmata, T.; Turnip, A. Sprayer System on Autonomous Farming Drone Based on Decision Tree. In Proceedings of the 2024 IEEE International Conference on Artificial Intelligence and Mechatronics Systems (AIMS), Bandung, Indonesia, 21–23 February 2024; pp. 1–6. [CrossRef]
59. Abioye, A.E.; Larbi, P.A.; Hadwan, A.A.K. Deep Learning Guided Variable Rate Robotic Sprayer Prototype. *Smart Agric. Technol.* **2024**, *9*, 100540. [CrossRef]

Groundwater Quality Assessment Using Multi-Criteria GIS Modeling in Drylands: A Case Study at El-Farafra Oasis, Egyptian Western Desert

Hanaa A. Megahed, Hossam M. GabAllah, Rasha H. Ramadan, Mohamed A. E. AbdelRahman, Paola D'Antonio, Antonio Scopa and Mahmoud H. Darwish

Pubblicazione: Rivista Water, editore MDPI (Volume 15, Issue 7, Articolo 1376, Anno 2023)
https://doi.org/10.3390/w15071376

water

MDPI

Article

Groundwater Quality Assessment Using Multi-Criteria GIS Modeling in Drylands: A Case Study at El-Farafra Oasis, Egyptian Western Desert

Hanaa A. Megahed [1], Hossam M. GabAllah [1], Rasha H. Ramadan [2], Mohamed A. E. AbdelRahman [2,*], Paola D'Antonio [3,*], Antonio Scopa [3] and Mahmoud H. Darwish [4]

[1] Division of Geological Applications and Mineral Resources, National Authority for Remote Sensing and Space Sciences (NARSS), Cairo 1564, Egypt
[2] Division of Environmental Studies and Land Use, National Authority for Remote Sensing and Space Sciences (NARSS), Cairo 1564, Egypt
[3] Scuola di Scienze Agrarie, Forestali, Alimentari ed Ambientali (SAFE), Università degli Studi della Basilicata, Viale dell'Ateneo Lucano, 10, 85100 Potenza, Italy
[4] Geology Department, Faculty of Science, New Valley University, El Kharga 72511, Egypt
* Correspondence: maekaoud@narss.sci.eg (M.A.E.A.); paola.dantonio@unibas.it (P.D.)

Abstract: The most critical issue that was the main research interest is its groundwater quality which is vital for public health concerns. Groundwater is a significant worldwide water supply for diverse communities, especially in dryland regions. Groundwater quality assessment in desert systems is largely hindered by the lack of hydrological data and the remote location of desert Oases. This study provides a preliminary understanding of the influences of climate, land usage, and population growth on the groundwater quality in El-Farafra Oasis in the Western Desert in Egypt from 2000 to now. Therefore, the study's main objective was to determine the extent of change in temporal water quality and the factors causing it. The present study integrates chemical analyses and geospatial modeling better to assess groundwater quality in the study area. A chemical analysis of thirty-one groundwater samples from wells representing each study area was carried out during three time periods (2000, 2010, and 2022). Several chemical properties of groundwater samples gathered from wells in the research area were analyzed. Furthermore, the groundwater quality trend from 2000 to the present was identified using three approaches: Wilcox and Schoeller Diagram in Aq.QA software, interpolation in the ArcGIS software, and Ground Water Quality Index (GWQI). Moreover, the influence of changing land usage on groundwater quality was studied, and it was found that the increase in agriculture and urbanization areas is linked to groundwater quality degradation. The findings revealed that the barren area in 2000, 2010, and 2022 was 371.7, 362.0, and 343.2 km^2, respectively, which indicates a substantial decrease of 6.2% within this research timeframe. In contrast, agriculture and human-made structures have expanded by 1.8%. Also, population growth has led to an increase in water consumption as the population has grown at a rate of 7.52% annually from 2000 to 2020. As the climatic condition increases from 2000 to 2022, these changes could extend to the water quality in shallow aquifers with increasing evaporation. Based on the water quality spatial model, it is found that, despite a declining tendency in the rate of precipitation and an expansion in agricultural areas and population growth, the water quality was still appropriate for human and farming consumption in large areas of the study area. The presented approach is applicable to the assessment of groundwater in desert regions in the Middle East area.

Keywords: groundwater quality; population pressure; spatial model; climate change; land use; western desert; El-Farafra Oasis; Egypt

Citation: Megahed, H.A.; GabAllah, H.M.; Ramadan, R.H.; AbdelRahman, M.A.E.; D'Antonio, P.; Scopa, A.; Darwish, M.H. Groundwater Quality Assessment Using Multi-Criteria GIS Modeling in Drylands: A Case Study at El-Farafra Oasis, Egyptian Western Desert. *Water* **2023**, *15*, 1376. https://doi.org/10.3390/w15071376

Academic Editors: Dionysia Panagoulia and Domenico Cicchella

Received: 15 February 2023
Revised: 26 March 2023
Accepted: 27 March 2023
Published: 3 April 2023

1. Introduction

Groundwater (GW) is a significant resource of drinkable water, and about 45% or more of the water is employed for agricultural purposes for almost 50% of the planet's

inhabitants [1], which denotes a significant volume of freshwater taken from the world [2]. GW resources have been impacted by climatic and land use changes, which represent major stressors and an influence on the groundwater quality and quantity [3,4] and may influence hydrologic cycle like as evapotranspiration and surface infiltration, leading to changes in surface and subsurface flows [5–7]. Naturally, the chemical composition of the groundwater depends on multiple factors including; recharge water quality, earth materials types, water-soil-rock interaction, groundwater dynamics, and hydrogeological setup, etc. [8]. Among the influences that change the quality of groundwater are human activities and geological formations that carry water [9–11]. Surface and Groundwater pass through a complex cycle in the atmosphere, the earth's surface, and the soil [12].

Recently, our world is currently subjected to unprecedented climate changes leading to serious environmental issues [13]. Many researchers have conducted their studies to analyze and interpret the hydrological influences of climate and land usage changes [14–16]. For instance, increased global temperatures; lowered water resources' pH, and varying levels of global precipitation from greenhouse gas emissions (CO_2) are caused by human activities [17]. Several studies [3,18] showed that the causes of the groundwater quality changes and a drop in groundwater amounts were climate change, the overuse of fertilizers, and the conversion of forests to farming, which resulted in increased pollutants and usage of artificial nitrogen fertilizer. Many studies demonstrated that modifications in the vegetative ecosystem produced by alterations in land use and land cover substantially impacted the local hydrological cycle [19,20]. Subsequently, the component of land cover/land use changes within the catchment affecting the hydrological cycle seems crucial in advancing hydrology [21,22]. On the other hand, groundwater quality is greatly affected by the surrounding human activities, and therefore groundwater supplies and water quality can be influenced by population growth and increasing urbanization rate [23–25].

The alteration in land usage was correlated with information on water quality, and it was shown that the regions around fast urban growth and industry contain groundwater of poor to unfit quality [26]. The capability to conduct a spatial study of fluctuations in groundwater quality is vital in environmental managers' decision-making processes. Several research papers used satellite imagery, Remote Sensing (RS), and Geographic Information System (GIS) techniques to investigate the phenomenon of temporal and geographical variations in land usage [27–30], also WQI which has been successfully used in the assessment of water quality [31], as well as the connection between the quality of groundwater and variations in land cover/land use [3,32–35]. During 2001–2005, Houben et al. [36] investigated the quality of groundwater in Afghanistan's Kabul watershed. They discovered that due to the repeated droughts, this area experienced a rise in the salinity and hardness of its groundwater. In addition, Ketata et al. [37] examined the behavior of variation in some groundwater hydrochemical parameters from 1995 to 2003 in Gabès, Tunisia. They concluded that salt concentration and other chemical parameters in groundwater streamlines have diminished over time. Elci and Polat [38] focused on the behavior of water quality fluctuations in Turkey's Nife groundwater. They found that during rainy seasons, chloride concentrations were lower than during dry seasons.

Furthermore, investigations conducted in Iran revealed a worsening in the groundwater quality in Iran's plains from 1998 to 2004 [39]. An examination of temporal and geographical variations of groundwater status in the Qazvin plain from 2003 to 2007 revealed that groundwater quality decreased during rainy seasons, demonstrating the effect of rains on groundwater quality [40]. Based on the results of Singh et al. [41], owing to modifications in land cover and land use trends, natural and artificial recharge resulted in a rise in groundwater volume (increased area of fallow land). Fertilizers, conversely, degraded the groundwater quality. Singh et al. [41] resolved that the deterioration in groundwater quality in many agricultural areas, as well as those near urban and industrial areas, has heightened conservation concerns among many governmental organizations.

In semi-arid and arid regions, groundwater is an increasingly significant resource for irrigation, industrial, and drinking. Egypt is a country located in these arid zones, and as

a result of this geographic location, Egypt may be highly susceptible to climate change. In the current area under consideration, groundwater and springs remain a key source of fresh water for drinking and irrigation purposes. Many Egyptian studies considered the changes in hydrological, geological, and land use [42–44]. This research explores the alteration in groundwater quality in EL-Farafa Oasis and the association between its land use modification and climate change from 2000 to the present. The New Valley Project, which started in the 1960s, is pumping water from the famous Nubian Sandstone Aquifer (NSA) to the oasis of El Farafra in the Western Desert so that the desert may be farmed and restored [45]. Even though a large number of deep-water wells were constructed for this project, the issue became immediately obvious since it threatened the oasis's primary spring water source [46]. Land use changes and climate changes in the present work are being applied for the first time in the Egyptian Western Desert to evaluate their possible effects on groundwater quality. The present work is carried out to explore the following objectives: (i) using remote sensing and satellite photos to evaluate the previous and current land use changes and their effects in the study region from 2000 to the present, (ii) analyzing the water quality indices for the groundwater samples and mapping their spatial distributions using remote sensing and GIS models, and (iii) study the possible influences of change in climate and land use on groundwater quality.

2. Study Area Description

Geographically, El-Farafra Oasis is placed in the Egyptian Western Desert (EWD) between latitude and longitude; 26°45′41″–27°13′40″ N and 27°42′51″–27°59′32″ E (Figure 1). El-Farafra Oasis has a hot hyper-arid desert climate, with hot and dry summers marked by a lack of precipitation and moderate winters with intermittent precipitation and a yearly mean air temperature of 25 °C [47]. Rainfall in the area is rare, with occasionally heavy rainfall in a short duration with yearly precipitation averaging below 10 mm [45].

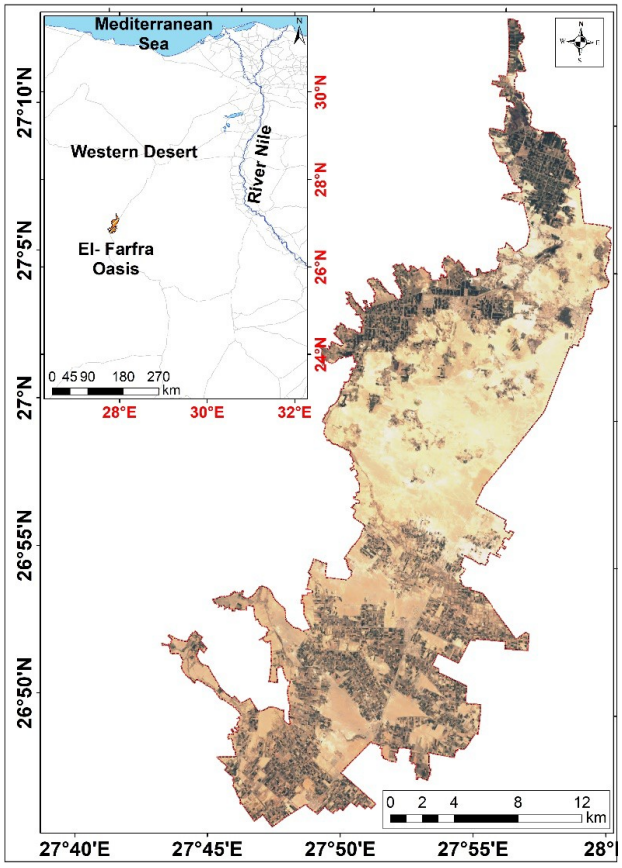

Figure 1. Location map of the study area (Landsat 8).

Geologically, the research area is covered with geologic rock formations that range in age from the Quaternary to the Upper Cretaceous. From top to bottom, the rock units are distinguished as follows: Quaternary deposits (containing sand sheets, sand dunes, and playa deposits), Tertiary formations (including Farafra limestone, Esna Shale, and Tarawan Chalk), and the Upper Cretaceous Khoman Formation. Upper Cretaceous to Pre-Cambrian geologic formations can be found in the subsurface. At the same time, the Upper Cretaceous and Paleozoic sediments that make up the Nubian Sandstone sequence are among the subsurface geological formations and are underlain by basement rocks [48] (Figure 2).

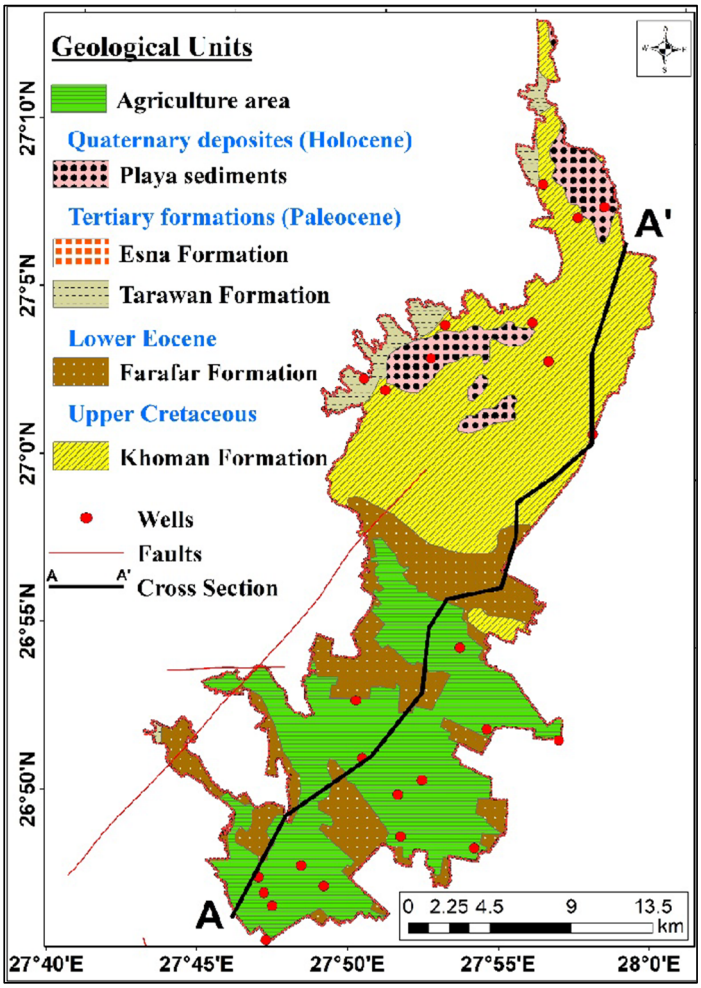

Figure 2. Geological map of the study area (modified by UNESCO, 2005).

From a hydrogeological perspective, the samples are collected from The Nubian Sandstone Aquifer System (NSAS)) (confined aquifer) with an average well depth of 600 m. The Nubian Sandstone Aquifer System (NSAS) is composed of two hydrological units namely; the Nubian Aquifer System (NAS) and the Post Nubian Aquifer System (PNAS) that are separated by the upper Cretaceous aquitard of the Dakhla Formation [49]. The NAS outcrops south of latitudes 28° and then it becomes a confined aquifer to the north in El-Farafra Oasis (Figure 3) [50,51]. The NAS groundwater has been mainly recharged during the previous wet climatic periods during the Pleistocene with a very limited recharge during the present arid conditions [52]. The PNAS mainly receives recharge through vertical connection with the NAS along major geological structures [49]. Therefore, both aquifers receive negligible volumes of modern recharge and thus avoiding potential contamination from surface water sources [53].

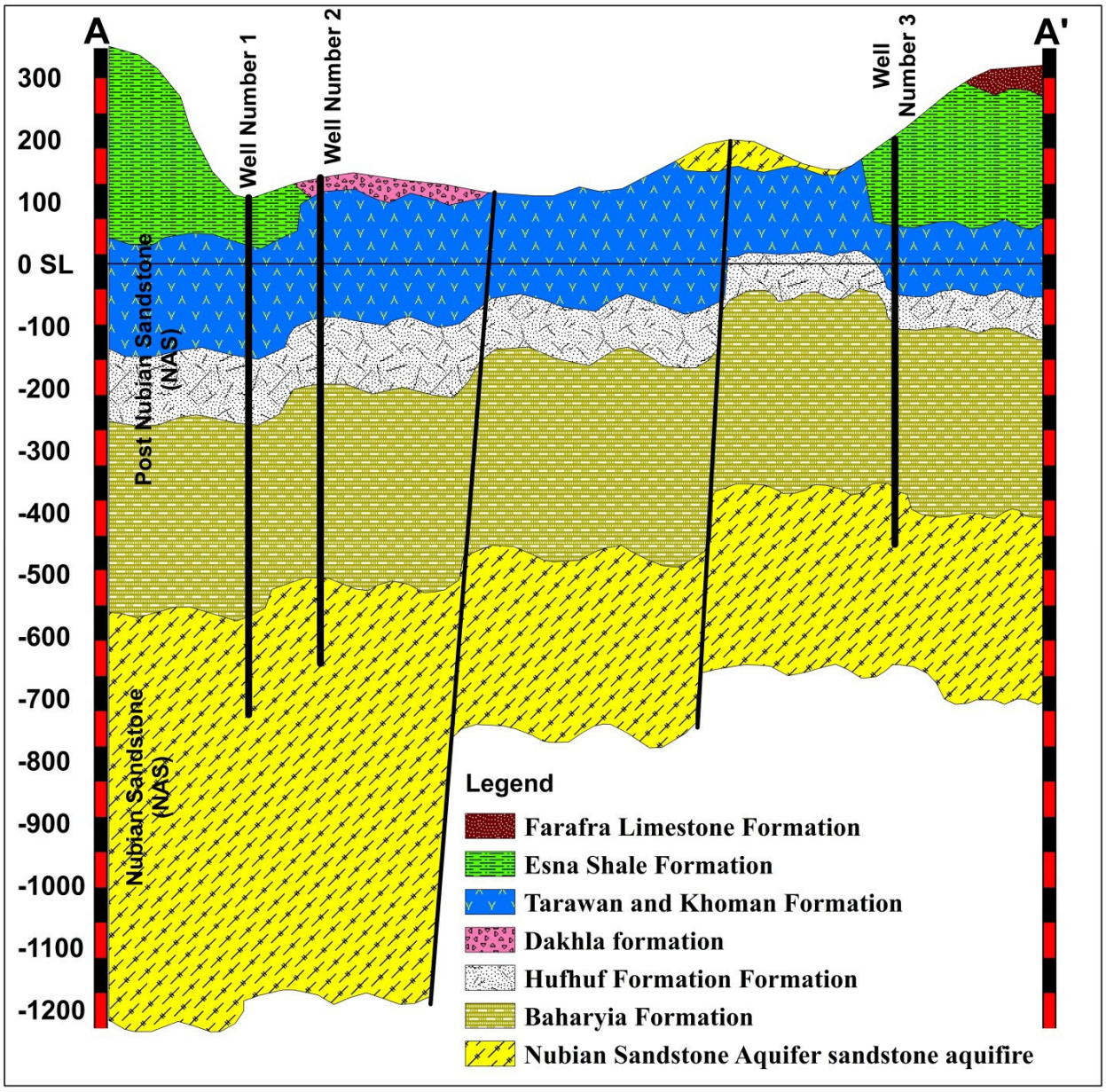

Figure 3. Hydrogeologic cross-section along SW-NE of the study area, (modified by UNESCO, 2005).

3. Materials and Methods

About 31 groundwater samples from the wells (Figure 4) were selected from all the wells in the study area (Figure 5). These selected wells were drilled before the year 2000 with different depths and water samples were taken during three time periods, 2000, 2010, and then 2022. Groundwater samples were collected in plastic containers for physical and chemical analysis. The physical parameters, pH, electrical conductivity, and dissolved solids were measured in the field by portable multiparametric devices. After about half an hour of pumping the wells, water samples were taken. All samples were sealed and kept until chemical analysis was carried out in the laboratory. Chemical analysis of the major cations and anions (Na^+, K^+, Ca^{2+}, Mg^{2+}, HCO_{3^-}, $SO_{4^{2-}}$, and Cl^-) was performed according to international standards. The flame photometer technique used to determine potassium and sodium, calcium, and magnesium was analyzed using atomic absorption spectrophotometer, Bicarbonate was determined by titration method, and sulfate and chloride were determined colorimetrically. Chemical analyses were carried out at the Central Water Laboratory in Kharga City. The chemical analysis results of the wells are given in

(Table 1). Various groundwater quality indices were produced in the present work using geographical information system (GIS) to assess and map changes in groundwater quality resulting from land use and climate alterations. Seven standard water quality indices were calculated. TDS, EC, SAR, SO_{42}-, and HCO_3- refer to total dissolved solids, electrical conductivity, sulfate, and bicarbonates, respectively. The research used various approaches to examine variations in groundwater quality, including interpolation techniques for mapping the changes, Wilcox and Schoeller Diagrams for measuring quality in farming, and the GWQI index for assessing the quality of drinking water. Therefore, three methods are applied to investigate groundwater quality using spatially based GIS (IDW, ordinary kriging, and RBF). The linear technique of displaying the spatial distribution of the concentration of the parameters was utilized in the kriging method, which was used for most parameters because it has the least error [54–56]. Wilcox [57] and Schoeller's [58] diagrams have been employed to assess the quality of water for consumption and agricultural purposes, based on the water's ionic compositions and total soluble salts [59].

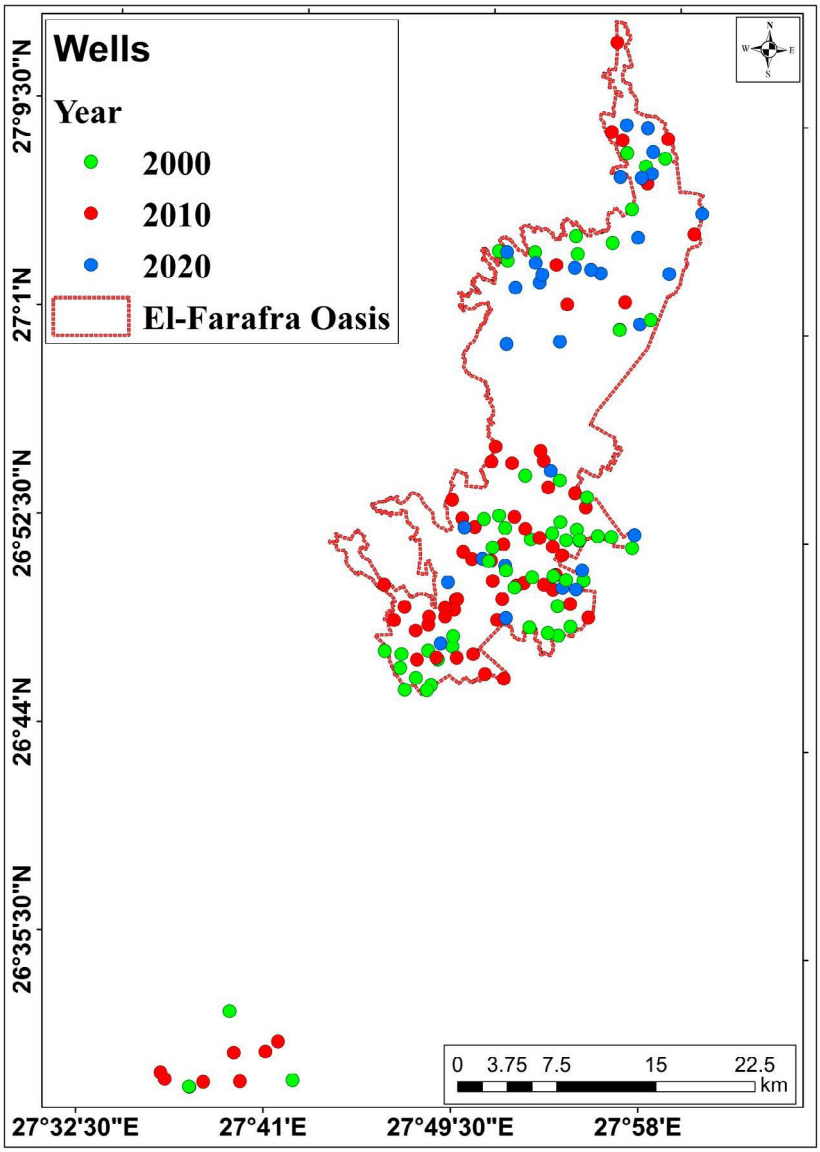

Figure 4. Location of the groundwater samples in the study area.

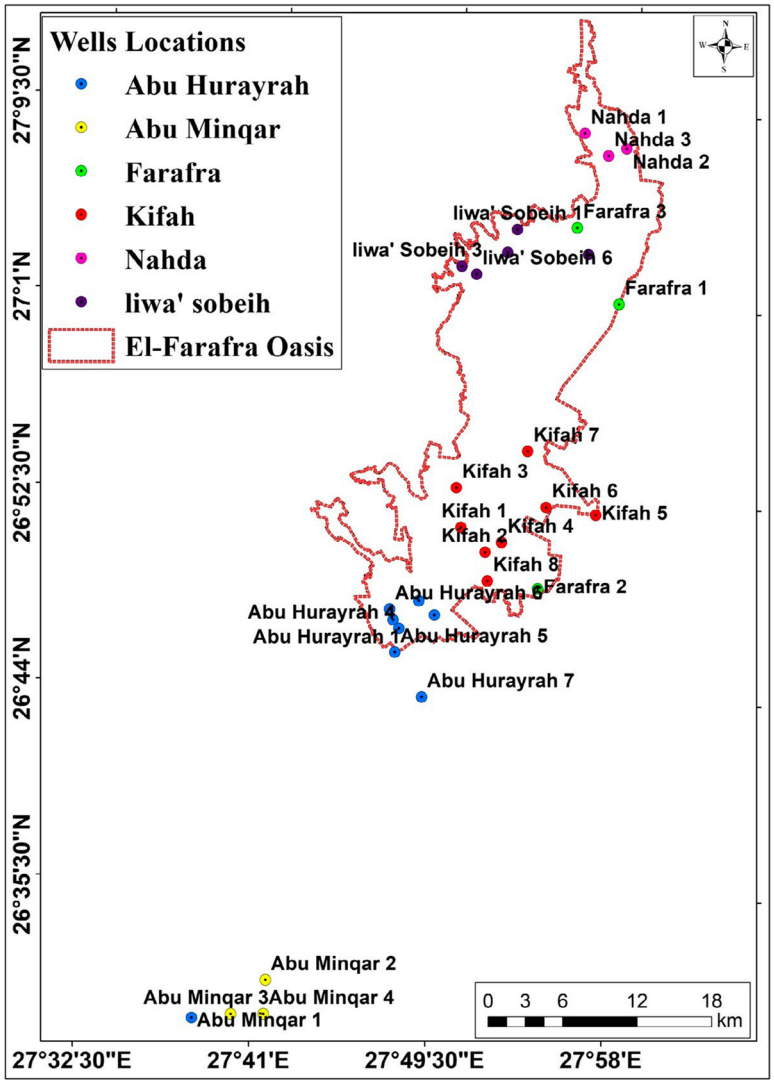

Figure 5. Location of the groundwater wells in the study area, (2022).

Table 1. Chemical analyses results of the groundwater samples.

Parameters			pH	TDS	Ca^{2+}	Mg^{2+}	Na^{+}	K^{+}	HCO_3-	Cl^{-}	SO_4^{-2}	Fe^{++}	Mn^{++}
Concentration (mg/l)	2000	Minimum	6.1	109	6.2	3	5.6	4	27	17.9	4	1.2	0.0
		Maximum	8.1	374	26	19	46	17	68	132	26	10	0.33
		Mean	6.9	139	12.1	7.3	14	9.2	40.4	37.6	14.6	5.3	0.08
	2010	Minimum	5.9	120	10	3.8	9	3	33	21	19	0.46	0.0
		Maximum	7.5	155	21	10	14.4	13	58	44	25.3	11.8	0.2
		Mean	6.5	134	13.9	6.9	11.9	8.5	42.2	30.0	22.3	5.5	0.15
	2022	Minimum	6.4	100	9.3	4.2	9	2.9	26.5	23	15	2.2	0.16
		Maximum	7.6	370	31.9	20.8	39.8	15	60.8	131	50	7.4	0.33
		Mean	6.7	138	12.1	7.3	13.5	8.2	40.2	34.6	20.2	4.7	0.25

4. Results and Discussion

4.1. Groundwater Quality Indices Trends

4.1.1. Interpolation Method

Groundwater quality assessment in the present work involves the calculation and evaluation of five quality indices, namely TDS, EC, SAR, SO_{42}- and HCO_3- over 22 years in three periods (2000, 2010, and 2022). Using the optimal interpolation model selection

shown in Figure 6a–e, and depending upon the least root-mean-square error, ordinary Kriging, IDW, and RBF were employed to assess groundwater quality. Generally, water containing dissolved solids greater than 1000 mg L^{-1} has an unpleasant flavor or is unfit for consumption [60]. Thus, in the research site, the levels of TDS varied from 109 to 374 mg L^{-1} in 2000, 120 to 155 mg L^{-1} in 2010, and 100 to 370 mg L^{-1} in 2022. Higher TDS values can be observed to decrease in both periods, 2000 and 2010, while in 2022, the TDS values increased in some spots in the southwest of the research region as a result of the increase in withdrawal rates in that area for agricultural activities (Figure 6a). It can see from Figure 6b that the amount of EC in 2000 was lower in the north and higher southeast of the research region (more than 584). Because of the land-use alterations and the reduction in precipitation, the EC values rose in some locations southwest of the research area in 2022. In contrast, the levels of SAR ranged from 0.55 to 1.67 in 2000, 0.50 to 0.80 in 2010, and from 0.50 to 1.40 in 2022. The spatial distribution map of SAR showed a significant increase in SAR values from 2000 to 2010 and in some spots in the southwest of the research region in 2022 (Figure 6c). SO_{42}- values varied greatly between 2000 and 2022, as shown in Figure 6d. In 2000, this parameter ranged from 27 meq L^{-1} on the north and south side to more than 68 meq L^{-1} in the area on the east and west sides of the Oasis. From 2000 to 2010, there was a considerable decline in HCO_3-, where the concentration dropped from 68 to 58 meq L^{-1}, while the HCO_3- values increased in some areas north and west of the study area to reach 60.8 meq L^{-1} in 2022 (Figure 6e). Both SO_{42}- and HCO_3- values exhibited significant increase trends from 2000 to 2010. The increasing trends of the SO_{42}- and HCO_3- values matched with the distribution map, which was slightly low over all the study sites in 2000 and then extremely high in most parts of the area between 2010 and 2022.

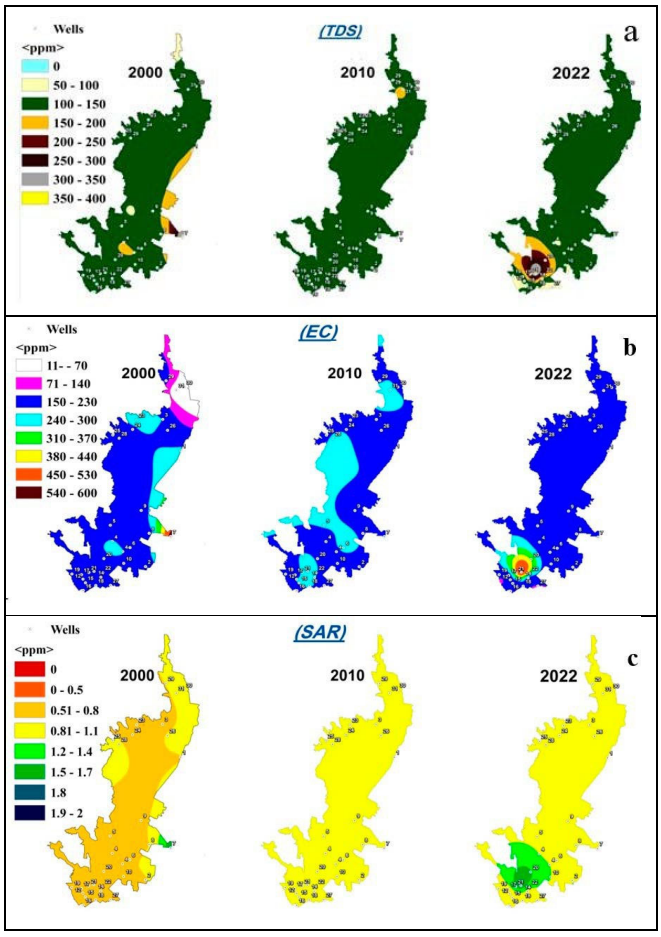

Figure 6. *Cont.*

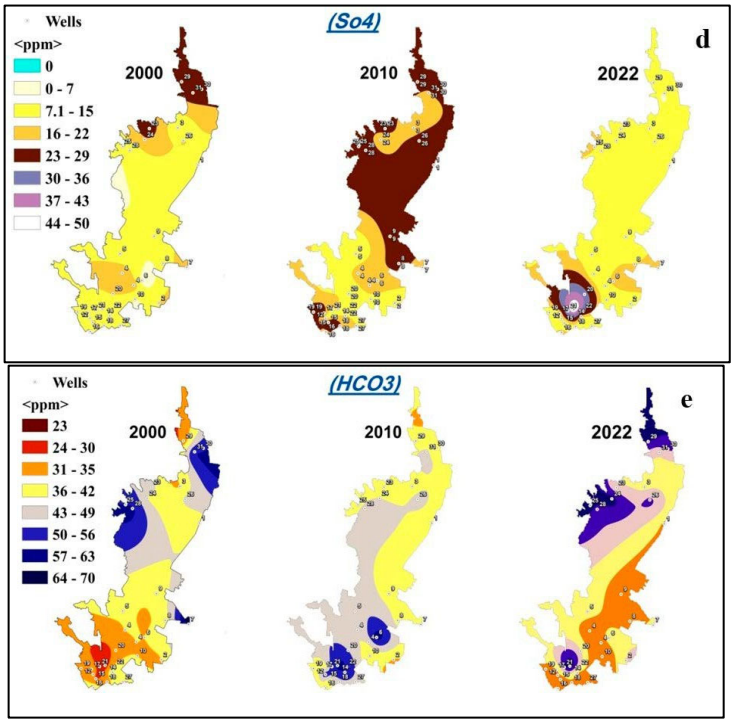

Figure 6. Spatial variations of (**a**) TDS, (**b**) EC, (**c**) SAR, (**d**) SO_{42-}, and (**e**) HCO_{3-} in 2000, 2010, and 2022.

4.1.2. Schoeller and Wilcox Diagrams

Based on the water's ionic compositions and total soluble salts, Wilcox and Schoeller's diagrams have been employed to assess the quality of water for agricultural and drinking purposes. In the Wilcox diagram [57], two parameters were determined using the Aq. Qa software (EC and SAR). In this method, salinity hazard is used to categorize water quality into S1, S2, S3, and S4 types, and sodium hazard into C1, C2, C3, and C4 types. The significance of quality ratings is described as follows: extremely good (C1S1), good (C1S2, C2S2, and C2S1), medium or acceptable (C3S3, C3S2, C3S1, C2S3, and C1S3), and poor (C4 or S4). The Schoeller diagram is a semi-logarithmic graph of the major ion concentrations in milliequivalents per liter that depicts many hydrochemical water sorts that share the same feature [58]. It is based on five chemical factors: hardness, total dissolved solids (TDS), sodium, chloride, and sulfate. By using this diagram, water is divided into six categories: good, acceptable, medium, poor, very poor, and unfit for anthropological usage.

The hydrochemical data were shown in standard graphs to compare the chemical characteristics of the region's groundwater with the World Health Organization's (WHO) standard recommendation for drinking and irrigation purposes [61]. Figure 7a,b depict the graphs created by Schoeller and Wilcox for 31 groundwater samples for the required time periods (2000, 2010, and 2022). The Schoeller graphic shows that the groundwater quality at the prescribed period was drinkable. The Wilcox graphic showed that most wells' groundwater quality has been good (C1S1) and (C2S1) for three years. Results of groundwater changes related to agriculture (Wilcox diagram) and drinking (Schoeller diagram) indicated that variations in the quality class of water were minimal and suitable for drinking and irrigation.

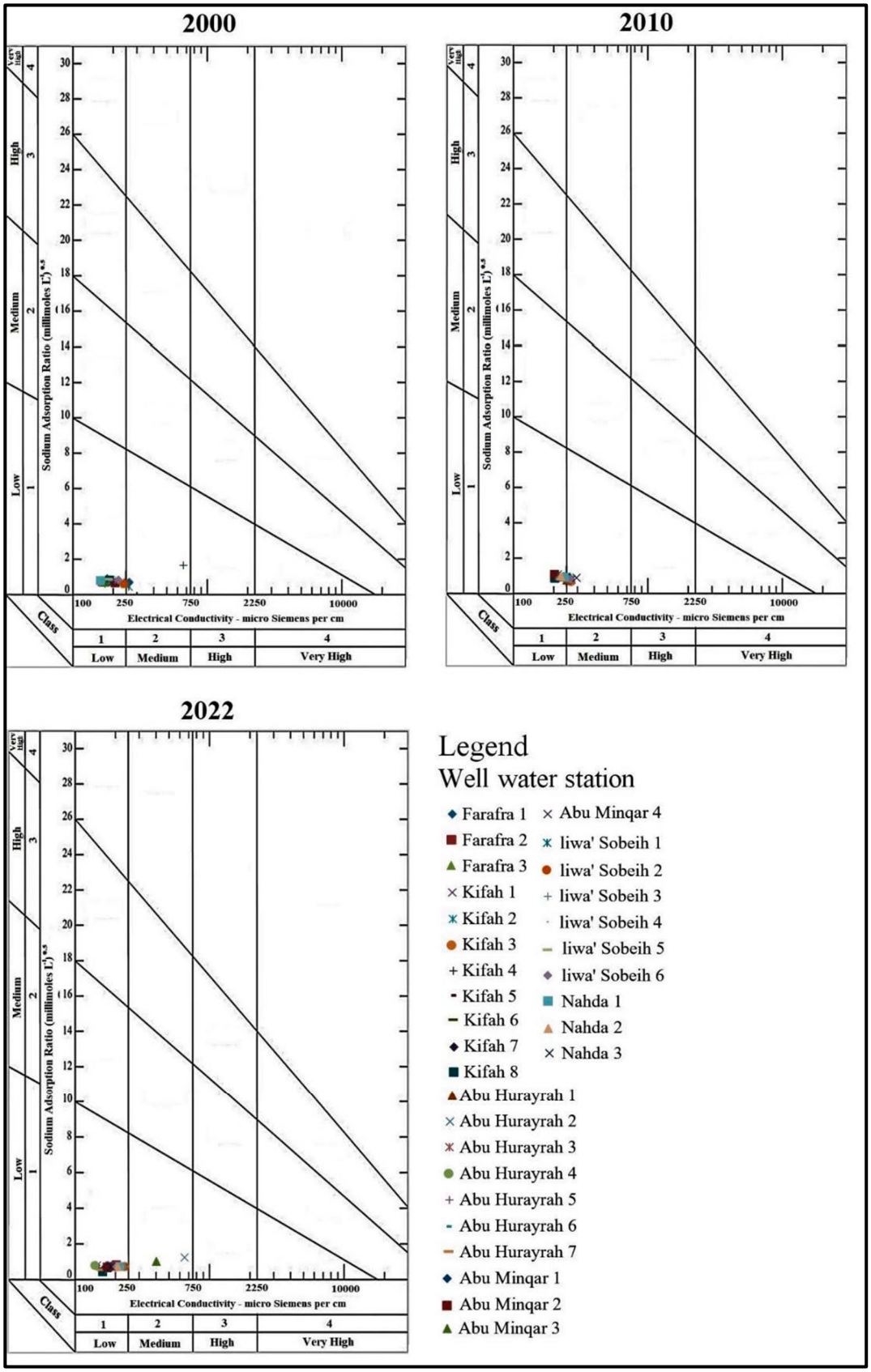

(**a**)

Figure 7. *Cont.*

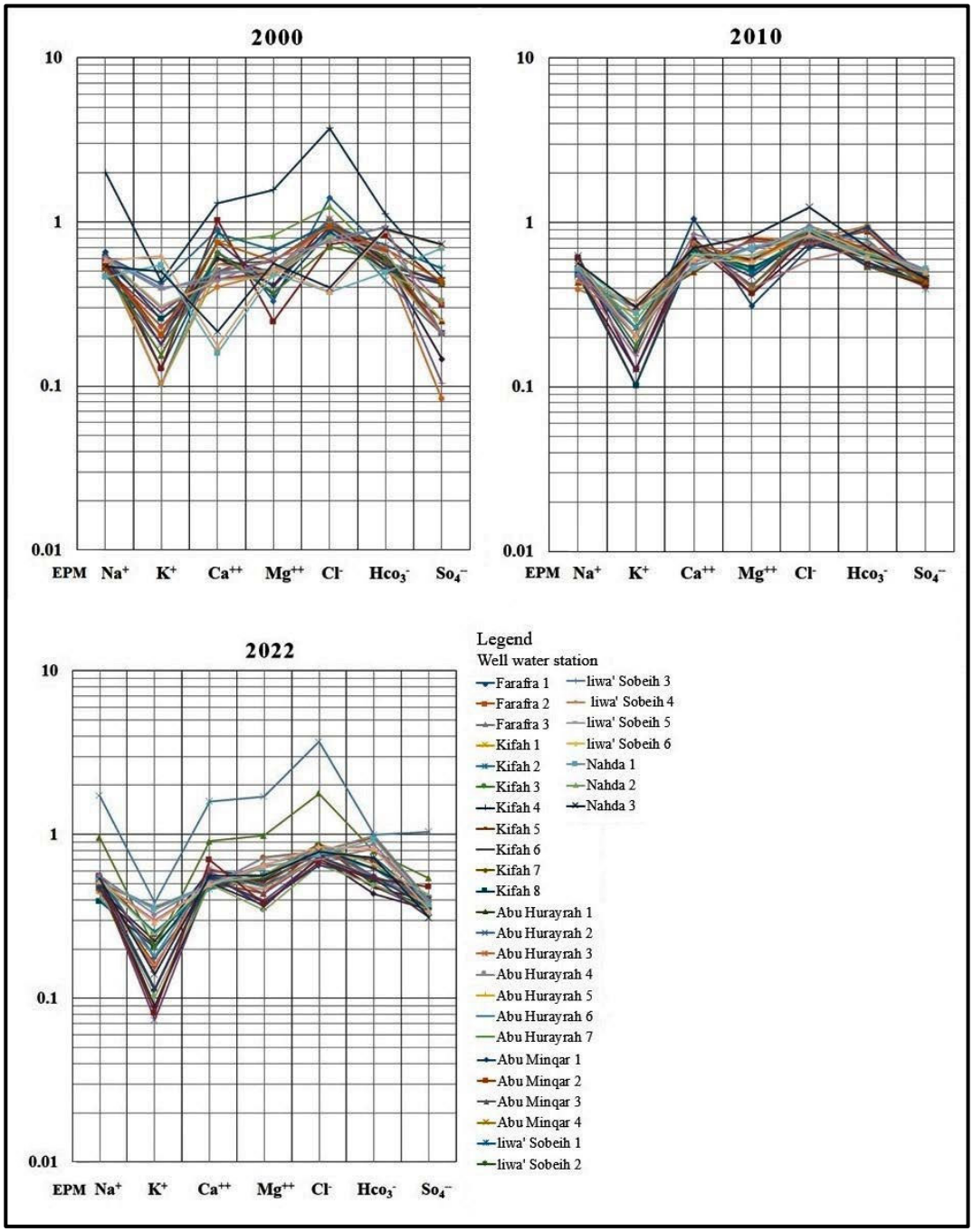

(**b**)

Figure 7. (**a**) Groundwater quality evaluation according (Wilcox diagrams, [57]). (**b**) Schoeller semi–logarithmic nomogram for the groundwater samples representation in the study area.

4.1.3. Groundwater Quality Index (GWQI)

The water quality index (WQI) method is used to assess the quality of surface and groundwater for drinking [62]. In this method, the weights of several quality characteristics are likely inversely correlated to their respective variables [63]. The weight factor (between 1 and 5) is then assigned to each of the ten parameters, including pH, TDS, EC, TH, Cl^-, HCO_3- , SO_{42}- , Mg^{2+}, Ca^{2+}, and Na^+, according to their impact on groundwater quality and health. Some equations are used to determine the GWQI index (Equations (1)–(3)), depicts the findings of this method. This method results in three classes of groundwater quality excellent, good, and bad for drinking in the presence of high concentrations of

iron and manganese. Without iron and manganese concentrations, the excellent class of groundwater quality for drinking in all groundwater samples.

$$W_{ri} = wi / \sum_{i=1}^{n} wi \quad (1)$$

where (w_i) and (W_{ri}) are, respectively, the weight and relative weight of each chemical parameter. Qualitative rank for each of them (q_i) calculated using Equation (2)

$$(q_i) = \frac{C_i}{S_i} \times 100 \quad (2)$$

where (C_i) is the concentration of each chemical parameter and (S_i) is WHO standard values. Finally, the GWQI index is calculated according to Equation (3).

$$\text{GWQI} = \sum_{i=1}^{n} (W_{ri} \times q_i) \quad (3)$$

Furthermore, land use change was mapped during the specified period of time to identify the areas where groundwater quality has changed as a consequence of land use modification using change detection and supervised classification methods by GIS techniques (ArcMap 10.5) [64]. Three Landsat satellite images (2000, 2010, and 2022) (Figure 8a–c) encompassing the research region were used by the American Geological Survey (https://pubs.usgs.gov/gip/gw_ruralhomeowner/) (accessed on 1 January 2023) after radiometric and atmospheric correction to them using ENVI 5.3 [65] software. Climatic condition data for the specific (2000–2022) were mainly acquired from the site (Earthexplorer.usgs.gov). While the Demographic data was collected from the official reports of the central agency for public mobilization & Statistics (CAPMAS).

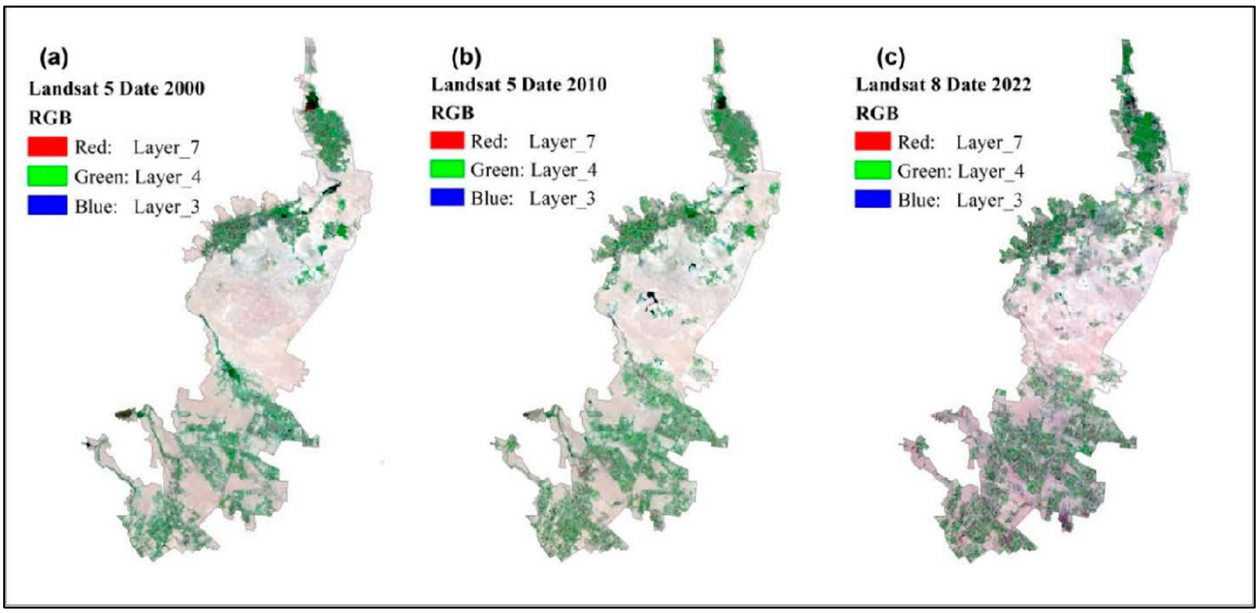

Figure 8. Landsat satellite image characteristics within the research region; (**a**) Landsat 5 from 2000, (**b**) Landsat 5 from 2010, and (**c**) Landsat 8 from 2022.

The chemical analyses from 2000, 2010, and 2022 were used to calculate the GWQI index, which was employed to evaluate changes in groundwater quality for consumption. In 2000, the GWQI index showed a significant decrease. While in 2010, the index shows that the quality of water in the research region has been high. However, in this period, changes were unregular. In 2010, water quality increased compared to 2022. In the research region,

the concentration of iron in the groundwater samples ranged from 1.16 to 10 mg L^{-1} (2000), 2.28 to 11.80 mg L^{-1} (2010), and 2.2 to 7.42 mg L^{-1} (2022). Additionally, the concentration of manganese ranged from 0.01 to 0.3 mg L^{-1} (2000), 0.00 to 0.20 mg L^{-1} (2010), and 0.17 to 0.33 mg L^{-1} (2022). In the presence of extremely high concentrations of iron and manganese as a consequence of soil degradation and the development of residential areas, the index has grown in all wells, indicating that the groundwater quality has worsened in almost all wells (Figure 9a,b).

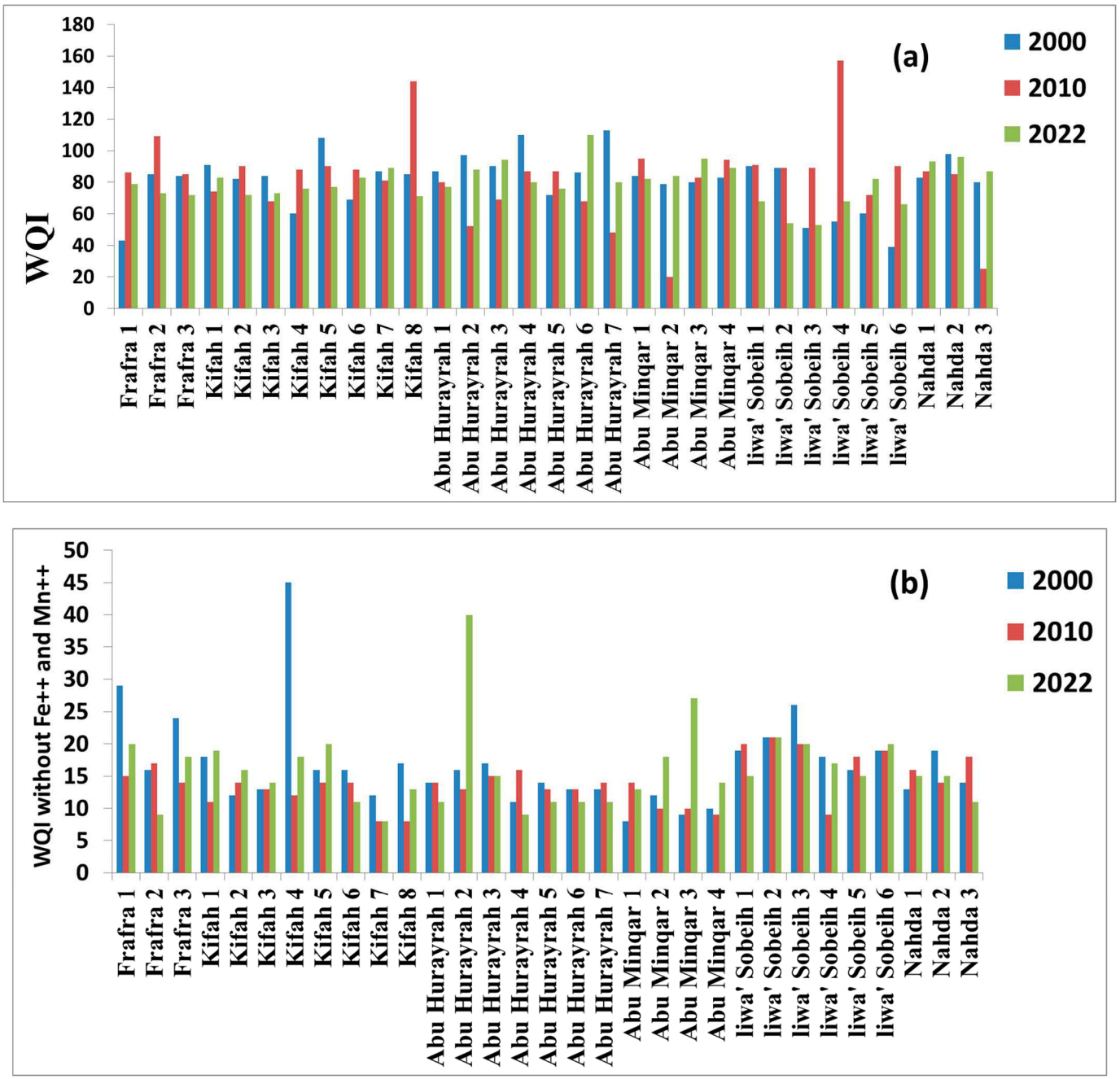

Figure 9. GWQI index; (**a**) with and (**b**) without Fe^{+2} and Mn^{+2} concentration in 2000, 2010, and 2022.

4.2. Impacts of Altering Land Use on the Quality of Groundwater

Various researchers [66–68] have investigated the impact of an extensive expansion of agriculture and other parameters on groundwater and soil quality. Alterations in land use are strongly implicated as one of the most important human-caused variables affecting

the soil and underground water system [69]. Although the footprint of the land used and climate changes on water quality degradation, this linkage has not been widely explored in Egypt; however, this linkage has long been recognized globally. Tang et al. [70] and Bhaduri et al. [71] concluded that land-use alterations significantly affect the watershed region's hydrology. In the latest two decades, the geographical distribution patterns of alterations in land use in the studied region revealed an expansion of agricultural fields.

The Oasis is 160.18 km^2 in total area. Four types of land usage were distinguished, urban, water, agricultural, and barren lands (Figure 10). Among the types of land use changes in the area is extending the agriculture area from 2000 to 2022 using flooded water for irrigation. This greatly influenced the quality of groundwater because of the too much water extraction in the region. Under arid conditions which characterized the study area, similarly, land use changes influenced aquifer recharge rates. The categorization of satellite images revealed that the proportion of agricultural land in the study region changed from 12.8% in 2000 to 13.3% in 2010 to 14.6% in 2022. Figure 11 depicts the changes in land use, while Table 2 provides a percentage comparison of these alterations. The change in percentage of the urban area was 6.4% in 2000, 7.8% in 2010, and it increased to 11.1% in 2022. As represented in the study area by springs, the water category was less than 1% in 2000, 0.3% in 2010, and decreased to 0.2% in 2022. The spreading out of farming land contributes to worsening groundwater quality; this deterioration is ascribed to the increased use of chemical fertilizers in the studied region. Alternatively, pollution and change in discharge may be a consequence of land use variations related to rigorous farming activities. Throughout the analysis of land use changes percentage through the study periods, especially the agricultural practice and anthropogenic activities may increase the degrading of groundwater quality in the area.

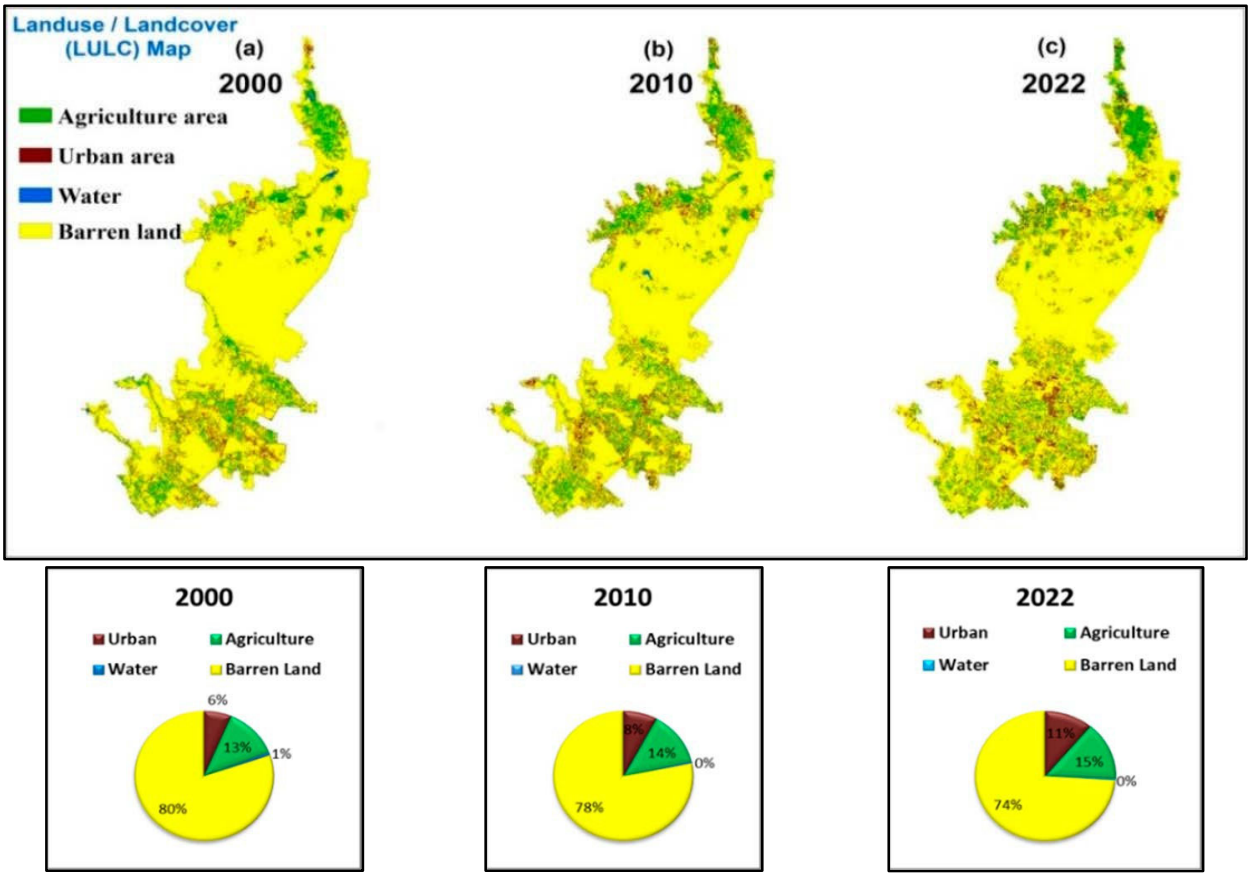

Figure 10. Land use/land cover map and percentage of the study area in (**a**) 2000, (**b**) 2010, and (**c**) 2022.

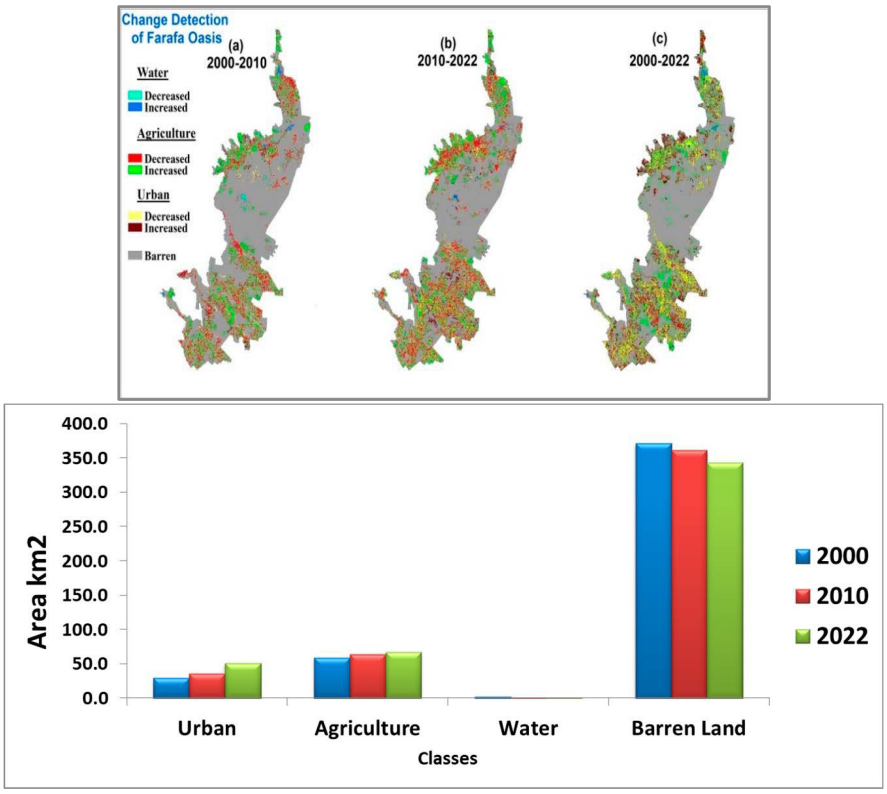

Figure 11. Change detection of land use in El-Farafra Oasis over the study periods. (a) represents changes between 2000 and 2010. (b) represents changes between 2010 and 2022. (c) represents changes between 2000 and 2022.

Table 2. Summary of the land use areas and percentage over the study periods.

Area (km^2) \ Years	Agriculture	Urban	Water	Barren lands	Total
2000	59.4 (12.8%)	29.6 (6.4%)	2.9 (0.6%)	371.7 (80.2%)	463.6 (100%)
2010	63.9 (13.8%)	36.3 (7.8%)	1.4 (0.3%)	362.0 (78.1%)	463.6 (100%)
2022	67.8 (14.6%)	51.3 (11.1%)	1.3 (0.2%)	343.2 (74.0%)	463.6 (100%)

4.3. Impacts of Climate Change on Groundwater Quality

Due to the lack of climatic stations on the study site, detailed knowledge of the climate condition in the study area was obtained from the power access data viewer web (https://power.larc.nasa.gov) (accessed on 1 January 2023). The acquired information includes maximum atmospheric temperature and means annual rainfall. The annual climate indicators (maximum temperature and mean precipitation) during 2000, 2010, and 2022 are shown in Figure 12. The highest average temperature was 39 °C and was recorded in July, while the lowest average through the last 22 years was recorded in January and was 10 °C. The highest mean relative humidity in the study area was 60%, recorded in December, and the lowest was 33% in May. In 2020, the maximum annual average precipitation in this area was 6.15 mm. The variation in precipitation indicates that the quantity of precipitation fell from 2000 to 2022 but was at its minimum in 2000, 2009, 2012 to 2015, and 2019, indicating dryness in such periods. However, the climate conditions in the area indicate a slight overall increase in the atmospheric temperature (Figure 12a), with an increase in annual rainfall during the years 2011, 2016, and 2020 (Figure 12b).

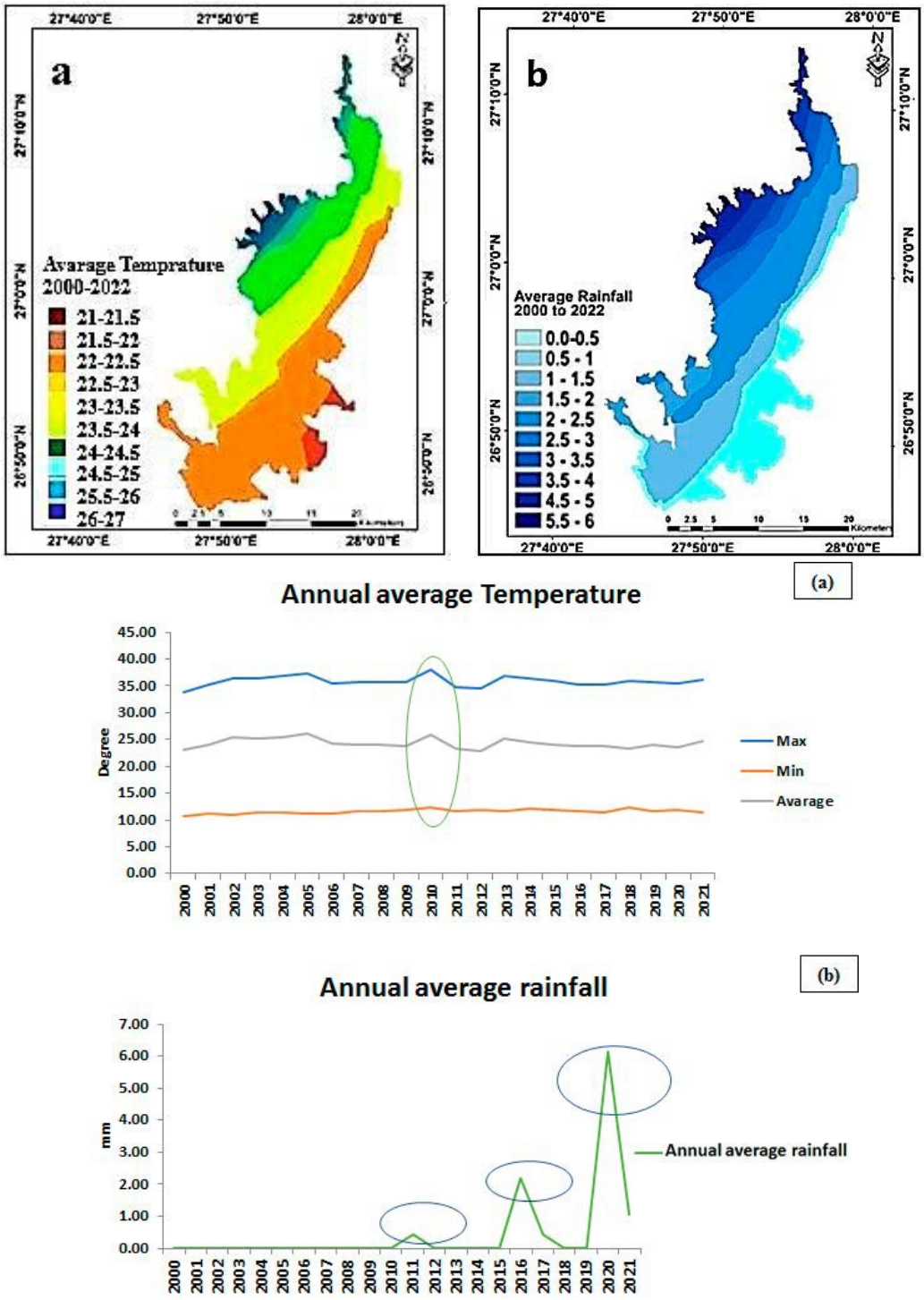

Figure 12. Climatological data of El-Farfra Oasis, Annual averages during the period (2000–2022) (average of latest 22 years) (https://power.larc.nasa.gov) (accessed on 1 January 2023). (**a**) annual average temprature. (**b**) annual average rainfall.

In 2009, the maximum atmospheric temperatures exhibited higher temperatures. On the other hand, comparing the annual maximum temperatures in the years 2000, 2010, and 2022, the results indicated that the approximate temperatures are 23.10, 25.35, and 24.72 °C, respectively. Furthermore, the increasing temperature will lead to an increased evaporation process, thus impacting the groundwater systems with a depth to the water table of 10 m or less. However, the precipitation trend during the study period showed slight changes and increases in the precipitation rates in 2010, 2016, and 2010. An increase in annual

precipitation is associated with an increase in the frequency of extreme precipitation events causing flash floods. The increasing precipitation in the area could lead to an increase in the aquifer recharge through surface runoff. These climatic conditions, linked with a geological context, may have led to the decreased water residence time in the aquifer, allowing water movement and degrading the water quality with greater water-rock interaction.

Finally, land use and climate change significantly affected groundwater quality degradation in the area. In particular, the increase in extreme and irregular climatic events such as rainfall and temperature have an impact on water quality. The higher temperatures in all cases are linked to higher evapotranspiration, which is most severe during summer. By comparing the precipitation during the study periods, no major change was observed in the rainfall rate except in the years 2010, 2016, and 2020. The annual precipitation in 2010 was 0.44 mm, then declined to 0.00 mm until it increased again to 2.20 mm in 2016 and 6.15 mm in 2020. From the perspective of geology combined with structural conditions, several investigations have underlined groundwater quality alterations induced by the seepage from different aquifers along with the fault system.

4.4. Population Growth Impacts on Groundwater Quality

The observed changes in population growth are closely related to the depletion of groundwater level and quality in the study area. El-Farafra Oasis in Egypt has experienced significant population growth, with an annual rate of 7.52% between 2000 and 2020 with a total population 35,820 per based on The Central Agency for Public Mobilization and Statistics (CAPMAS) reports (Figure 13). Farafra has a relatively high population density ranging from 207 to 1573 individuals per square kilometer (Figure 14). However, this growth has put pressure on the limited natural resources in the area, particularly the groundwater supplies which are decreasing at a rate of 284.34 × 106 m^3/year. Maintaining water quality is crucial for the well-being of society, especially with the increasing demand for water, energy, land, and infrastructure due to urbanization. Neglecting the issue of water pollution could result in a future where polluted water is the only option for drinking.

El-Farafra Oasis heavily relies on groundwater for drinking water due to its distance from the Nile River, making it critical to maintain its quality during population growth. However, population growth has created a disproportion between the availability of fresh water and the number of people relying on it, resulting in pressure on groundwater quality. The effects of this pressure are complex and depend on a range of factors, including scientific, social, economic, and management factors.

4.5. Water Quality Spatial Model

The research employed several water quality spatial models (WQSM) using ArcGIS software (V.10.8) to identify the most areas where the groundwater quality is most affected based on the main implemented factors. The models' input included main variables, i.e., chemical analysis, land uses, population growth and climatic data. The results of each model are classified into five classes including; high-risk, moderately high, moderate, moderately low, and low-risk areas (Figure 15). Accordingly, chemical analysis and land use had the highest importance values in the modeling process. On the other hand, climate change and Population growth had the least important values. Inspection of the final model output (Figure 16) indicates that, the area where the groundwater quality is the most affected lies in the north of the Oasis (Alamil Oasis) which is an area where agricultural areas are increasing, elements concentrations and population density. While the central region of the Oasis is found to be the least affected (Al shaykh Marzuq and Al shaykh Marzuq Aljadida area) where agricultural areas and populations decrease significantly from models for different indices (Figure 16).

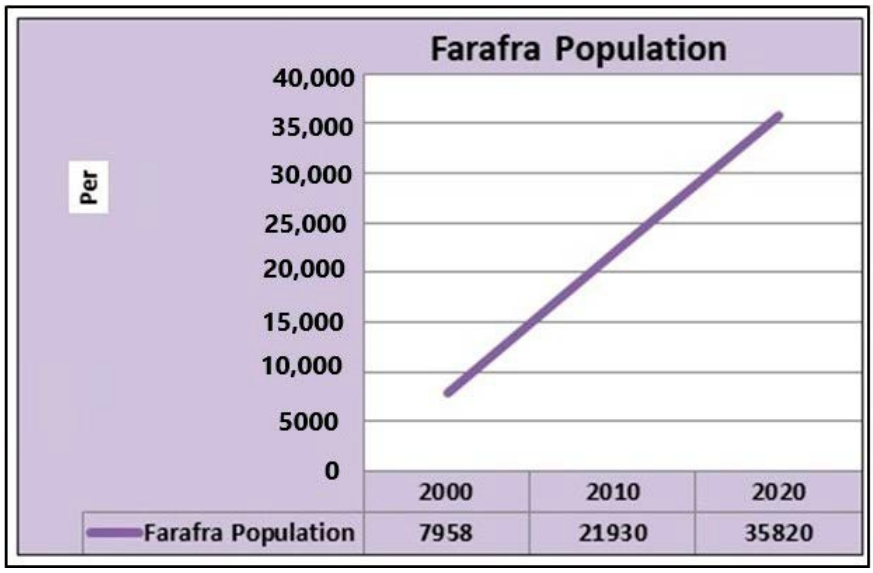

Figure 13. Population growth of El-Farafra Oasis from 2000 to 2020.

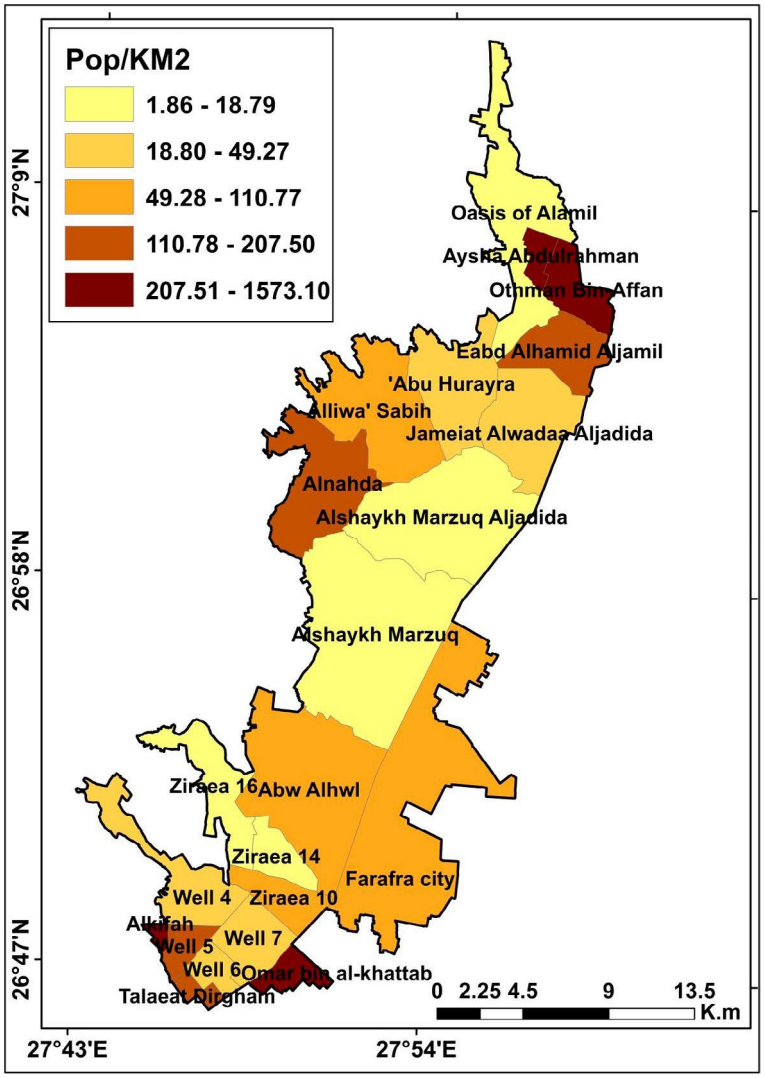

Figure 14. Geographical distribution of the population density of Farafra Oasis in 2020.